A matrix population forecasting model for *Aedes aegypti* considering basic sanitation environment, daily weather, and its impact over the dormancy state

Luana Tais Bassani

Thesis presented to the
Institute of Mathematics and Statistics
of the University of São Paulo
in partial fulfillment
of the requirements
for the degree of
Doctor of Science

Program: Applied Math
Advisor: Prof. Dr. Pedro da Silva Peixoto

During the development of this work, the author received financial support from
CAPES – Finance Code 001, CNPq and NSERC of Canada

São Paulo
November, 2023

A matrix population forecasting model for Aedes aegypti considering basic sanitation environment, daily weather, and its impact over the dormancy state

Luana Tais Bassani

This is the original version of the thesis
prepared by candidate Luana Tais Bassani,
as submitted to the Examining Committee.

Acknowledgments

The world always seems brighter when you've
just made something that wasn't there before.
— Neil Gaiman

I thank the Lord for all the blessings around me, which includes thank to Pedro, Huaiping, Salete, Cerilo, Maiton, Gabriele, Eduardo, Rodney, João, Sérgio, Grigori, Marcos, Petrônio, Paulos, Fernanda, Silvia, Wnilson, Luciano, Liane, Deise, Gilmar, Antônio, Luciana, Daisy, Silvana, Jéssicas, Graziane, Amanda, Athauana, Luana, Taís, Susane, Marcelo, Samara, Therezinha, Albino, Marinês, Marla, Rafael, Antunino, Lucas, Larissas, Irene, Eurico, Amelina, Bruna, André, Thomas, Pei, Longbin, Sherry, Teresa, Stan, Tony, Frederick, Vanessa, Simone, Erick, Anas, Diego, Geise, Edina, Leane, Sonia, Luis, Izanildes, Rosani, Kátia, Nérimo, Marciele, Jucélia, Terezina, Bernard, and everyone who contributes to my life in their own way. It's amazing I have all these friends to support me! I wish God bless all of us.

I also thank to Claudia Codeço and Denise Valle from Fiocruz (Brazil), for providing the data which supported our work.

I'm honored to thank Professors Pedro da Silva Peixoto and Huaiping Zhu, you both trusted me many times.

I thank Bill, Melinda Gates and their foundation for their projects and beliefs. They made me recognize the basic sanitation importance, and catch the math behind it, to improve the public health.

I thank to USP, CAPES and CNPq for all the opportunities and support these institutions offered me.

You all helped me to become this and continue.

Deus faz maravilhas em minha vida, fé que me moveu tantas vezes, que me move e continuará movendo na eternidade, Não deixaria de agradecer da forma como conheço desde pequena, em português, Obrigada por tudo Deus.
— Lua

Resumo

Luana Tais Bassani. **Modelo matricial de projeção populacional para Aedes aegypti com influência de saneamento básico, condições climáticas diárias e impactos sobre o estágio de quiescência** . Tese (Doutorado). Instituto de Matemática e Estatística, Universidade de São Paulo, São Paulo, 2023.

Modelos matriciais de populações estruturadas por estágios são úteis para investigar a dinâmica populacional e têm sido aplicados com sucesso na modelagem de vetores. Para construí-los, considera-se que os blocos que compõem a matriz do sistema correspondem a processos biológicos que conectam o indivíduo à população. Propomos um modelo com a finalidade de investigar o comportamento da dinâmica populacional do *Aedes aegypti* e estimar a sua abundância em municípios brasileiros. Há quatro estágios, que correspondem ao ovo quiescente, não-quiescente, ao desenvolvimento aquático (larva e pupa) e à fêmea adulta. Cada coordenada do vetor mosquito representa o número de indivíduos no estágio atual com mesma idade. Para isso, considera-se a matriz de projeção populacional, composta por funções de oviposição, transição e mortalidade. São funções dependentes da temperatura média diária ou acumulada, de idade e estágio do indivíduo, da precipitação diária ou acumulada, bem como do saneamento básico. Assim, para cada passo de tempo, há uma matriz esparsa associada que rege o sistema e possibilita análise de sensibilidade e estabilidade com condições climáticas constantes. Comparamos os resultados gerados pela simulação do modelo com dados coletados de armadilhas, a fim de validar a médio prazo o modelo de predição da dinâmica populacional e de estimar a abundância das fêmeas adultas, vetor transmissor de doenças em humanos. Percebemos que a influência da temperatura e da precipitação, em conjunto com a abordagem da quiescência e do saneamento básico urbano, possibilitaram compreender a interferência do clima e do saneamento básico para o desenvolvimento e a manutenção da população de *Aedes aegypti*. Por meio da modelagem, avaliamos o impacto de melhorias nos sistemas de saneamento sobre a dinâmica populacional, e fundamentamos a importância de coletas de dados reais das regiões urbanas endêmicas mensalmente, com a realização de programas de vigilância contínuos.

Palavras-chave: Modelos matriciais. Abundância de *Aedes aegypti*. Condições climáticas. Quiescência. Saneamento básico urbano.

Abstract

Luana Tais Bassani. **A matrix population forecasting model for Aedes aegypti considering basic sanitation environment, daily weather, and its impact over the dormancy state** . Thesis (Doctorate). Institute of Mathematics and Statistics, University of São Paulo, São Paulo, 2023.

Stage-structured matrix population models are useful to investigate population dynamics and have been successfully applied to vector modeling. To construct this model, we consider that these matrices' blocks correspond to biological processes, which allows for building a bridge from the level of the individuals to the whole population. With this purpose, we developed a model to investigate the behavior of *Aedes aegypti* population dynamics and to estimate its abundance in Brazilian municipalities. There are four stages, corresponding to the quiescent eggs, nonquiescent eggs, the aquatic development (larvae and pupae), and the adult female mosquitoes. Each coordinate of the mosquito vector represents the number of individuals in the current stage over the same age. We considered a population projection matrix composed of oviposition, transition, and mortality functions, which depend on the daily mean or accumulated temperature, the individual age and stage, as well as the daily or accumulated precipitation and the basic sanitation of acity. There is an associated sparse matrix governing the system for each time step. Due to its structure, when we set constant weather conditions, we are able to evaluate stability and sensitivity analysis by calculating the net reproductive value. We compared the model simulation results to real data collected from mosquito traps as we attempted to validate the forecasting of the model's population dynamics for a medium-range period and to estimate the eggs and adult females abundance. We pointed out that the use of temperature and precipitation, together with the quiescence and urban sanitation approach, allowed us to verify the interference of the weather and basic sanitation for the development and maintenance of the population. Through modeling, we assessed the impact of sanitation improvements on *Aedes aegypti* fluctuation and the importance of collecting monthly data from urban endemic regions to encourage and support continuous surveillance schemes.

Keywords: Matrix models. *Aedes aegypti* abundance. Weather conditions. Quiescence. Urban basic sanitation.

List of Figures

2.1 Five Brazilian cities' locations and their neighborhoods (A, B, C), according to the figure extracted from Codeço *et al.* (2015). 11
2.2 Fuzzy set for the input about percentage of urban population, which is blue for few and red for many. 17
2.3 Fuzzy set for the input about percentage of the served population by frequents solid waste collection services, which is green for defective and brown for ideal. 17
2.4 Fuzzy set for the input about percentage of the served population by sanitary sewerage services, which is green for defective and blue for ideal. 18
2.5 Fuzzy set for the input about the served population by water supply services, which is purple for defective and red for ideal. 18
2.6 Fuzzy logic system structure. 21
2.7 Fuzzy set for the output about sanitation influence, which is green for precarious, brown for inadequate, red for adequate, and blue for ideal. . 23
2.8 Rules 11 and 15 are active for Parnamirim. 24
2.9 Fuzzy Rule-Based System output for Parnamirim/RN, with inputs [100 91.61 100 0.77]. 25
2.10 Fuzzy Rule-Based System output for Campo Grande/MS, with inputs [98.66 98.15 99.03 62.33]. 25
2.11 Fuzzy Rule-Based System output for Santarém/PA, with inputs [72.68 48.28 74.17 22.83]. 25
2.12 Fuzzy Rule-Based System output for Nova Iguaçu/RJ, with inputs [99.18 87.3 93.33 44.02]. 26
2.13 Fuzzy Rule-Based System output for Duque de Caxias/RJ, with inputs [99.69 81.73 99.01 43.45]. 26

3.1 (a) The lower mortality in the aquatic development stage is around 17°C. (b) The transition is improved around 27°C. (c) The lower mortality is around 29°C. (d) The oviposition is stimulated around 30°C. 33

3.2 (a) The biggest transition is stimulated around 31°C. (b) The lower mortality is around 7°C. . . . 34
3.3 Modeling the viability versus temperature using a sum of sines (Farnesi *et al.*, 2009). . . . 37
3.4 Gaussian fitting for the viability sample from Soares-Pinheiro *et al.* (2017). 39
3.5 Eclosion from then two calculations (H. Silva and I. Silva, 1999). . . . 41

4.1 Compartments of the model. . . . 44
4.2 *Aedes aegypti* life cycle. Adapted from Ishikawa (2012), E. Souza (n.d.), Diáriogaúcho (2015), and Loyola (2016). . . . 45
4.3 The flow chart of mosquito's life cycle as established in the model. . . . 48
4.4 The flow chart of mosquito's life cycle as established in the model. One color represents the path trends in the same class. . . . 49
4.5 *Dipsacus sylvestrix*. Source: the authors (Jul. 2020). . . . 71

5.1 Scheme for identifying the individuals that sum a total of 5 days old on the day $t + 4$ from day t. . . . 76
5.2 BG-Sentinel and ovitrap used by Codeço *et al.* (2015). . . . 78
5.3 Campo Grande's BG and ovitrap data for the surveillance period. The red line represents ovitrap data, while the blue line is for BG-Sentinel data. . 78
5.4 Santarém's BG and ovitrap data for the surveillance period. The red line represents ovitrap data, while the blue line is for BG-Sentinel data. . . . 79
5.5 Parnamirim's BG and ovitrap data for the surveillance period. The red line represents ovitrap data, while the blue line is for BG-Sentinel data. . . . 79
5.6 Nova Iguaçu's BG and ovitrap data for the surveillance period. Instead of July to June, as BG was collected on June, 29th, in June 2012 they did not collect ovitrap, and it was collected lately, on July, 3rd. The red line represents ovitrap data, while the blue line is for BG-Sentinel data. . . . 80
5.7 Duque de Caxias's BG and ovitrap data for the surveillance period. The red line represents ovitrap data, while the blue line is for BG-Sentinel data. 80
5.8 Weather, ovitrap and BG-Sentinel data over Nov. 2009 to Oct. 2010 in Duque de Caxias. . . . 81
5.9 *Aedes aegypti* population dynamics for Duque de Caxias. . . . 82
5.10 Model output and trap data along the year. The red lines represent the data, and the blue lines are the model output. While the first plot is about new individuals, the second one is about adult females. . . . 82
5.11 Dependence between variables. . . . 83

5.12 Weather, ovitrap and BG-Sentinel data over Dec. 2009 to Nov. 2010 in Parnamirim. 83
5.13 *Aedes aegypti* population dynamics for Parnamirim. 84
5.14 Model output and trap data along the year. The red lines represent the data, and the blue lines are the model output. While the first plot is about newly individuals, the second one is about adult females. 85
5.15 Dependence between variables for Parnamirim results. 85
5.16 Weather, ovitrap and BG-Sentinel data over Dec. 2009 to Nov. 2010 in Campo Grande. 86
5.17 *Aedes aegypti* population dynamics for Campo Grande. 87
5.18 Model output and trap data along the year. The red lines represent the data, and the blue lines are the model output. While the first plot is about newly individuals, the second one is about adult females. 88
5.19 Dependence between variables for Campo Grande results. 89
5.20 Weather, ovitrap, and BG-Sentinel data for Nov, 2011 to Oct, 2012 in Nova Iguaçu. 89
5.21 *Aedes aegypti* population dynamics for Nova Iguaçu. 90
5.22 Model output and trap data along the year. The red lines represent the data, and the blue lines are the model output. While the first plot is about newly individuals, the second one is about adult females. 91
5.23 Dependence between variables for Nova Iguaçu results. 91
5.24 *Aedes aegypti* population dynamics over extreme constant conditions in Duque de Caxias. 94
5.25 *Aedes aegypti* population dynamics over extreme weather constant conditions in Duque de Caxias. 95
5.26 *Aedes aegypti* population dynamics over extreme constant conditions in Santarém. 96
5.27 *Aedes aegypti* population dynamics over extreme constant conditions in Santarém. 97
5.28 *Aedes aegypti* population dynamics over extreme constant conditions for different basic sanitation panoramas. We selected Santarém (first column) and Duque de Caxias (second column). 99
5.29 *Aedes aegypti* population dynamics over extreme constant conditions for different basic sanitation panoramas. We selected Santarém (first column) and Duque de Caxias (second column). 100

List of Tables

2.1 Tpop: Total population; Upop: Urban population percentage; Twat: Percentage of the total population with water supply; Uwat: Percentage of urban population with water supply; Tsew: Percentage of the total population with sewerage service; Usew: Percentage of urban population with sewerage service; Twas: Percentage of the total population with solid waste collection. We calculate the percentages according to SNIS data (SNSA, n.d.). The lines which include averages among the 2009 and 2012 periods carry the fuzzy system entries. 12
2.2 The rules of the fuzzy logic system. 19
2.3 Percentages of basic sanitation indicators according to an average of 2009-2012 period. *Legend for the Table; Tpop: Total population; Upop: Urban population percentage; Twat: Percentage of the total population with water supply; Uwat: Percentage of urban population with water supply; Tsew: Percentage of the total population with sewerage service; Usew: Percentage of urban population with sewerage service; Twas: Percentage of the total population with solid waste collection; Sanitation parameter: output value for the city's sanitation influence. 24

3.1 Characteristics of *Aedes aegypti* (time period counted by day). 29
3.2 Parameters description. 32
3.3 Results of laboratory experiments from Farnesi *et al.* (2009). 35
3.4 Results of experiments from Soares-Pinheiro *et al.* (2017). 37
3.5 Basic rates of *Aedes aegypti*. 40

4.1 Compartments description. 50
4.2 Matrices blocks description. 51
4.3 Matrices entries and rates description. 53
4.4 Functions and parameters description. 58

5.1 Critical days and characteristics (Climate-Data, n.d.[b]; Climate-Data, n.d.[c]; Climate-Data, n.d.[a]; Climate-Data, n.d.[d]; Spark, n.d.[a]; Spark, n.d.[b]; Spark, n.d.[c]; Spark, n.d.[d]; Spark, n.d.[e]). *Mean of the minimum daily temperature (average T_{min}, not average daily temperature). ♦The annual mean accumulated precipitation. †Half of the annual mean accumulated precipitation per 365 days multiplied by 24 days. 75
5.2 Organizing data, inputs, and outputs of the model. 81
5.3 *Net reproductive number n, growth rate λ and mean generation time γ* for daily temperature (θ in °C) and precipitation (q_p in mm) for Duque de Caxias scenarios. 93
5.4 *Net reproductive number n, growth rate λ and mean generation time γ* for daily temperature (θ in °C) and precipitation (q_p in mm) for Santarém scenarios. . . 95
5.5 The net reproductive number n, for a fixed daily temperature (θ in °C) and precipitation (q_p in mm for Duque de Caxias and Santarém basic sanitation panorama. 98

Contents

1 Introduction **1**

2 Basic sanitation and Fuzzy systems **5**

2.1 Basic sanitation in Brazilian cities 6

2.2 Urban versus rural zones 13

2.3 System Components 15

2.3.1 Input variables and Sets 15

2.3.2 Rules Basis 18

2.3.3 System structure: Fuzzy Relation and Compositional Inference . 18

2.3.4 Output set 22

2.3.5 Active rules for each city 23

3 Mosquito Population Dynamics **27**

3.1 General concepts about *Aedes aegypti* 27

3.2 Literature based functions 31

3.3 Novel functions 34

4 Model construction **43**

4.1 Model assumptions and some considerations 43

4.2 Model development 50

4.3 Composing all functions 57

4.4 System Structure 64

4.5 The theory behind general structured models 65

4.5.1 Net reproductive number n 67

4.5.2 Single Newborn Class Model 69

4.5.3 Structure example 70

5 Numerical simulations **73**

5.1 The cities' weather characteristics 73

5.2 Setting the initial conditions 74
5.3 Data, model simulation, and discussion 77
5.4 Population dynamics for Duque de Caxias/RJ 79
5.5 Population dynamics for Parnamirim/RN 83
5.6 Population dynamics for Campo Grande/MS 86
5.7 Population dynamics for Nova Iguaçu/RJ 88
5.8 Discussion for Santarém/PA 91
5.9 Weather scenarios and extreme conditions 92
5.10 Sensitivity analysis for the basic sanitation parameter α_c 97
5.11 What if Brazilian policies for sanitation are achieved? 98

6 Final considerations **101**

References **103**

Chapter 1

Introduction

Vector-borne diseases like Dengue, Zika, and Yellow Fever affect the human population (Gould and Solomon, 2008). They are spread by the adult female of *Aedes aegypti*, which has its biological stimuli influenced by environmental conditions.

Mathematical models are used to study this kind of phenomenon, helping to explain the population dynamics of the vectors and the incidence of the diseases. The modeling aims at vector control, and it can catch population fluctuations, forecast the epidemic periods, and send warnings to public health programs and the whole population.

However, building a forecasting model able to predict health risks and apply prevention strategies is a challenge (Morin and Ebi, 2018). The study of the dynamics of the adult mosquito has contributed to the detection of fluctuations in this population (H. Yang *et al.*, 2009). The ability to accurately estimate the mosquito abundance has shown a way to develop vector control (M. R. d. Silva, 2022; H. Yang *et al.*, 2009; G. Yang *et al.*, 2009).

Matrix population models are usually governed by stage and or age structure (Ahumada *et al.*, 2004; Cushing and Yicang, 1994; Usher, 1966; Werner and Caswell, 1977; Loncaric and Hackenberger, 2011; Newman *et al.*, 2014; Schaeffer *et al.*, 2007; Yusoff *et al.*, 2012b; Yusoff *et al.*, 2012a). Historically, based on Cushing and Yicang (1994), in the Leslie, Lefkovitch, and Usher models, as well as the generalized structured population models, the configuration allows associating an individual with all individuals. It occurs according to biological characteristics in common, like age, life stage, survival, transition, and a minimum and maximum time spent in each step of the development (Cushing and Yicang, 1994). As a result, matrix models can provide a tool for understanding population development phenomena, especially those related to the dynamics of structured populations.

Age and stage-structured models were developed to model the population dynamics of vectors, such as *Aedes vexans, furcifer, africanus*, and *aegypti* as well as *Culex pipiens* (Loncaric and Hackenberger, 2011; Schaeffer *et al.*, 2007; Yusoff *et al.*, 2012b). These models consider that the matrix blocks correspond to biological processes (Newman *et al.*, 2014), which build a bridge from the individual level to the whole population (Cushing and Yicang, 1994). An advantage of this model is that the block structure produces a sparse matrix that governs the dynamical system. We then study the properties of the

model while we assume a weather-independent projection matrix for each city, based on its typical weather and sanitation. Additionally, the matrix population model has a net reproductive number, which allows the evaluation of the asymptotic dynamics of the population (Cushing and Yicang, 1994).

The structured population approach allows exploring egg development in two stages, the quiescent and nonquiescent eggs. Despite recent efforts in mosquito life cycle research, few studies have focused on mosquito dormancy (DL Denlinger and Armbruster, 2014). The *Ae. aegypti* dormancy ability allows survival during seasons since the characteristics of the egg allow accumulation even in heat and precipitation absence (S. Souza *et al.*, 2010), and this has contributed to the mosquito abundance (R *et al.*, 2014; Barrera *et al.*, 2014; Vieira, 2008; Trpis, 1972) apud (Lega *et al.*, 2017). Therefore, we include embryonic quiescence in a model as a stage to understand the success of the *Aedes aegypti* vector (DL Denlinger and Armbruster, 2014).

In Brazil, one season produces a variability of environmental conditions due to its continental size. The geographical location is intercepted by the parallel lines of the equator and the tropic of Capricorn. Thus, Brazil's summer starts on December 21st and ends on March 20th, and its winter is from June 21st to September 22nd. Indeed, there are four seasons, which have different characteristics according to the region (Jerônimo *et al.*, 2011).

In the same way as the model built for the climate diversity along an island by Johansson *et al.* (2009), we can model the Brazilian areas despite the different weather conditions. We consider city conditions like temperature, precipitation, and sanitation, which we apply to stem information about seasonality and environmental water abundance. The photoperiod has a small variability in Brazil compared to temperate areas. For example, in regions like the Northeast, the dryness period is a limitation for the *Aedes aegypti* population. Besides, the floating periods may help in understanding the fluctuations and dynamics.

The eggs can remain for a longer period waiting for environmental conditions to develop. A usual tool to maintain surveillance in the city is monitoring houses. Unfortunately, the Brazilian surveillance programs for mosquito development are temporary. This ineffective monitoring of the situation can influence the risk of outbreaks by promoting mosquito breeding once it increases by factors resulting from human behavior, such as a temporary pause in disease control activities or overcrowding, and susceptibility to changes in the habitat like deforestation or river damming (WHO, n.d.[a]).

Therefore, we studied possible relationships between the abundance data with the surrounding variables (Reisen *et al.*, 2008; G. Yang *et al.*, 2009), as an attempt to predict peaks in the mosquito population.

The Brazilian Fiocruz institution collected data about surveillance schemes using traps for adults and eggs, arranged in 5 mid-sized cities located in Brazil (Codeço *et al.*, 2015). Each city has a distinct dengue-endemic region, provided by different environmental conditions.

The vector-borne disease or population abundance modeling can provide information to improve public health. In recent years, dengue has been considered an international

public health concern, predominantly in urban and peri-urban areas (WHO, n.d.[b]).

Recently, *Aedes aegypti* spreading is a concern for cold cities in the South of Brazil. For example, Santa Catarina is a Brazilian state above the Tropic of Capricorn (the Southern Tropic). It combines severe winters and characteristics that used to be a hindrance to *Aedes aegypti*'s development. However, health secretariats from Santa Catarina reported an increase in cases of vector-borne diseases transmitted by *Aedes aegypti*, such as dengue in humans (Gov, 2020; DIVE, 2022). The number of infested cities in 2022 represented an increase from 2021 (DIVE, 2022).

Therefore, we built a model to investigate the behavior of *Aedes aegypti* population dynamics and estimate its abundance in Brazilian municipalities. Through the city data of weather, sanitation, and traps, we built a forecasting population model to predict the *Aedes aegypti* population in different stages. After all, by predicting the abundance of females, it was possible to study the transmission dynamics of the diseases caused by them. This model can work as a warning of outbreak periods, and it is possible to couple it with predictive models of diseases spread by *Aedes aegypti*.

The contribution of our model's approach was that we relate weather with the city's sanitation characteristics and the *Aedes aegypti* population's biological stages. The model considers the basic sanitation panorama as an output of a fuzzy system and works with development stages that combine quiescent egg characteristics, besides weather data, through temperature and precipitation on a daily average and accumulated.

We cannot directly control the weather fluctuations. Despite this, humans are capable of helping in the preservation of the environment, and "efforts to prevent their global dissemination in the near future will be most effective if focused on preventing human-mediated spread and establishment" (Kraemer *et al.*, 2019).

In what follows, we describe the basic sanitation and fuzzy systems (Chapter 2), the dynamics of the mosquito population including the basic biology of *Aedes aegypti* (Chapter 3), the model construction including the assumptions and development (Chapter 4), the numerical simulations (Chapter 5), the final considerations (Chapter 6), and the appendix.

Chapter 2

Basic sanitation and Fuzzy systems

In mathematical applications, the modeling process can require a representation that involves graduations, such as patterns of best and worst scenarios (Barros and R. Bassanezi, 2006). For some diagnostics, we justify the fuzzy set theory approach for categorizing the weather predictions and basic sanitation services supply.

We considered there exists an influence of basic sanitation on the maintenance of breeding sites of *Aedes aegypti*. Klafke *et al.* (2023) concluded that solid waste management and *Aedes aegypti* infestation are connected. Similarly, Almeida *et al.* (2020) concluded a relationship between urban settlement, water supply, sanitation, and *Ae. aegypti* development.

We will set a parameter (α_c) that will play a role over *Aedes aegypti* development in our mathematical model. This parameter will be considered an output of a fuzzy rule-based system (FRBS), due to the subjectivity to measure it. This aims to quantify the contribution attributed to the basic sanitation of the city on the maintenance of breeding sites of *Aedes aegypti*. The rain absence has less influence on the dynamics of the *Aedes aegypti* population as α_c grows, because the sanitation panorama provides environmental conditions for vector-borne development (J. Silva and Machado, 2018; WHO, 2020; WHO, n.d.[a]; WHO, n.d.[b]).

After we search about Brazilian sanitation systems and the environmental influence over *Aedes aegypti* development, a FRBS will be designed to supply the expert's intuition. Thus, the analysis of the system output will allow a municipality to predict outbreaks and manage public policies, as they can discern the fluctuation in vector population dynamics in an outcoming period while improving basic sanitation and controlling the vector. Therefore, fuzzy logic allows us to expand classical logic, in addition to representing and relating imprecise information, that helps in decision-making Barros and R. Bassanezi, 2006.

Instead of government spending on controlling outbreak consequences, such as releasing insecticides and hospital beds, public policies can contribute earlier, by improving the basic sanitation in the municipality and surveillance programs. The supply service

companies measure a price to offer the service and cover structure repairs, acquire chemicals necessary for the waste treatments, and also make a profit, to continue to provide a quality service. However, there must be a balance between investment and profit (G1, 2019). As long as the structure is not repaired and universalized, there are always goals to achieve.

There is a Brazilian web school that offers free courses to the city hall staff, and any interested person (GOV, 2024). Some courses explain how the system data are released and provided by each city hall, and how sanitation works for each city. In this way, we selected for the fuzzy system inputs variables the percentage of the urban population, and the served population with basic sanitation of water supply, solid waste, and sewerage treatment.

2.1 Basic sanitation in Brazilian cities

Basic sanitation refers to the set of services, infrastructures, and operational installations for the supply of drinking water, sanitary sewerage (collection, transportation, treatment, and final disposal), urban cleaning, and management of solid waste and rainwater (BRASIL, 2007).

Ancient civilizations concluded that the population needed the promotion of basic sanitation for the maintenance of public health (Brasil, 2013b). We emphasize that the term sanitation comes from the verb to sanitize, which means to make it hygienic (Brasil, 2013b).

Therefore, the concept of sanitation is based on health prevention (Brasil, 2013c), which means the effort to avoid diseases, and involves a larger dimension related to the quality of life (C. Souza *et al.*, 2015; Brasil, 2013c).

Organizations are concerned about control measures to guarantee public health. World Human Organization indicates that the proper disposal of solid waste helps to reduce water availability (WHO, n.d.[b]). Plus, the organization understands that an efficient method to avoid dengue consists of harming the *Aedes aegypti* development through the removal of mosquito breeding sites, which means that human interventions are required to contain the spreading once there is no vaccine to protect against dengue (WHO, n.d.[b]).

Those diseases related to a poor sanitation infrastructure can occur due to the lack of a collection and treatment system for solid waste, sewerage, as well as adequate rainwater management (Brasil, 2013c).

The United Nations adopted a resolution in 2010 that recognized “the right to safe and clean drinking water and sanitation as a human right”, which means they are essential for the full enjoyment of life and all human rights (Nations, 2010, p. 2).

Previously, in 2007, the Law 11445, known as the Basic Sanitation Law, made it mandatory for serviceholders to prepare for the basic sanitation policy. From that law, the Ministry of the Cities was subject to organizing a broader basic sanitation plan (BRASIL, 2010). Building a plan helps a city to guide the needed steps for a healthy sanitation panorama.

Nowadays, experts from the United Nations point out the benefits of providing funding for basic sanitation (Brasil, 2014). According to them, each US$ 1 spent on sewerage treatment implies an economy of around US$ 4 with health care (Brasil, 2014).

Brazilian public sanitation services aim to universalize access through a progressive expansion of all occupied households to basic sanitation (BRASIL, 2007).

As an attempt to surveillance and plan the next steps, Brazil has its own sanitation system. Indeed, SNIS means *Sistema Nacional de Informações Sobre Saneamento*, which is a Brazilian sanitation information system (Brasil, 2019a). It is the most important Latin American system of sanitation reports, created in 1996 through 1995 data of water and sewerage (Brasil, 2019a). Since 2002 it has included solid waste management (Brasil, 2019a).

The Brazilian system SNIS calculates indicators about the sanitation basic information for each municipality and all Brazilian territory (Brasil, 2019a). This tool helps the construction of the Municipality Plan of Sanitation (Brasil, 2019a). Each company that provides Water and/or Sewerage Services is responsible for providing information to SNIS (Brasil, 2019a).

The system has two components, the first is about Water and Sewerage services, and the second is Solid waste treatment (Brasil, 2019a). SNIS indicators are generated by crossing at least two types of information (Brasil, 2019a).

The system processes information through the data inputted from the basic sanitation service municipal providers, which can be state, public, and private companies, or the Municipality city hall, through their secretariats or departments (Brasil, 2019c). It evaluates the situation related to sanitation and assists in the preparation of the Municipal Sanitation Basic Plan (Brasil, 2019a; Brasil, 2019c).

The companies have a local, micro-regional, or regional scope, which depends on how many municipalities the entity is providing services (Brasil, 2019c).

The population that receives benefits from the water and/or sewerage service is connected to the network and served (Brasil, 2019d). Otherwise, it is classified as not served. Plus, the total population served is composed of urban and rural (Brasil, 2019d).

Based on the Brazilian National basic sanitation plan (PLANSAB - *Plano Nacional de Saneamento Básico*), an adequate service of sanitation includes the following items (Brasil, 2011):

1) Water Supply: the supply of drinking water through a distribution network or well, spring, or cistern, with internal channeling and without intermittent (Brasil, 2011).

2) Sanitary Sewage: the collection of sewage followed by treatment, as well as the use of a septic tank (Brasil, 2011).

3) Solid Waste Management: For urban areas, it requires direct collection with daily frequency or on alternate days and appropriate destination (Brasil, 2011). On the other hand, in rural areas, direct or indirect waste collections are classified as adequate (Brasil, 2011).

Water treatment is a set of physical and chemical procedures that are applied to the water to become drinkable (Brasil, 2019e). It is not all municipalities that have a Water Treatment Station (Brasil, 2019e). However, disinfection and fluoridation operations can be carried out as a Simplified Treatment Unit of water (Brasil, 2019e).

There are water supply alternatives such as well, springs, fountains, and cisterns, which are adequate methods, while they are continuous and depend on internal channeling (Brasil, 2012; Brasil, 2013b; Brasil, 2011). Weir, water truck, and structures with intermittent or without internal channeling are inadequate (Brasil, 2013b; Brasil, 2011).

If the water supply has frequent intermittent, the population often use water tanks, pots, and barrels, which are covered or not (Fiocruz, 2016; J. Silva and Machado, 2018; Sardão, 2016). The SNIS carries information about the frequency of problems occurred with the supply service through indicators.

We point out that alternative ways to obtain water supply may increase the breeding sites when the structures are inadequate. Thus, people may carefully use and maintain them, for example, by sealing the water tanks and putting grille in the drains (Fiocruz, 2017).

Public health organizations need to carry on measures aiming for an adequate universal supply with no intermittent.

Aedes aegypti develops mainly in sites where collections of water are available in artificial containers in the environment of human settlements (Fiocruz, 2016; Fiocruz, 2017; WHO, 2020), unlike wild species, which lay their eggs in the hollows of trees (Fiocruz, 2017). It implies that the solid waste may influence the breeding sites, due to the increase in the environmental capacity (WHO, 2020; WHO, n.d.[b]).

Indeed, prevention of mosquito breeding can be realized by checking drinking-water containers, covering them, frequently emptying them, or treating them (Fiocruz, 2016; WHO, 2020). Therefore, solid waste collection can help in collecting containers, mainly those placed in urban public areas. The rhythm is important to supply and avoid breeding sites. In favorable environmental conditions, after the egg hatches, the pupa mosquito develops into an adult and winged form, taking a period of around ten days (minimum of nine days according to the model hypothesis). Therefore, if the water change is accompanied by washing once a week, the mosquito's life cycle will be interrupted. Thus, we note the importance of conducting a weekly collection of solid waste (Vieira, 2008).

For example, everybody can give the right destination for an abandoned tire, but how could we suggest to people not to store water in buckets, while nowadays some populations still do not have intermittent services and do not know if they will have their daily basic sanitation right guaranteed tomorrow?

Environmental sanitation involves the control of physical characteristics from where the human acts or can exercise activities that result in harmful effects on own self's well-being, physical, social, or mental (Brasil, 2013b).

In 2023, the Brazilian government purposed to postpone goals for basic sanitation, despite the sanitation program discussed during the last years and the measures proposed

in the 2018-2022 period (Ribeiro, 2023; Brasil, 2011; Brasil, 2019g; Brasil, 2020a). Unfortunately, it implies that a part of some Brazilians continue without basic sanitation, such as water supply services and sewage treatment (SNSA, n.d. G1, 2019; Ribeiro, 2023).

Through the analysis, we discussed *Aedes aegypti* population fluctuations concerning sanitation variables related to public health.

We add the term urban to categorize solid waste from urban cleaning and households (Brasil, 2013c). According to Law 12305/2010, solid waste includes many types, as well as those from health and civil construction (BRASIL, 2010).

In this context, solid waste characterizes material, substance, object, or discarded goods (BRASIL, 2010). It results from human activities in society, and the appropriate destination must keep it as solid or semi-solid states (BRASIL, 2010). In addition to that, the waste may contain gases that cannot be discharged into sewage or water channels (BRASIL, 2010). Some types of waste require solutions inviable given the best available technology (BRASIL, 2010).

The National solid waste Policy defines instruments as firstly a selective collection, that must be implemented through the earlier separation of solid waste (Brasil, 2013c). Secondly, the reverse logistics systems, which are characterized by the set of actions, procedures, and means for collecting and returning solid waste to the business sector for reuse in its life cycle or other production cycles (Brasil, 2013c).

Moreover, companies treat solid waste with sorting (separation of materials), recycling (transformation into raw material again), and final disposal in landfills (Brasil, 2013c). For that, the collection of usual waste requires a compactor truck, while for recyclables, it needs a bucket truck or similar (Brasil, 2013c).

Adequate disposal of solid waste requires transporting it to a place called a sanitary landfill (BRASIL, 2010). This technique is for disposing of urban solid waste on the soil, avoiding damage to public health and safety, and minimizing environmental impacts (BRASIL, 2010). The method uses engineering principles to confine solid waste to the smallest possible area and allowable volume, covering them with a layer of soil between short time intervals (BRASIL, 2010; Brasil, 2013a).

Brazil incinerates only 0.03% of the waste (Brasil, 2013a). Usually, the alternative is a sanitary landfill, despite current generations of big cities having problems in finding places for it since a closed landfill continues to generate pollutants, such as gas, and percolate, for at least 15 years (Brasil, 2013a).

The sewage starts to be produced from the use of water, mainly coming from homes (Brasil, 2019f). The natural process is that the sewage formed is taken by the sewerage collection network to a Sewerage Treatment Station, which treats the effluent before the final disposal (Brasil, 2019f; Brasil, 2013c).

In some places where there is no sewage direct collection and treatment, an adequate alternative is the construction of a septic tank, which refers to a projected unit that treats, at the primary level, household sewage (Brasil, 2013b; Brasil, 2019b). It is mainly found in rural homes and performs the physical separation of the solid matter (Brasil, 2019b).

This treatment serves as a great benefit to basic sanitation due to the prevention of diseases related to hygiene care (Brasil, 2019b).

There are irregular and not recommended options for the disposal of household sewage, which are rudimentary tanks, release into rainwater galleries, release into watercourses, and open ditch (Brasil, 2013b; Brasil, 2019b).

A precarious sewerage service can pollute the environment, and pollution contributes to floods. Besides, floods can expand the number and range of vector-borne habitats (WHO, n.d.[a]).

Moreover, rainwater management interferes with flood periods, as it involves structures to control drainage and measures for significant infiltration in the forest, as an attempt to reduce runoff (Brasil, 2013a). However, they are subjective to evaluate. We assume that daily and accumulated precipitations are enough to predict population fluctuations, which means that flooding does not represent a direct impact on the model.

From the map in Figure 2.1, we located cities and their respective regions. Santarém-PA is located in the North Region, Parnamirim-RN in the Northeast Region, Duque de Caxias-RJ and Nova Iguaçu-RJ in the Southeast Region, and finally Campo Grande-MS in the Central-West Region (more details in (Codeço *et al.*, 2015)).

The percentage of the population served in each municipality is described in Table 2.1. Basic sanitation was provided to a different proportion of households for each studied city in urban and rural areas (SNSA, n.d.).

From the Table 2.1 we notice that zero means there is no service, while empty entries mean unknown information (Brasil, 2019c). However, we associate that Santarém has void information due to a precarious sewerage service reported in 2012 (SNSA, n.d.).

Nowadays, Santarém presents an alarming reality yet (Brasil, 2020b). Among the 100 most inhabited cities in Brazil, it received the 97th ranking position in 2019 and 2020, due to its inadequate water and sewerage service, as well as investments and structures, i.e., only three Brazilian cities among those 100 obtained a worse panorama for sanitation (Brasil, 2020b). The ranking scores did not consider waste collection.

We note that Duque de Caxias (91st ranking position in 2019 and 89th in 2020) and Nova Iguaçu (82nd in 2019 and 72nd in 2020) are also classified with a ranking position that indicates the city indicators shall be improved.

Campo Grande (31st ranking position in 2019 and 32nd in 2020) occupied a better ranking position among the five studied cities.

The Parnamirim population (261,469) (IBGE, 2019) was not included in the ranking of the 100 most inhabited cities, once the city with fewer inhabitants estimated by IBGE in that ranking was Governador Valadares (278,685) located in the state of Minas Gerais (Brasil, 2020b).

Based on the information in Table 2.1, we note that both cities did not evolve significantly, from 2010 up to 2020. Indeed, the actual panorama for Duque de Caxias is one of the worst in Rio de Janeiro (G1, 2019).

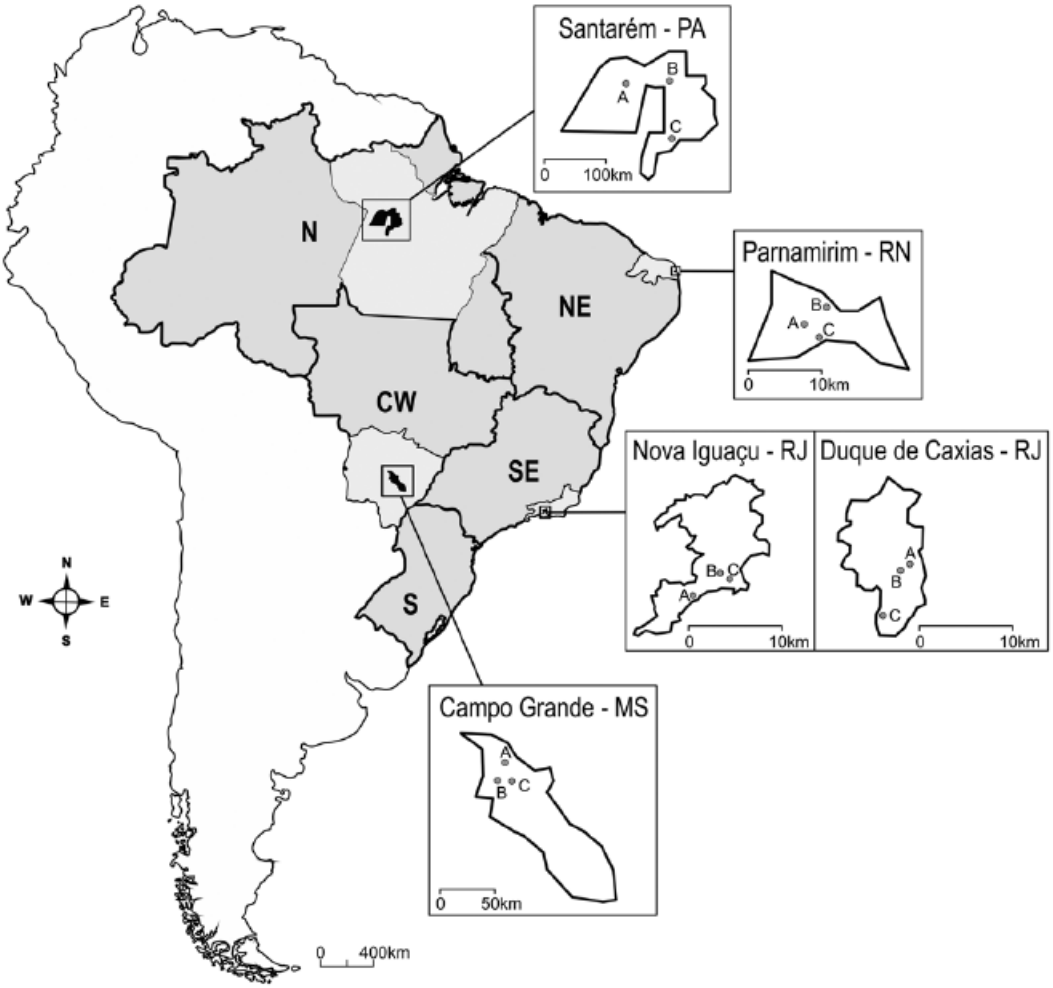

Figure 2.1: *Five Brazilian cities' locations and their neighborhoods (A, B, C), according to the figure extracted from* Codeço *et al. (2015).*

As we cited previously, inadequate sanitation service can develop related diseases (Brasil, 2013c), and provide a surrounding environment for mosquito development (WHO, 2020; WHO, n.d.[b]).

As activities aimed at disease control are not carried out continuously in Brazil (J. Silva and Machado, 2018; WHO, n.d.[a]), any outbreak risk identified through weather forecasting can be potentially increased when followed by the high percentage of households without sanitation services. Especially Santarém and Rio de Janeiro scenarios indicate a potential to increase the breeding sites' availability.

Recently, researchers found that 9 PM is adequate to control mosquitoes by using spraying interventions in Florida, where *Aedes aegypti* is abundant (Wilke *et al.*, 2023). However, basic sanitation control can provide an effective method to reduce *Aedes aegypti* population in Brazil, without insecticide techniques.

From Table 2.1, we focused on total population and services, even that *Aedes aegypti* mosquito is frequent in urban areas, due to the discussion about the difficulty of categorizing urban and rural areas.

Municipality	Year	Tpop	Upop	Twat	Uwat	Tsew	Usew	Twas
Campo Grande	2018	885711	98.66	100.00	100.00	82.71	83.83	99.00
Campo Grande	2012	805397	98.66	98.36	99.70	68.42	69.35	100.00
Campo Grande	2011	796252	98.66	98.20	99.54	61.28	62.11	98.81
Campo Grande	2010	786797	98.66	97.72	99.05	60.26	61.08	98.66
Campo Grande	2009	755107	98.66	98.32	99.66	59.35	60.16	98.66
Campo Grande/MS	09-12	785888	98.66	98.15	99.49	62.33	63.18	99.03
Santarém	2018	302667	73.25	51.29	70.02	4.19	5.72	73.25
Santarém	2012	284401	73.25	45.78	62.50	22.83	31.16	75.60
Santarém	2011	297040	73.25	41.44	56.58			73.25
Santarém	2010	294580	73.25	50.80	69.35			73.25
Santarém	2009	276665	70.96	55.09	77.63			74.57
Santarém/PA	09-12	288172	72.68	48.28	66.52	22.83	31.16	74.17
Duque de Caxias	2018	914383	99.66	84.50	84.79	43.07	43.22	99.90
Duque de Caxias	2012	867067	99.66	85.51	85.80	44.40	44.55	98.96
Duque de Caxias	2011	861158	99.66	85.41	85.70	44.35	44.50	99.29
Duque de Caxias	2010	855048	99.66	85.09	85.39	41.60	41.75	97.80
Duque de Caxias	2009	872762	99.60	70.92	71.21			100.00
Duque de Caxias/RJ	09-12	864009	99.64	81.73	82.02	43.45	43.60	99.01
Nova Iguaçu	2018	818875	98.91	93.15	94.18	45.03	45.53	97.06
Nova Iguaçu	2012	801746	98.91	93.97	95.01	45.08	45.58	85.00
Nova Iguaçu	2011	799047	98.91	93.70	93.70	44.99	45.49	95.00
Nova Iguaçu	2010	796257	98.91	92.09	92.10	42.00	42.46	100.00
Nova Iguaçu	2009	865089	100.00	69.43	69.43			
Nova Iguaçu/RJ	09-12	815535	99.18	87.30	87.56	44.02	44.51	93.33
Parnamirim	2018	255793	100.00	100.00	100.00	5.49	5.49	100.00
Parnamirim	2012	214199	100.00	98.77	98.77	0.89	0.89	100.00
Parnamirim	2011	208426	100.00	91.35	91.35	0.81	0.81	100.00
Parnamirim	2010	202456	100.00	86.17	86.17	0.71	0.71	100.00
Parnamirim	2009	184222	100.00	90.13	90.13	0.65	0.65	100.00
Parnamirim/RN	09-12	202326	100.00	91.61	91.61	0.77	0.77	100.00

Table 2.1: *Tpop: Total population; Upop: Urban population percentage; Twat: Percentage of the total population with water supply; Uwat: Percentage of urban population with water supply; Tsew: Percentage of the total population with sewerage service; Usew: Percentage of urban population with sewerage service; Twas: Percentage of the total population with solid waste collection. We calculate the percentages according to SNIS data (SNSA, n.d.). The lines which include averages among the 2009 and 2012 periods carry the fuzzy system entries.*

We perceived that the most inhabited cities of Brazil often have a higher percentage of the urban population supplied with basic sanitation than rural ones, once the total population percentage is lower than that for urban (SNSA, n.d.).

Indeed, an important question is how to classify urban areas. This classification helps in understanding the geography of countries and mainly in directing funding for public policies (IBGE, 2017).

2.2 Urban versus rural zones

The relationship between urban and rural places shall consider the connections among rural, peri-urban, and urban zones, which can be represented by flows of people, material goods, resources, work, services, technologies, et cetera (IBGE, 2017).

Instead of a large percentage of the served population in each city, some studies indicate that the urban population is about to double by 2050 (IBGE, 2017). It represents a trend where several rural areas can transform into urban ones. Thus, we expect that companies supply the demand for sanitation services, following this evolution.

Often government agencies are not able to follow a quickly increasing amount of urban population (IBGE, 2017). Besides, official limits are subject to fiscal objectives from the city hall, which implies that the definitions are obtained through a selection of aspects, and can hinder public policies and investments (IBGE, 2017).

Moreover, the urban-rural classification can misrepresent that an urban area is well-served. Consequently, the municipality could be considered as a reference, even if there is a rural area classified conveniently and needing improvements.

Indeed, one question is how to classify urban-rural areas. This categorization helps in understanding the geography of countries, and mainly in directing funding for public policies and actions.

Usually, the procedure followed for categorizing areas includes some management and classification techniques (Endlich, 2010 apud IBGE, 2017). We highlight aspects such as administrative or political-administrative delimitation, demographic density, the economic occupation of the population, and lifestyle (Bernardelli, 2010 apud IBGE, 2017).

Plus, another challenge to considering a portion urban of the population is that we can find spaces inside an urban zone that seem rural, and vice-versa, which suggests considering how they are connected and overlapped (Castree *et al.*, 2013 apud IBGE, 2017). The criteria are criticized for not including a closer dimension to reality, capturing it partially (IBGE, 2017).

International agencies, such as WHO and the United Nations, use different approaches for classifying urban-rural areas, which depend on the characteristics of the countries (IBGE, 2017). However, a proposal mixing rural and urban, as the “continuum” sight, also has problems (Rosa and Ferreira, 2010 apud IBGE, 2017). If we recognize those areas as isolated or continued, it is a partial approximation of reality (IBGE, 2017).

Society needs parameters to statistically categorize and evaluate the areas to guide and promote public policies (IBGE, 2017). Both England and Wales and the USA characterized around 19% of the rural population in the country (IBGE, 2017). Differentiating criteria in Brazil can assign a larger rural population than the country could have. Often, waste collection is carried out in rural areas on a small scale, while the percentages of inadequate water supply and sewage treatment are high.

The decree law no. 311/1938 associated urban and rural zones, pointing out some differences between city and village, which previously did not exist (IBGE, 2017). This

decree-law presented a political-administrative definition to identify an urban area that was the target of much criticism (IBGE, 2017).

The territorial manual edited by IBGE maintained the provisions of that decree law. It established that the municipality defines the limits of the urban area and, by exclusion, the rural area (IBGE, 2017).

Specifically, the IBGE territorial basis manual considers the legal reference for the definition of urban and rural areas. The first area is internal to the urban perimeter, created through municipal law, whether for tax purposes or urban planning. For cities or villages where there is no legislation regulating these areas, a census collection can guide the urban perimeter (IBGE, 2014).

The rural area is the one not included in the urban perimeter by municipal law (IBGE, 2014). It is usually a land destined for rustic land use, with large tracts of land and low housing density (IBGE, 2014). They include fields, forests, crops, and pastures (IBGE, 2014).

Urbanization tends to reduce the natural permeability of the soil (Brasil, 2013c). It increases surface runoff, reduces underground flow, and decreases evapotranspiration (Brasil, 2013c).

For the statistical approach, IBGE works with a particular classification which includes transition groups between urban and rural areas. The diversity of territorial aspects guided IBGE to use more than one legal and political-administrative division to classify the areas (IBGE, 2017). In this context, IBGE established census sectors, according to the morphological aspects of the territory (IBGE, 2017).

Therefore, IBGE considers the number of households and the distance between residences inside a sector (IBGE, 2017). There are eight sectors, from which those contained in the urban perimeter are urban areas, non-urbanized areas, and isolated urban areas (IBGE, 2017). On the other hand, those outside are a rural agglomeration of urban extension, thorp, nucleus, village, and rural area (IBGE, 2017).

The rural agglomeration of urban extension can be a potential area for spreading once it constitutes an occupation with urban characteristics, near the urban perimeter (IBGE, 2014), besides human populations becoming ever more connected (Kraemer *et al.*, 2019).

We can access urban occupation by population density because it is related to built areas (IBGE, 2017). In this way, possible problems with sanitation and breeding sites are encouraged.

Consequently, we realize that it is important to consider the population to measure the breeding site capacity in a municipality.

Usually, our FRBS evaluates an approximate reality of the total population, which means rural and urban groups compose the inputs together. The urban population approach is isolated only in one fuzzy system input. Therefore, we apply the percentage of the total population served for the rules.

2.3 System Components

A fuzzy inference system uses fuzzy set theory to map inputs to output. It has three components (Pedrycz and Gomide, 2007):

- Dictionary: it defines the fuzzy sets of linguistic variables. Membership values express the degrees to which each element of a universe is compatible with the properties distinctive to the class. We define variable inputs and outputs.
- Rules basis: they establish a relationship among variables.
- Inference method: it determines the system output according to the given inputs.

Eventually, we add a component called defuzzification: it transforms the fuzzy output into a real number or a classic set.

2.3.1 Input variables and Sets

The system inputs involve the percentage of the urban population, as well as the percentage of served population by water supply, frequent solid waste collection, and sanitary sewerage.

To define a fuzzy (sub)set, the range of the characteristic function - found in classical mathematics, whose set is $\{0, 1\}$ - is expanded to the interval $[0, 1]$ (Barros and R. Bassanezi, 2006; Pedrycz and Gomide, 2007).

Starting from U a classical universe set, a fuzzy (sub)set A of U is defined as the application:

$$\varphi_A \ : \ U \rightarrow [0, 1], \tag{2.1}$$

where φ_A is a pre-fixed function called the membership function of the fuzzy subset A.

In an attempt to quantify the degree of membership with which the element x of the universe U is in the fuzzy set A, the membership value $\varphi_A(x) \in [0, 1]$ is used, where $\varphi_A(x) = 0$ and $\varphi_A(x) = 1$ represent non-membership and total membership to the set.

We observed that A is composed of elements x belonging to a classical set U and which have a membership value associated with A, represented by $\varphi_A(x)$. According to the literature, the membership function φ_A can be conventionally denoted by just A, with the notation $\varphi_A(x)$ becoming just $A(x)$ (Barros and R. Bassanezi, 2006).

Given the fuzzy subset A and $\alpha \in [0, 1]$, the α-level of A is the classical subset of U of the form:

$$[A]^\alpha = \{x \in U \ : \ \varphi_A(x) \geq \alpha\}; \ 0 < \alpha \leq 1. \tag{2.2}$$

The establishment of α-levels helps in the relationship between different subsets. A fuzzy subset is formed by elements that can be represented by degrees, such that an element x of U belongs to the given class if it presents a degree of membership with a value greater

than a given level $\alpha \in [0, 1]$, which defines the class. Therefore, the concept is necessary for cases in which the sets are not classical, that is, that have a transition from membership to non-membership gradually, and not abruptly (Castanho, 2005).

From this definition, a fuzzy number can be characterized. According to (Barros and R. Bassanezi, 2006), a fuzzy subset A is a fuzzy number if A is defined in the universe set of real numbers $\mathbb{R}$, and satisfies the following conditions:

i) All α-levels of A are non-empty, where $0 \leq \alpha \leq 1$;

ii) All α-levels of A are closed intervals of $\mathbb{R}$;

iii) $\overline{\text{supp}}(A) = \{x \in \mathbb{R} \, : \, A(x) > 0\}$ is limited.

Thus, $[A]^\alpha$ is a closed and non-empty interval. In particular, one can represent the α-levels of the number A in the form $[A]^\alpha = [a_I^\alpha, \, a_S^\alpha]$.

Furthermore, every real number is a fuzzy number in which its membership function coincides with its characteristic function (Barros and R. Bassanezi, 2006).

The fuzzy numbers that will be used later are classified as triangular - whose membership function has the form of a triangle based on the interval $[a, b]$ and a single vertex that does not belong to the basis, the point $(u, 1)$, where $a, \ b, \ u \ \in \mathbb{R}$, with $a \leq u \leq b$ defined as:

$$A(x) = \begin{cases} 0, & \text{se } x \leq a \\ \frac{x-a}{u-a}, & \text{se } a < x \leq u \\ \frac{x-b}{u-b}, & \text{se } u < x \leq b \\ 0, & \text{se } x > b \, . \end{cases}$$

Therefore, with the numbers a, b, u the triangular fuzzy number A is defined, denoted by the triple $(a; u; b)$, so that the representation of the α-levels is of the form

$$[a_I, \ a_S] = [(u - a)\alpha \ + \ a, \ (u - b)\alpha \ + \ b], \ \forall \ \alpha \ \in \ [0, 1].$$

Now, as the possibility of $a \neq b$ exists, it is possible that the fuzzy number is not symmetric.

For our system, the state variables are triangle fuzzy numbers, which we selected according to Section 2.1, and categorized them in subsets.

For example, three among four inputs work on 0 to 100% percentage of the population served, with a gradual membership degree, where 100% is ideal.

i) Percentage of urban population (SNSA, n.d.):

Previously, we noticed that *Aedes aegypti* breeding sites are spread in urban regions.

We set this variable as Few [0 0 100] or Many [0 100 100], as the Figure 2.2.

ii) Percentage of the served population by frequents solid waste collection services (SNSA, n.d.):

We set this variable as Defective [0 0 100] or Ideal [0 100 100], as the Figure 2.3.

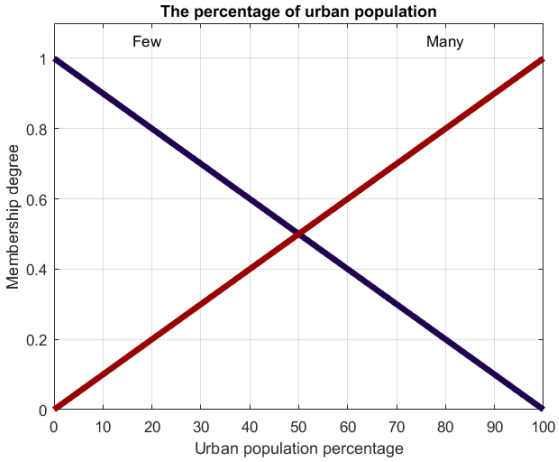

Figure 2.2: *Fuzzy set for the input about percentage of urban population, which is blue for few and red for many.*

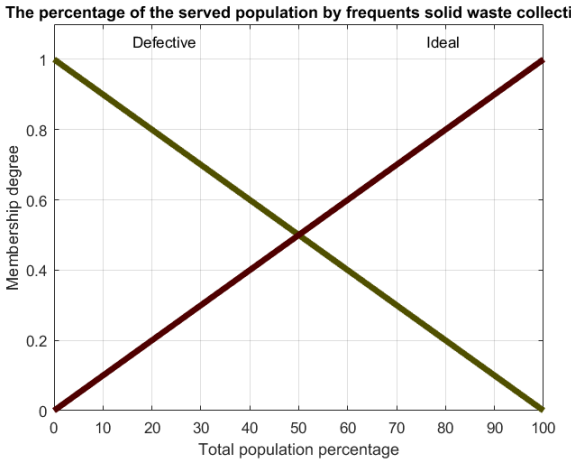

Figure 2.3: *Fuzzy set for the input about percentage of the served population by frequents solid waste collection services, which is green for defective and brown for ideal.*

iii) Percentage of the served population by sanitary sewerage services (SNSA, n.d.):

We set this variable for the percentage of the served population by sanitary sewerage as Defective [0 0 100] or Ideal [0 100 100], as the Figure 2.4.

iv) Percentage of the served population by water supply services (SNSA, n.d.):

We set this variable as Defective [0 0 100] or Ideal [0 100 100], as the Figure 2.5.

Remark: Periods of rain absence are not considered as a system entry once both cities (Campo Grande (SPARK, n.d.[a]), Duque de Caxias (SPARK, n.d.[b]), Nova Iguaçu (SPARK, n.d.[c]), Parnamirim (SPARK, n.d.[d]), and Santarém (ADAMS *et al.*, 2006; SPARK, n.d.[e])) present around 6 months of the dry season.

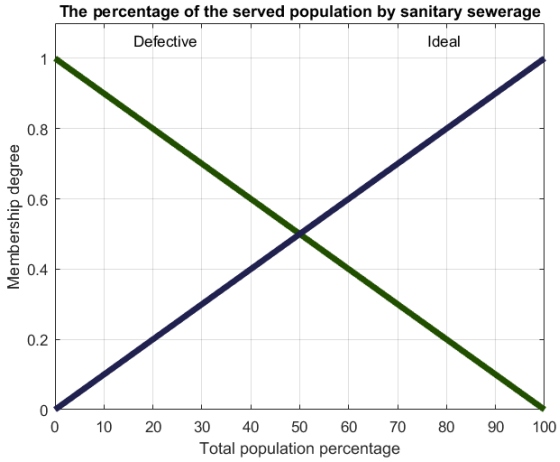

Figure 2.4: *Fuzzy set for the input about percentage of the served population by sanitary sewerage services, which is green for defective and blue for ideal.*

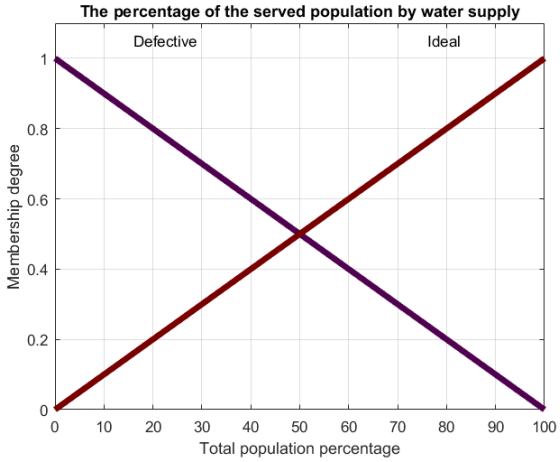

Figure 2.5: *Fuzzy set for the input about the served population by water supply services, which is purple for defective and red for ideal.*

2.3.2 Rules Basis

The system considers that water supply and solid waste are the main characteristics of sanitation associated with *Aedes aegypti* development, followed by sewerage service and urban population percentage.

There are 16 rules to build the inference, where 4 inputs are combined, according to Table 2.2, and produce one output.

2.3.3 System structure: Fuzzy Relation and Compositional Inference

We built the system as 2.6. It used Mamdani's fuzzy inference method and the center of gravity as the defuzzification technique.

A fuzzy relation R is defined by the membership function $\varphi_R = R : U_1 \times U_2 \times \cdots \times U_n \rightarrow$

Rule	Urban Population	Water Supply	Solid Waste	Sewerage	Sanitation Power
1	Few	Defective	Defective	Defective	Precarious
2	Few	Defective	Defective	Ideal	Inadequate
3	Few	Defective	Ideal	Defective	Adequate
4	Few	Defective	Ideal	Ideal	Adequate
5	Few	Ideal	Defective	Defective	Adequate
6	Few	Ideal	Defective	Ideal	Adequate
7	Few	Ideal	Ideal	Defective	Ideal
8	Few	Ideal	Ideal	Ideal	Ideal
9	Many	Defective	Defective	Defective	Precarious
10	Many	Defective	Defective	Ideal	Precarious
11	Many	Defective	Ideal	Defective	Inadequate
12	Many	Defective	Ideal	Ideal	Adequate
13	Many	Ideal	Defective	Defective	Inadequate
14	Many	Ideal	Defective	Ideal	Adequate
15	Many	Ideal	Ideal	Defective	Adequate
16	Many	Ideal	Ideal	Ideal	Ideal

Table 2.2: *The rules of the fuzzy logic system.*

$[0, 1]$. Thus, the number $R(x_1, x_2, \cdots, x_n) \in [0, 1]$ indicates the degree to which the elements $x_i,\ i = 1, \cdots, n$ are related according to the relation R (Barros and R. Bassanezi, 2006).

Regarding the inference relationship, we can highlight the Cartesian product, which is used in controllers. We notice it is similar to the intersection. However, at the intersection, there are subsets of the same universe, while with the Cartesian product, it is possible to use different subsets. The Cartesian product of $A_1,\ A_2,\ \cdots,\ A_n$ belonging to $U_1, U_2, \cdots, U_n$ respectively, is represented by $A_1 \times A_2 \times \cdots \times A_n$, where the membership function is given by:

$$A_1 \times A_2 \times \cdots \times A_n(x_1, x_2, \cdots, x_n) = A_1(x_1) \wedge A_2(x_2) \wedge \cdots \wedge A_n(x_n),$$

where $\wedge$ is the minimum.

One way to obtain the relationship is by considering the compositional rule of inference. Given U and V two sets, $F(U)$ and $F(V)$ are the classes of fuzzy subsets of U and V, respectively, and R is a binary relation over the Cartesian $U \times V$. Then the relation R defines a functional of the form $R : F(U) \to F(V)$, in order to associate each element $A \in F(U)$ with the element $B \in F(V)$, through the equation

$$B(y) = (A \circ R)(y) = A(x) \circ R(x, y) = \sup_{x \in U}[A(x) \triangle R(x, y)],$$

where $\triangle$ represents any t-norm.

A t-norm is an operator $\triangle : [0, 1] \times [0, 1] \to [0, 1],\ \triangle(x, y) = x \triangle y$ that satisfies the following conditions:

i) Neutral element: $\triangle(1, x) = 1 \triangle x = x$;

ii) Commutative: $\triangle(x, y) = x \triangle y = y \triangle x = \triangle(y, x)$;

iii) Associative: $x \triangle (y \triangle z) = (x \triangle y) \triangle z$;

iv) Monotonicity: if $x \leq u$ and $y \leq v$, then $x \triangle y \leq u \triangle v$.

Note that t-norms extend the operator $\wedge$, which models the connective "and" in classical theory. There are still t-connorms, which model the connective "ou" (Barros and R. Bassanezi, 2006), and will be used in the compositional rule, to calculate the supreme .

The t-connorms, in turn, are operators $\triangledown : [0,1] \times [0,1] \to [0,1]$, $\triangledown(x,y) = x \triangledown y$ that satisfy the following conditions:

i) Neutral element: $\triangledown(0,x) = 0 \triangledown x = x$;

ii) Commutative: $\triangledown(x,y) = x \triangledown y = y \triangledown x = \triangledown(y,x)$;

iii) Associative: $x \triangledown (y \triangledown z) = (x \triangledown y) \triangledown z$;

iv) Monotonicity: if $x \leq u$ and $y \leq v$, then $x \triangledown y \leq u \triangledown v$.

The term linguistic variable refers to a variable in which the assumed values are fuzzy subsets, that is, it is a noun with values that correspond to adjectives, which in turn are represented by fuzzy sets (Barros and R. Bassanezi, 2006).

Linguistic terms serve to transcribe knowledge in the form of a collection of rules. In this way, the rule includes possible combinations between input and output variables, which builds a collection of propositions (B. Bassanezi *et al.*, 2011) .

In agreement with Barros and R. Bassanezi (2006), it can be mentioned that there is the elaboration of the ruled basis that mathematically represents the information available in the knowledge basis of the fuzzy system, created considering the selected linguistic variables. Given an FRBS, each input is associated with one or more outputs through the controller - capable of approximating continuous functions -, the system being a function of $\mathbb{R}^n$ in $\mathbb{R}^m$ constructed in a way that uses the membership functions of each fuzzy set involved in the process, obtained from among some possibilities, through curve adjustments and intuition.

The classical relationship between two elements or sets indicates whether there is an association between them, while in the fuzzy relationship, in addition to indicating the existence, it also indicates the degree, which provides an adequate approximation when displaying an extensive rule basis, which brings together propositions of the form: if 'state' then 'response' Barros and R. Bassanezi, 2006. In this way, each state and each response comes from the adjective values that the linguistic variables assume, represented by the fuzzy sets Barros and R. Bassanezi, 2006, with each fuzzy proposition being assigned a name R_i, $i = 1, \cdots, r$, with r being the number of rules.

From the arrangement of the data, we identify the important variables in the process, both input and output from the system, as well as the intervals to classify their state in linguistic terms. With this, the terms are translated by a membership function, which characterizes a fuzzy subset, and in this way, the phase called fuzzification is obtained. At this stage the discussion through literature or specialists is important.

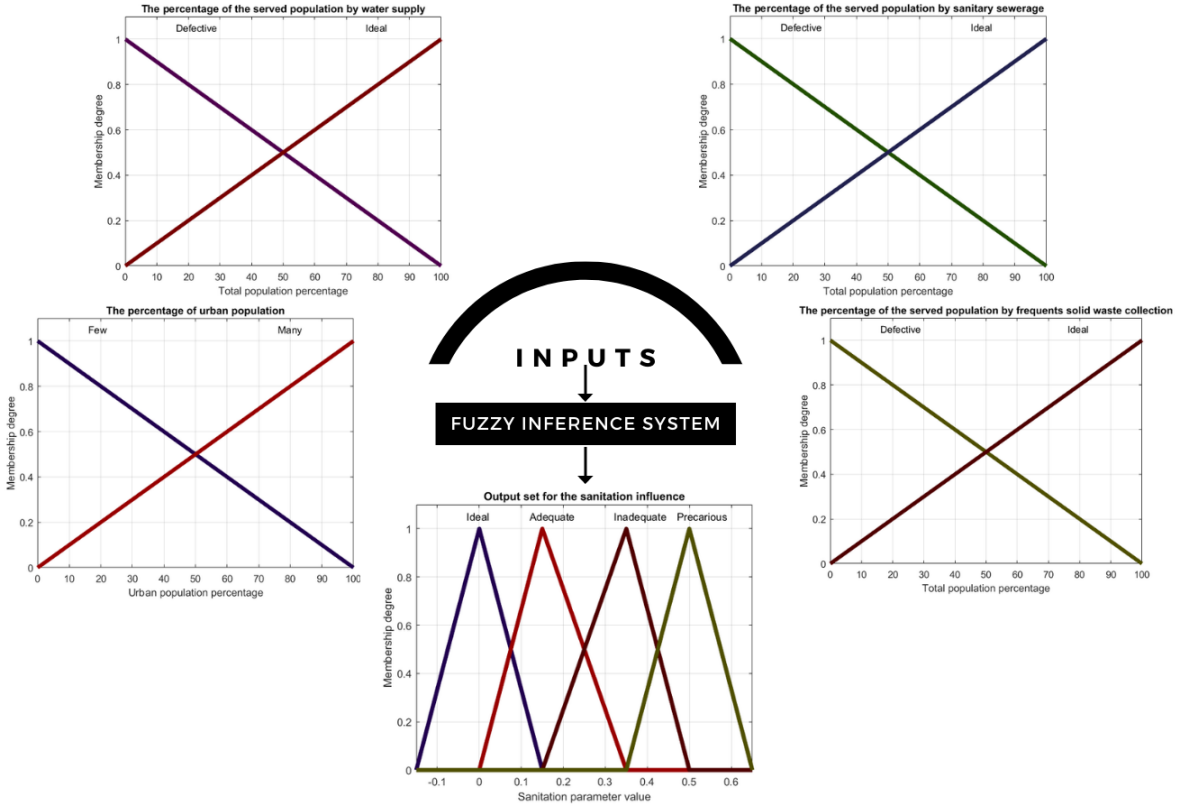

Figure 2.6: *Fuzzy logic system structure.*

Then, a fuzzy inference is used, created to mathematically translate each fuzzy proposition, among which the Mamdani method stands out. The purpose of inference methods is to calculate the response variable (output) of the FRBS based on the values of the input variables, as with the values of the degrees of relevance of the input variables it is possible to find the value of the degree of relevance of the response variable. Finally, a defuzzification method is performed, which consists of a process that makes it possible to represent the fuzzy set by a real number.

In effect, after fuzzification and elaboration of the rule basis, with rules of the form:

If x_1 is A_1 and x_2 is A_2 and $\cdots$ and x_n is A_n, then u_1 is B_1 and u_2 is B_2 and $\cdots$ and u_m is B_m,

Mamdani's inference method was used, in addition to the area center method for defuzzification.

The inference method allows mathematical translating of fuzzy propositions, and Mamdani's method proposes a binary fuzzy relation which means that for each rule R_i of the rule basis, the conditional "If x is A_i, then u is B_i" be modeled by the minimum, since the t-norm $\wedge$ is adopted for the connective "and".

Thus, we have the fuzzy relation M, a subset of the Cartesian $X \times U$, with membership

function:

$$M(x,u) = \max_{1\leq i\leq r}(R_i(x,u)) = \max_{1\leq i\leq r}[A_i(x) \wedge B_i(u)] \tag{2.3}$$

Note the use of the *max-min* composition, which becomes the union after making the intersection, that is, the union of the partial outputs of each rule is used.

Mamdani's inference method has been discussed in the literature and is considered to have good results (Barros and R. Bassanezi, 2006; Bassani, 2016). In this method, we use the t-norm operator, based on the t-norm of the minimum, which refers to the use of the connective "and".

Given a rule basis system, where $A = A_1 \times A_2$, the following rules and inference structure are obtained for two inputs and one output (Barros and R. Bassanezi, 2006; Bassani, 2016):

$$\text{If } x_1 \text{ is } A_{11} \text{ and } x_2 \text{ is } A_{12}, \text{ then } u \text{ is } B_1$$

Or

$$\text{If } x_1 \text{ is } A_{21} \text{ and } x_2 \text{ is } A_{22}, \text{ then } u \text{ is } B_2$$

So when considering the triple $t = (x_1, x_2, u)$, we have:

$$M(t) = \{A_{11}(x_1) \wedge A_{12}(x_2) \wedge B_1(u)\} \vee \{A_{21}(x_1) \wedge A_{22}(x_2) \wedge B_2(u)\} \tag{2.4}$$

$$= \max\{A_{11}(x_1) \wedge A_{12}(x_2) \wedge B_1(u),\ A_{21}(x_1) \wedge A_{22}(x_2) \wedge B_2(u)\} \tag{2.5}$$

Obtaining partial outputs through inference, the union is performed and the final output is obtained. In general, this output is a surface, and if it is necessary to translate it into a crisp value, we process a defuzzification, which is possible with the center of area method, among others.

After the activation of each input set A_i, the minimum is performed, with $i = 1, 2$ according to the rule basis. The resulting value represents membership in the partial output set B_i. After obtaining activation in each partial output set through each rule, these B_i sets are joined to compose the output set.

With computational tools, the center of the area can be obtained through a sum, given a significant number of surface partitions, under a finite domain,

$$D(B) = \frac{\sum_{i=0}^{n} u_i B(u_i)}{\sum_{i=0}^{n} B(u_i)}\,. \tag{2.6}$$

Furthermore, it may be favorable to use integral calculus, in a continuous case.

$$D(B) = \frac{\int_{\mathbb{R}} uB(u)du}{\int_{\mathbb{R}} B(u)du} \tag{2.7}$$

2.3.4 Output set

The fuzzy system provides as output a number. It represents the sanitation influence for each city.

We considered this variable with four states, as Ideal [-0.15 0 0.15], Adequate [0 0.15 0.35], Inadequate [0.15 0.35 0.5], or Precarious [0.35 0.5 0.65], as the Figure 2.7.

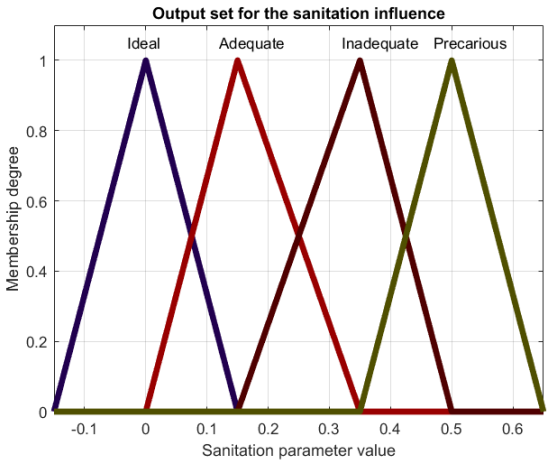

Figure 2.7: *Fuzzy set for the output about sanitation influence, which is green for precarious, brown for inadequate, red for adequate, and blue for ideal.*

A value closer to 0 means that the sanitation panorama of the city is ideal, and the *Aedes aegypti* population development is limited, according to lower precipitation periods, i.e., water sources' lack.

Unlike Campo Grande/MS, both Santarém/PA, Parnamirim/RN, and Rio de Janeiro's cities have a higher parameter α_c, as we will calculate later.

2.3.5 Active rules for each city

The system output feeds the parameter α_c, which aims to quantify the contribution attributed to the basic sanitation of the city on the maintenance of breeding sites of *Aedes aegypti*, mainly during periods without rain.

We use data disclosed by the Brazilian institutions IBGE and SNIS (*Instituto Brasileiro de Geografia e Estatística* - Brazilian Institute of Geography and Statistics; *Sistema Nacional de Informações sobre Saneamento* - Brazilian sanitation information system). We present the data in Table 2.3, the lines that include averages among the 2009 and 2012 periods carry the fuzzy system inputs.

The system entries are fuzzy sets that involve four linguistic variables, which are the percentage of the urban population, as well as the percentage of served population by water supply, frequent solid waste collection, and sanitary sewerage.

We show the membership activation, that is, how the system works for two rules in Figure 2.8. Mamdani's inference takes the minimum among the *if* inputs and combines them as a membership for the consequence set "then". The maximum works to compose an output set through the union of the rules.

City	Year	Tpop	Upop	Twat	Uwat	Tsew	Usew	Twas	α_c
Campo Grande	09-12	785888	98.66	98.15	99.49	62.33	63.18	99.03	0.086
Santarém	09-12	288172	72.68	48.28	66.52	22.83	31.16	74.17	0.250
Duque de Caxias	09-12	864009	99.64	81.73	82.02	43.45	43.60	99.01	0.142
Nova Iguaçu	09-12	815535	99.18	87.30	87.56	44.02	44.51	93.33	0.147
Parnamirim	09-12	202326	100.00	91.61	91.61	0.77	0.77	100.00	0.182

Table 2.3: *Percentages of basic sanitation indicators according to an average of 2009-2012 period. *Legend for the Table; Tpop: Total population; Upop: Urban population percentage; Twat: Percentage of the total population with water supply; Uwat: Percentage of urban population with water supply; Tsew: Percentage of the total population with sewerage service; Usew: Percentage of urban population with sewerage service; Twas: Percentage of the total population with solid waste collection; Sanitation parameter: output value for the city's sanitation influence.*

After the activation of each input set, the minimum is performed according to the rule basis. The resulting value represents membership in the partial output set. After obtaining activation in each partial output set through each rule, these sets are joined to compose the output set.

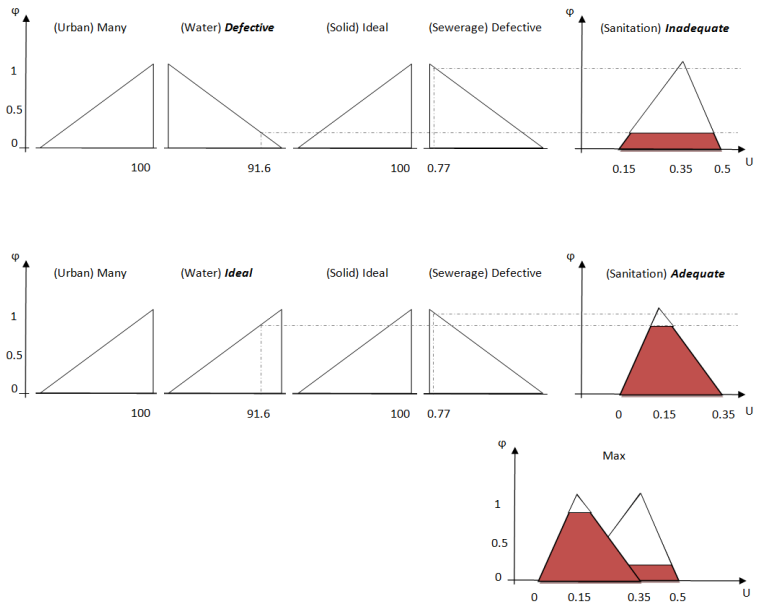

Figure 2.8: *Rules 11 and 15 are active for Parnamirim.*

Obviously, we have 16 rule actives for each city, as we see in the following Figures (2.9, 2.10, 2.11,2.12,2.13).

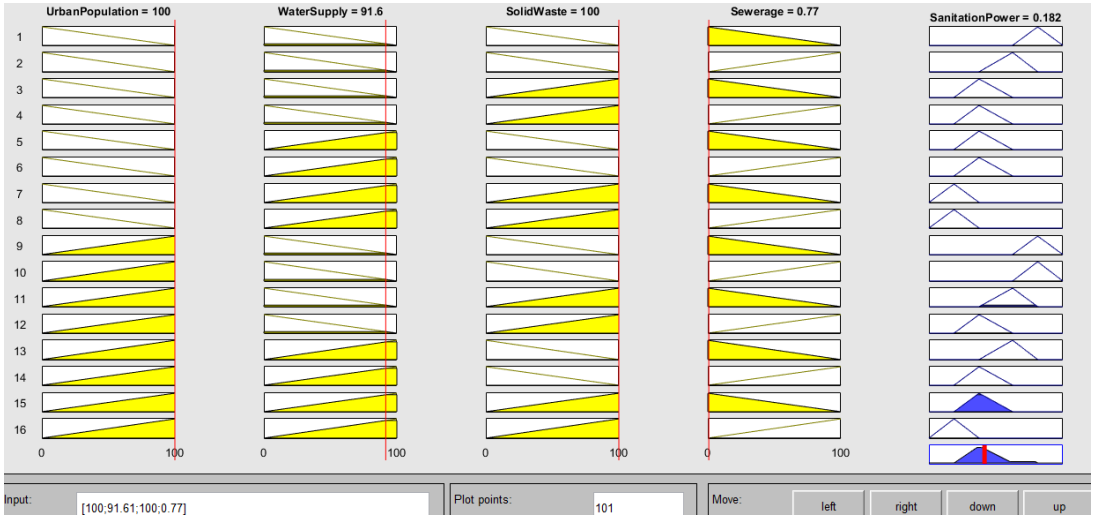

Figure 2.9: *Fuzzy Rule-Based System output for Parnamirim/RN, with inputs [100 91.61 100 0.77].*

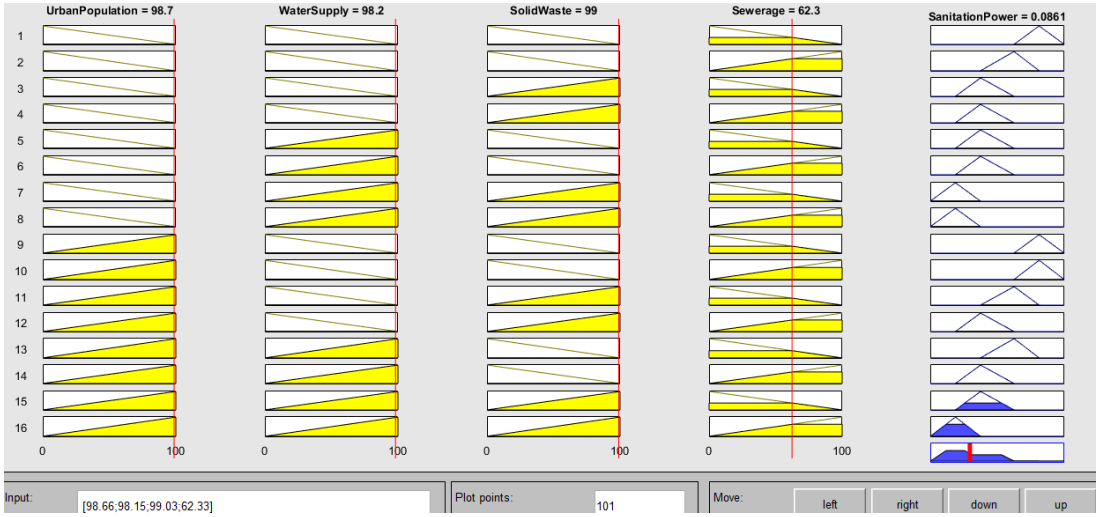

Figure 2.10: *Fuzzy Rule-Based System output for Campo Grande/MS, with inputs [98.66 98.15 99.03 62.33].*

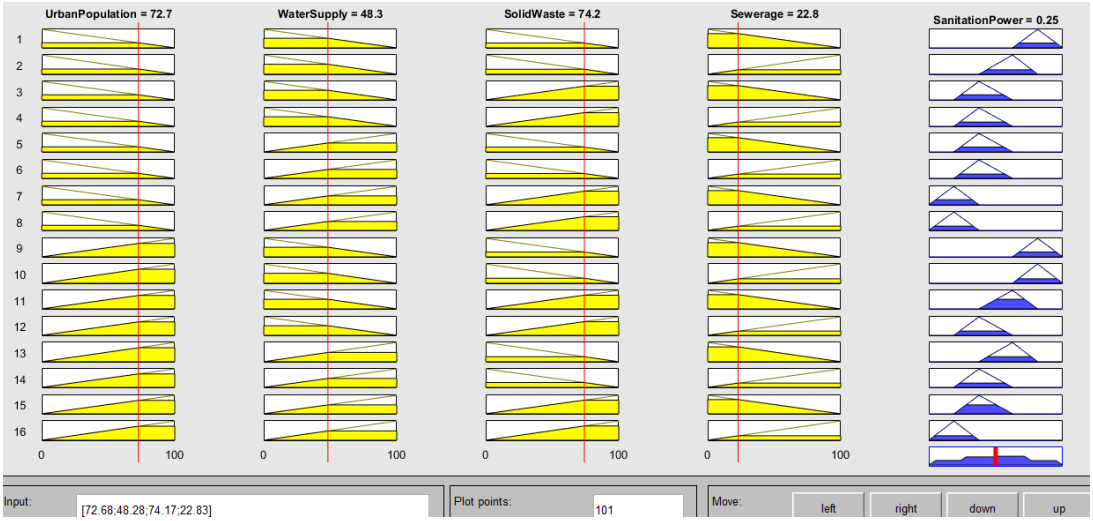

Figure 2.11: *Fuzzy Rule-Based System output for Santarém/PA, with inputs [72.68 48.28 74.17 22.83].*

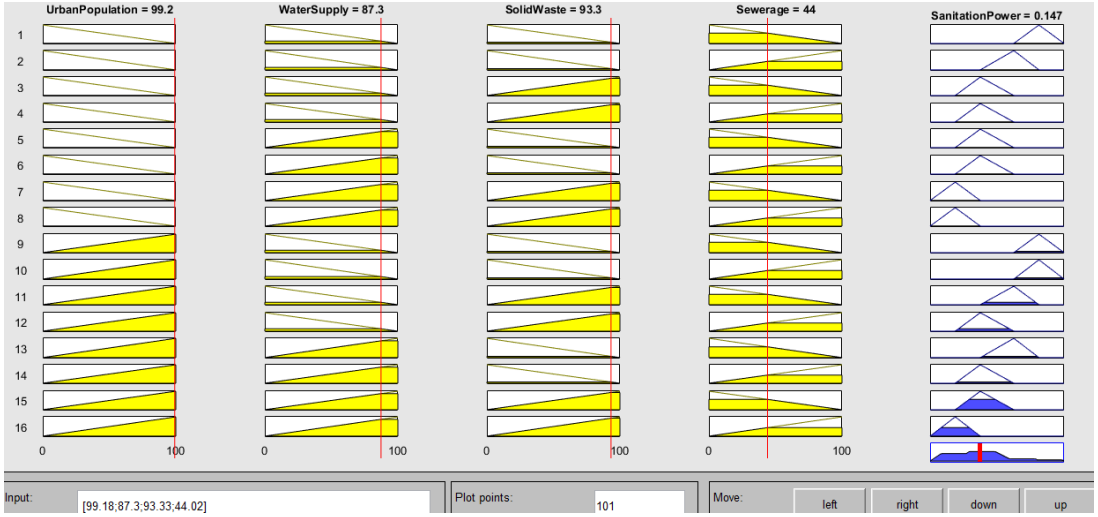

Figure 2.12: *Fuzzy Rule-Based System output for Nova Iguaçu/RJ, with inputs [99.18 87.3 93.33 44.02].*

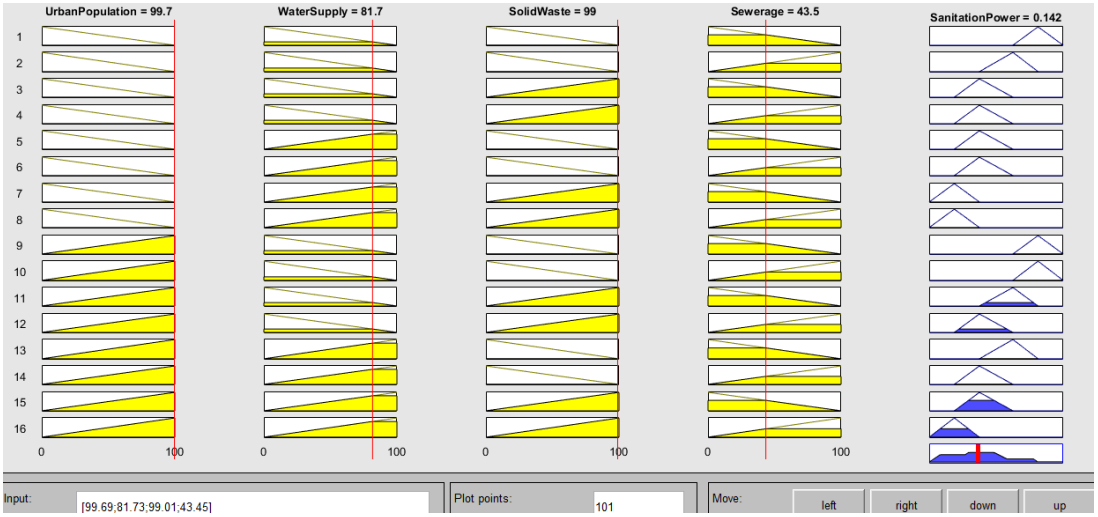

Figure 2.13: *Fuzzy Rule-Based System output for Duque de Caxias/RJ, with inputs [99.69 81.73 99.01 43.45].*

Chapter 3

Mosquito Population Dynamics

Mosquitoes are insects belonging to the order *Diptera* and family *Culicidae* and their evolution allowed various survival strategies developed by them, in both tropical and temperate regions (Diniz, Albuquerque, *et al.*, 2017). Among the approximately 3500 species, about 300 have medical and veterinary importance (Diniz, Albuquerque, *et al.*, 2017).

Some characteristics of *Aedes aegypti* and the remaining mosquito species are significantly different. Dengue, Zyka, and Yellow fever are spread by the adult female *Aedes aegypti*, which are important viral diseases transmitted by arthropods (Gould and Solomon, 2008).

Diapause and quiescence are two different categories of dormancy. Nevertheless, the literature often assumes them as synonyms (DL Denlinger and Armbruster, 2014; Diniz, Albuquerque, *et al.*, 2017; H. Silva and I. Silva, 1999). In the embryonic phase, both biological devices allow the inhibition of larval hatching (Diniz, Albuquerque, *et al.*, 2017). However, during the larval and adult stages, the dormancy is caused only by the diapause device (Diniz, Albuquerque, *et al.*, 2017).

With respect to diapause, the arrested development starts in any stage of insect development according to an environmentally preprogrammed period (DL Denlinger and Armbruster, 2014). It is hormonally programmed and is not immediately terminated due to favorable conditions, because it happens with a fixed period of latency, which needs to be completed, and from this, there exists the continuity of the development (DL Denlinger and Armbruster, 2014). On the other hand, quiescence is a dormancy caused due to unfavorable environmental conditions and immediately terminated if favorable (DL Denlinger and Armbruster, 2014). The embryonic quiescence contributes to the maintenance and the spread of the *Aedes aegypti* population (Diniz, Albuquerque, *et al.*, 2017).

3.1 General concepts about *Aedes aegypti*

The egg of *Aedes aegypti* measures approximately 1 mm in length (Vieira, 2008). The female deposits it on the inner walls of breeding sites, close to the water surface

(Vieira, 2008). It means that an *Aedes aegypti* egg, which is probably quiescent, is an offspring deposited above the water surface line. It can be prompted immediately with immersion into the water (Schaeffer *et al.*, 2007; Yusoff *et al.*, 2012a), and (Denlinger *et al.*, 2012) apud (Diniz, Albuquerque, *et al.*, 2017)). As this species lacks diapause ability, it is restricted to subtropical and tropical habitats (DL Denlinger and Armbruster, 2014). For example, the *Aedes albopictus* diapause is programmed during a fixed interval of time, such that the submersion does not change the time that the eggs can respond to the water stimulus (Pener, 1992) apud (Diniz, Albuquerque, *et al.*, 2017).

Likewise, there is no diapause period for the *Aedes aegypti* larvae, pupae, or adult mosquitoes, and the dormancy period occurs only for eggs (Diniz, Albuquerque, *et al.*, 2017). When the egg dormancy period starts, the incubation period can extend up to 492 days (Vieira, 2008; H. Silva and I. Silva, 1999). This ability helps mosquito survival.

According to Rezende *et al.* (2008), the authors concluded that the formation of a serosal cuticle along with the eggshell provides desiccation resistance because they developed experiments using eggs 10, 11, 13, and 20 hours after egg-laying. The eggs were exposed to chlorine digestion, from which the thirteen-hour-eggs were able to resist the desiccation, while the ten and eleven-hour-eggs groups did not resist and disintegrated (Rezende *et al.*, 2008). After all, when the egg had a dry exposition till 20 hours after the egg-laying, it developed a desiccation resistance (Rezende *et al.*, 2008). Often, it happens around 15 hours later (Vieira, 2008).

To lay eggs, the female needs to mate with a male adult mosquito once in her lifetime (Schaeffer *et al.*, 2007; Laboissière, 2016). Starting each gonotrophic cycle, females need to find a blood meal host, and they posit eggs when the cycle ends (Schaeffer *et al.*, 2007). The oviposition relapses with a similar periodicity (Schaeffer *et al.*, 2007).

Another typical behavior is related to the water preference concerning the salinity of the oviposition site (Tracey, 2019). Researchers found that *Aedes aegypti* females prefer pure fresh water, with an aversion to sites with seawater (Tracey, 2019). The salinity is decisive for the larva since it starts to die when water is as little as 12.5% of seawater (Tracey, 2019).

Several biological characteristics of *Aedes aegypti* are in Table 3.1. Besides, the mathematical modeling for some biological experiments is in Sections 3.2 and 3.3. Using Table 3.1, we note a convergence in the reported number of days spent over the phases. However, the period length, and consequently the developmental rates, depend on environmental conditions. One of the main factors that produce this variability is temperature (Couret and Benedict, 2014), which we point out from a review of several papers (Beserra, Castro Jr., *et al.*, 2006; Beserra, Fernandes, *et al.*, 2009; Couret and Benedict, 2014; Farnesi *et al.*, 2009; Loncaric and Hackenberger, 2011; Otero *et al.*, 2006; Schaeffer *et al.*, 2007; H. Silva and I. Silva, 1999; Soares-Pinheiro *et al.*, 2017; H. Yang *et al.*, 2009; Yusoff *et al.*, 2012b; Yusoff *et al.*, 2012a).

Aedes aegypti eggs develop faster in warm temperatures until a certain threshold is reached since studies suggested that warmer temperatures harm dengue transmission and decrease the population (Nakhapakorn and Tripathi, 2005; Beserra, Fernandes, *et al.*, 2009; M. R. d. Silva, 2022). While temperatures are around 26°C, the *Aedes aegypti*

population development is faster, and dengue cases increase (Beserra, Fernandes, *et al.*, 2009; M. R. d. Silva, 2022). Until the egg accumulates enough heat, it remains quiescent over a long period (H. Silva and I. Silva, 1999), and the environmental condition provides a stimulus for the quiescent eggs to develop faster or slowly.

Characteristic	Information (unit and reference)
Lifetime egg waiting for the water	1 - 492 days (H. Silva and I. Silva, 1999).
Incubated eggs that will hatch to larva	1 - 85 days (H. Silva and I. Silva, 1999).
Larval period	5† - 21 days (Beserra, Castro Jr., *et al.*, 2006).
Pupal period	1 - 7 days (Beserra, Castro Jr., *et al.*, 2006).
Larval and pupal	Average of 53 days with a final time of 103 days (H. Yang *et al.*, 2009). Another study reported a range of 6† - 28 days (Beserra, Castro Jr., *et al.*, 2006).
Life time adult female mosquito	1 - 63 days (H. Silva and I. Silva, 1999).
Eggs total/female	Range of [3.4, 610.6], it varies with temperature (Beserra, Fernandes, *et al.*, 2009).
Mosquito bite	Adult female (H. Yang, 2014).
Egg quiescence	Present (Diniz, Albuquerque, *et al.*, 2017).
Other dormancy	Absent (Diniz, Albuquerque, *et al.*, 2017).
Number of annual generations	It used to be above 20 generations, and up to 38 generations under laboratory conditions (Beserra, Fernandes, *et al.*, 2009).

† The lower threshold does not consider natural death.

Table 3.1: *Characteristics of Aedes aegypti (time period counted by day).*

Results found in the literature and reported through laboratory experiments indicate a wide range of time spent at the aquatic development stage. From Beserra, Castro Jr., *et al.* (2006) they evaluate the development over 5 temperatures (18, 22, 26, 30, and 34°C with similar water temperatures), while H. Silva and I. Silva (1999) used only one fixed temperature (28±1°C). By doing this, the studies obtained a similar lower threshold for the larval and pupal period, around 6 and 7 days (Beserra, Castro Jr., *et al.*, 2006; H. Silva and I. Silva, 1999; Yusoff *et al.*, 2012b). Plus, for adult females, the maximum age reported is also similar, around 56.2 ± 2.38 and 57.8 ± 4.85 (Beserra, Castro Jr., *et al.*, 2006; H. Silva and I. Silva, 1999). However, we found a report that one female laid 752 eggs over 72 days in 1960 (Christophers, 1960).

In breeding site conditions, we assume the water stimuli are necessary for the egg hatching (Chen *et al.*, 2007), the larva or pupa development, and the female oviposition since females lay eggs in standing water (Tracey, 2019) and water from storm drains (Chen *et al.*, 2007).

Besides, the life cycle of *Aedes aegypti* is short, and natural death is different during the development stages. We define the mortality rate as a function that determines individuals who died during each time step. In general, it depends on the temperature (H. Silva and I. Silva, 1999; H. Yang *et al.*, 2009).

According to the literature review, we assumed that the daily mean temperature and the precipitation are the main environmental variables that stimulate *Aedes aegypti* development in tropical or subtropical regions (Lega *et al.*, 2017; Loncaric and Hackenberger, 2011; CW Morin *et al.*, 2015; Rossi, Lopez, *et al.*, 2015; Yusoff *et al.*, 2012b; Yusoff *et al.*, 2012a). The temperature dependence is motivated by the fluctuations along the year and its effect on *Aedes aegypti* biology. After all, it influences insect physiology and behavior (Loncaric and Hackenberger, 2011; Siraj *et al.*, 2017; M. R. d. Silva, 2022; M. R. d. Silva *et al.*, 2022).

We will study the influence of temperature and precipitation during the population dynamics through numerical simulations, then we set a table for precipitation and temperature fixed values. Also, the population dynamics of a municipality will be estimated according to its historical weather data and sanitation panorama, to compare with collected data. There are several studies using temperature and precipitation to forecast the dynamics of the mosquito population. Nevertheless, we set a quiescent stage and a basic sanitation parameter to organize the population development, and to construct the transition and mortality functions depending on the egg age and the weather data during previous days.

Through our model, we are building functions for understanding *Ae. aegypti* population development. For this purpose, we established that the oviposition, transition, and mortality functions always depend on the daily mean temperature. And often the individual age, the accumulated temperature, and the daily or accumulated precipitation. The daily mean temperature threshold is 6.8 to 36°C, and it incorporates all cities during the period for which we have surveillance data, as well as most Brazilian municipalities.

The temperature and precipitation influence, together with the quiescence and sanitation approach, will help us to verify the interference of the weather and basic sanitation for the development and maintenance of the population.

From table 3.1, similar to Maimusa *et al.* (2016) we got a minimum of 8.9 days for females to emerge from the egg. This occurs if the temperature and humidity are favorable to this emergence (Maimusa *et al.*, 2016). To account for the minimum periods of our study, we got a minimum of 1 day (quiescent egg) plus 1 (nonquiescent egg) plus 5 (aquatic development, as larva and pupa) equals 7 days. Therefore, the individual needs 7 days during the previous stages, and it could emerge adult female during its 8th day. Otherwise, it will become a fertile adult female after its 9th day. For the number of offspring n and the mean duration time γ, we note that they vary according to the weather and the basic sanitation.

We believe that even the older eggs were younger than 500 days in Brazil because the weather had some fluctuation and was well-defined in four seasons. Besides, precipitation was not a problem for more than six months in Brazil.

We used the term individuals as a generic way to refer to eggs, larvae, pupae, or adult

female mosquitoes. Concerning the stages, the individual moves due to age or growth. These movements describe the maturing of the individuals and we are using transition matrices to represent them.

3.2 Literature based functions

In some mortality and transition functions, we use the parametrized functions modeled by H. Yang *et al.* (2009) for *Ae. aegypti* according to temperature-controlled experiments carried out over approximately one year and a half.

Briefly, in these experiments, the mosquitoes were placed in a cage with water and honey, where their blood meal was an immobilized mouse. The way to count eggs was from the amber glass with filter paper for egg-laying. Furthermore, the numbers of survival of males and females were recorded.

To monitor the development of the newly hatched eggs, they were put in a bowl and fed with freely available fish, then it was possible to measure the time spent in this stage over different temperatures. After the procedure, the pupae were transferred and remained inside the chamber (H. Yang *et al.*, 2009).

To fit the data and calculate the functions, they chose a polynomial of degree m given by $P_m(\theta) = \sum_{i=0}^{m} b_i \theta^i$, and used probability functions to estimate the b_i parameters considering the period between the individual emergence at the new stage until its death, as well the temperature dependence (H. Yang *et al.*, 2009).

The fittings were functions of temperature, and the coefficients were usually determined for $10 \leq \theta \leq 35$°C or $10 \leq \theta \leq 40$°C (H. Yang *et al.*, 2009), referring to the daily mean temperature.

We adopt all transition and mortality functions for the range between $6.8 \leq \theta \leq 36$°C due to their biological meaning in the interval. H. Yang *et al.* (2009) worked with a probability distribution, calculating parameters for functions such that the range gives values near zero, and they do not represent a significant change between a rate and a probability distribution, while we assume low rates.

- The aquatic development mortality rate (only larvae and pupae, based on H. Yang *et al.* (2009) and represented in Figure 3.1(a).

$$R_D^0(\theta) = 6.794{\times}10^{-6}\,\theta^4 - 6.778{\times}10^{-4}\,\theta^3 + 2.457{\times}10^{-2}\,\theta^2 - 3.797{\times}10^{-1}\,\theta + 2.130\,. \quad (3.1)$$

  This means the rate of individuals who died on the day t according to the temperature.

- The aquatic development transition rate (only larvae and pupae, based on H. Yang *et al.* (2009)):

Symbol	Definition
θ	The daily mean temperature on the day t, that is $\theta(t)$.
$R^0_{Eq}(\theta)$	The mortality rate of quiescent eggs who died on the day t according to the temperature.
$R^0_E(\theta)$	The mortality rate of nonquiescent eggs who died on the day t according to the temperature.
$R^0_D(\theta)$	The aquatic development mortality rate of individuals (larva and pupa), who died on the day t according to the temperature.
$R^0_A(\theta)$	The mortality rate of adult female mosquitoes who died on the day t according to the temperature.
$R^{Et}_{Eq}(\theta)$	The rate of quiescent eggs that move to the nonquiescent stage on the day t according to the temperature.
$R^{Ej}_{Eq}(j)$	The rate of quiescent eggs that move to the nonquiescent stage on the day t according to the age j.
$R^D_E(\theta)$	The rate of nonquiescent eggs that move to larva on the day t according to the temperature.
$R^A_D(\theta)$	The aquatic development transition rate represents the rate of individuals (only larva and pupa) who move on the day t to adult female according to the temperature.
$R^{Eq}_A(\theta)$	Oviposition rate of quiescent eggs laid by an adult female on the day t according to the temperature.

Table 3.2: *Parameters description.*

$$\begin{aligned} R^A_D(\theta) &= -3.420\times10^{-10}\,\theta^7 + 5.153\times10^{-8}\,\theta^6 - 3.017\times10^{-6}\,\theta^5 \\ &+ 8.723\times10^{-5}\,\theta^4 - 1.341\times10^{-3}\,\theta^3 + 1.164\times10^{-2}\,\theta^2 \\ &- 5.723\times10^{-2}\,\theta + 1.310\times10^{-1}\,. \end{aligned} \tag{3.2}$$

For $\theta < 10.12$°C, we set the aquatic transition as 0, as Figure 3.1(b). It represents the rate of individuals who move on the day t according to the temperature.

- The mortality rate of the female mosquito was adapted from H. Yang *et al.* (2009) and represented in 3.1(c):

$$R^0_A(\theta) = 3.809\times10^{-6}\,\theta^4 - 3.408\times10^{-4}\theta^3 + 1.116\times10^{-2}\,\theta^2 - 1.590\times10^{-1}\,\theta + 8.692\times10^{-1}\,. \tag{3.3}$$

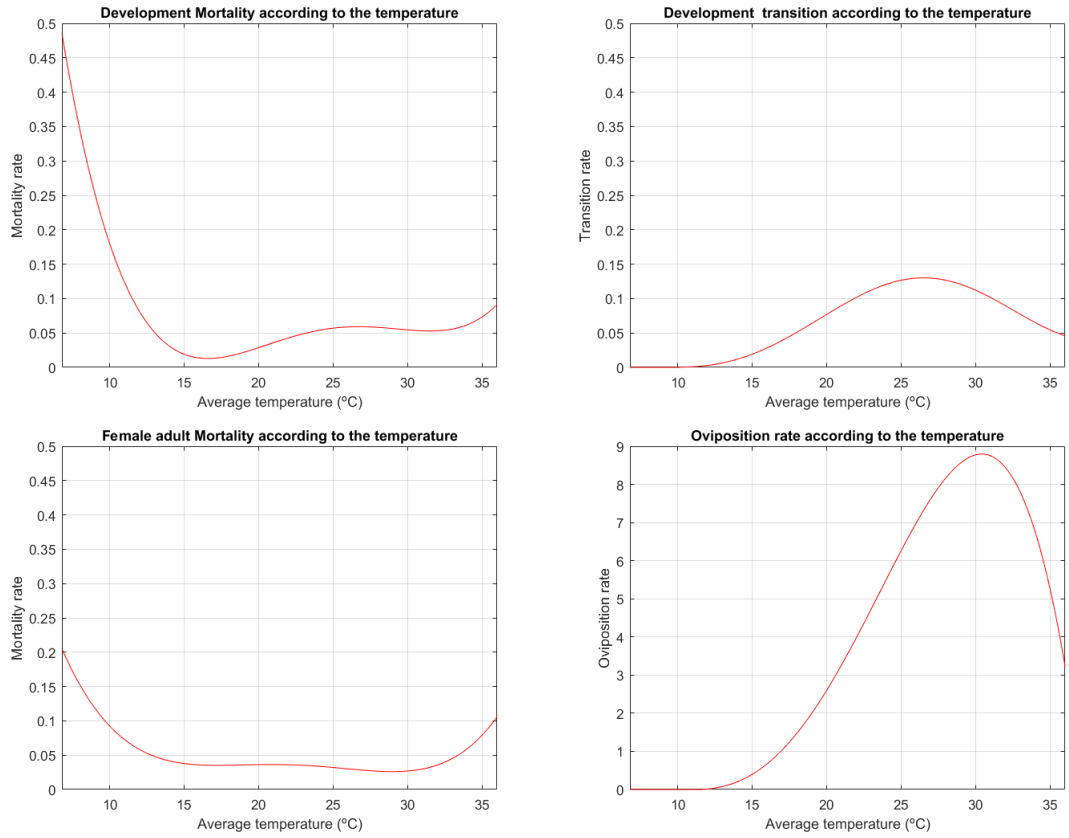

Figure 3.1: *(a) The lower mortality in the aquatic development stage is around 17°C. (b) The transition is improved around 27°C. (c) The lower mortality is around 29°C. (d) The oviposition is stimulated around 30°C.*

- Oviposition rate, based on H. Yang *et al.* (2009):

$$R_A^{Eq}(\theta) = -1.515\times10^{-4}\,\theta^4 + 1.015\times10^{-2}\,\theta^3 - 2.124\times10^{-1}\,\theta^2 + 1.800\,\theta - 5.400\,. \quad (3.4)$$

For $\theta < 11.624$°C, the oviposition depending on temperature is 0, as Figure 3.1(d).

Equation (3.4) represents the rate of quiescent eggs laid by an adult female on day t according to the temperature.

However, the transition and mortality functions from quiescent to nonquiescent eggs, and also that of nonquiescent eggs to aquatic development phase were not reported in H. Yang *et al.* (2009).

We found a temperature dependence function for the transition between nonquiescent egg and larva from Rossi, Ólivêr, *et al.* (2004) that does not consider the water influence, as we see in (3.5),

$$R_E^D(\theta) = 0.00764\,(\theta + 273)\,\frac{e^{40.55-\frac{13094.10}{\theta+273}}}{1+e^{92.501-\frac{28169.2}{\theta+273}}}\,. \quad (3.5)$$

Equation (3.5) determines the rate of nonquiescent eggs that become larvae on day t according to the temperature. The temperature influence over this transition can be seen in Figure 3.2(a).

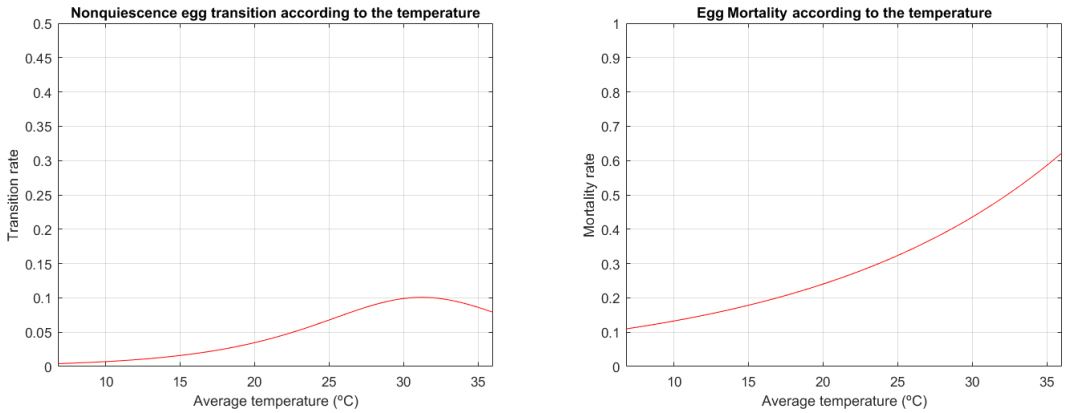

Figure 3.2: *(a) The biggest transition is stimulated around 31°C. (b) The lower mortality is around 7°C.*

We selected this model since Rossi, Ólivêr, *et al.* (2004) also considers the standard unit of measure as Celsius degree, although θ was truly a number in a similar range to the daily mean temperature but it was composed of the daily average temperature together with geographical coordinates. In our model, we are not interested in all those environmental aspects.

We considered the same mortality rate for quiescent and nonquiescent eggs who died on day t according to the temperature (see Figure 3.2(b)). According to Rossi, Ólivêr, *et al.* (2004),

$$R^0_{Eq}(\theta) \;=\; R^0_E(\theta) \;=\; 0.0731\,(\exp(\,0.0595\,\theta\,))\,. \tag{3.6}$$

However, we combine transition, mortality, and fertility rates, and they compose the entries of the probabilities matrix in the same way as Yusoff *et al.* (2012b). There are temperature-dependent functions combined with sanitation or precipitation parameters calculated based on data from experiments or the environment. For example, about the oviposition function from equation (3.4), we include precipitation influence according to Chen *et al.* (2007). From Rossi, Lopez, *et al.* (2015), they set an oviposition function also depending on temperature and rain information, although with a different approach.

Finally, we built the functions described in Section 3.3 and Chapter 4 considering biological and environmental aspects as follows.

3.3 Novel functions

We note from Farnesi *et al.* (2009) that the embryonic development was evaluated using a temperature ranging between 12 and 36°C (at 12, 16, 22, 25, 28, 31, 35, and 36°C).

The main results are described in Table 3.3.

Temperature (°C)	Days (≈)	Hours †	Eclosion (%)
12	40	960*	-
16	20	489.3	81.1
22	4	98.3	93.9
25	3	77.4	96.0
28	3	61.6	93.3
31	2	48.4	82.8
35	2	50.3	48.5
36	-	-	-

† Hours elapsed for eclosion of 50% of larvae specimens between 16 and 35°C. *While for 12°C it is about the first larva eclosion reported.

Table 3.3: *Results of laboratory experiments from* Farnesi *et al. (2009).*

Through these experiments, they reported that the velocity of the complete development was directly proportional to the temperature till 31°C because at 35°C it was slower.

According to Table 3.3, at 12°C the first egg hatching was observed after 40 days. Regarding 16°C, the number of days required for the completion of embryogenesis of half of the sample eggs was reported as 20 days. Quickly development was obtained at 28°C and 31°C (a little over 48 hours). Then we assume 2 as a minimum of days spent by an egg during the quiescence and nonquiescence stages.

In this way, we considered a minimum of 1 day of quiescence, plus 1 day in the nonquiescence stage. In fact, the quiescent egg needs at least 1 day, because the egg will be fertilized when it is laid, that is, the embryo will be generated after the egg laying once the procedure happens outside of the female organs.

Furthermore, the egg spent more than 2 days to complete its embryogenesis at 35°C, if completed (Farnesi *et al.*, 2009). Around 36°C, they did not observe any eclosion (Farnesi *et al.*, 2009). These duration times were counted by hours during the experiment, and often the difference between the time spent for the first egg eclosion was approximately equal to the time performed for half of the sample eggs.

The study justifies the hatching rates once the three-day-old egg has more probability to hatch than a forty-day-old one (Table 3.3). This kind of behavior we noticed from other studies, as follows (see Figures 3.4 and 3.5).

From then on, the biggest eclosion rates were obtained between 22-28°C (approximately 90%) (Farnesi *et al.*, 2009). For exposition considering the temperatures of 16°C and 31°C, they decreased to 80% while at 35°C the eclosion rate was approximately 50%. Despite this, they concluded 35°C as the maximum temperature supported during embryonic development since no hatching was observed above 36°C (Farnesi *et al.*, 2009).

While we consider this sample, we have the velocity of the completion of embryonic development. However, we need the information of temperature around forty previous days, including other surrounding conditions, and it is costly computer-wise. Besides, the

experiment means the eclosion time for half of the eggs, but they felt the environmental stimulus before the reported time, and we are interested in investigating it. Let us consider the data about the percentage of egg hatching. According to Table 3.3, we fit the data as a sum of sines,

$$R_{Eq}^{Et}(\theta) = a_1 \sin(b_1\theta + c_1) + a_2 \sin(b_2\theta + c_2), \tag{3.7}$$

calculating the coefficients as defined by

$$a_1 = 478.7,\ b_1 = 0.1435,\ c_1 = -1.63,$$

$$a_2 = 384.5,\ b_2 = 0.1579 \text{ and } c_2 = 7.491.$$

The resulting curve is represented by Figure 3.3 and normalized in the following equation,

$$R_{Eq}^{Et}(\theta) = \frac{478.7 \sin(0.1435\theta - 1.63) + 384.5 \sin(0.1579\theta + 7.491)}{100}, \tag{3.8}$$

where $\theta = \theta(t)$. We set (3.8) once the unknown percentage is around 10 and 15°C and we expect it to be significantly lower than that for 16°C. Besides, through these six coefficients, according to the range 16-36 Celsius degrees, that is, a set of 7 points, we observe the R-square reaches the maximum of 1.

We built a model using data about seven points with six parameters, but more than looking at the R^2 to choose the fitting, we paid attention to the biological behavior. From then on the sum of sines provides a decrease in the extremes (12°C and 36°C) of the experiment, as the references, we mentioned about *Aedes aegypti*.

Equation (3.8) determines the rate of quiescent eggs that move to nonquiescent eggs on day t according to the temperature θ. Therefore, given good humidity, the temperature influence over the eclosion was evaluated (Farnesi *et al.*, 2009).

The modeling from (3.8) is due to that we assumed the dormancy ends through stimuli according to a rate, and this biological mechanism has a similar behavior to the eclosion, which means it has a similar temperature dependence.

Obviously, faster development is highly determined by temperature, but we also investigate the age influence on it.

In order to justify our point of view, we found results showing that eggs were exposed for 3 days to the water stimulus adhered in sheets of filter paper (Soares-Pinheiro *et al.*, 2017). Afterward, the eggs were left outdoors for 1 day. Therefore they were dried through evaporation and stored in groups in paper envelopes, plastic bags, or plastic cups.

Despite the absence of water, those three days were enough to hatch a lot of eggs. Indeed, from this stimulus, the hatching rates of egg batches stored during 12 to 61 days were bigger with rates between 84 to 90% (Soares-Pinheiro *et al.*, 2017). A significant decrease was reported between 89 to 118 days, with 63 and 48%, respectively. Besides, this study looked for eclosion up to 8 months where the viability of *Aedes aegypti* remained high until 4 months. From the viability tests, they reported a rate for 12, 19, 32, 61, 89, 118, 158, 186, 240, and 271 storage days, as described in Table 3.4.

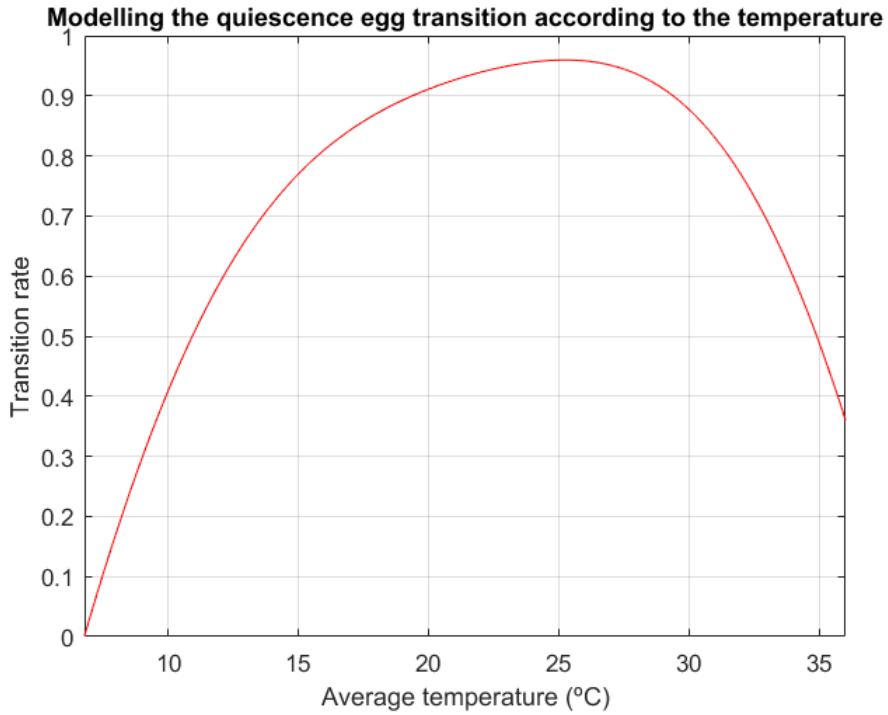

Figure 3.3: *Modeling the viability versus temperature using a sum of sines (Farnesi et al., 2009).*

Storage days	Eclosion (%)
12	90.0
19	80.7
32	88.9
61	83.7
89	63.5
118	48.2
158	10.6
186	2.7
240	0.2
271	0.0

Table 3.4: *Results of experiments from Soares-Pinheiro et al. (2017).*

According to the research, the egg was not counted daily immediately upon its hatching so the eclosion number was accumulated (Soares-Pinheiro *et al.*, 2017). However, they did not report how many days they watched the eggs. Through the pilot experiment and comparisons with the development of the three-day-old eggs during 10 days (Soares-Pinheiro *et al.*, 2017), we conclude they watched the eggs for over 10 days.

Starting with this behavior we could be invited to set models such as Gompertz, logistic curve, or Bertalanffy for fitting the data. However, those models produce curves with a limited growth, which reaches a maximum value in a mid-point between the asymptotes (R. Bassanezi, 2012; Winsor, 1932) and usually, they represent some relationship between age and growth, from where it is possible to analyze the growth behavior of a unique

individual over time (Freitas, 2005; L. Souza, Caires, *et al.*, 2010; Carneiro *et al.*, 2009; L. Souza, Carneiro, *et al.*, 2011). This means that the individual had a weight on time t and on the next day $t+1$, it still had some weight. In this approach, the biological meaning was related to age and eclosion. Thus, since the individual hatched, it did not continue to hatch during the following days.

On the other hand, another experiment reported that 492 days old eggs could hatch according to a rate of 0.2% (H. Silva and I. Silva, 1999). Even though the rate eclosion from Table 3.4 was reported as null for 271 days old eggs (Soares-Pinheiro *et al.*, 2017), we do not consider this information because we assumed that the watching period for the study was short. Assuming a partial sample from Table 3.4 given by

$$\begin{aligned} a &= [12\ 19\ 32\ 61\ 89\ 118\ 158\ 186\ 240] \quad \text{and} \\ b &= [90.0\ 80.7\ 88.9\ 83.7\ 63.5\ 48.2\ 10.6\ 2.7\ 0.2], \end{aligned} \tag{3.9}$$

we point out that the behavior can be represented by a Gaussian curve, such that

$$R_{E^q}^{E^j}(j) = a_1\, \mathrm{e}^{-\left(\frac{j-b_1}{c_1}\right)^2}, \tag{3.10}$$

where j means the quiescent egg age and we fit the data available during 12-240 days because the percentage for 271 days is unknown and it could be near but not equal to zero (H. Silva and I. Silva, 1999).

Thus, we plot the curve in Figure 3.4 and obtain the coefficients (with 95% confidence bounds) given by

$$a_1 = 89.95\,(82.61, 97.29);\ b_1 = 36.8\,(22.33, 51.28)\ \text{and}\ c_1 = 91.9\,(70.68, 113.1), \tag{3.11}$$

where $R^2 = 0.985$.

Mathematically, this gives a good fitting. In practice, the transition of quiescence to nonquiescence happens before eclosion. However, we assume eclosion rates carry information about the development.

Finally, we represent a rate depending on age (j) given by

$$R_{E^q}^{E^j}(j) = \frac{89.95\ \exp\left(-((j-36.8)/91.9)^2\right)}{100}. \tag{3.12}$$

Despite a smooth increase and an unworthy hatchability rate for the 300-day-old individuals, we use this model for fitting the data, which composes the transition function.

From Figure 3.4, we concluded that age influences hatchability. Our approach is justified by the fact that eggs were stored in different containers and places (Soares-Pinheiro *et al.*, 2017), which means the study produced a tendency to model how the quiescent egg felt enough stimulus according to its age. Indeed, the eggs were exposed over three days in the water, and afterward they were stored (Soares-Pinheiro *et al.*, 2017). Some of them received air humidity also, that is, the eggs stored in cups received a few more stimuli

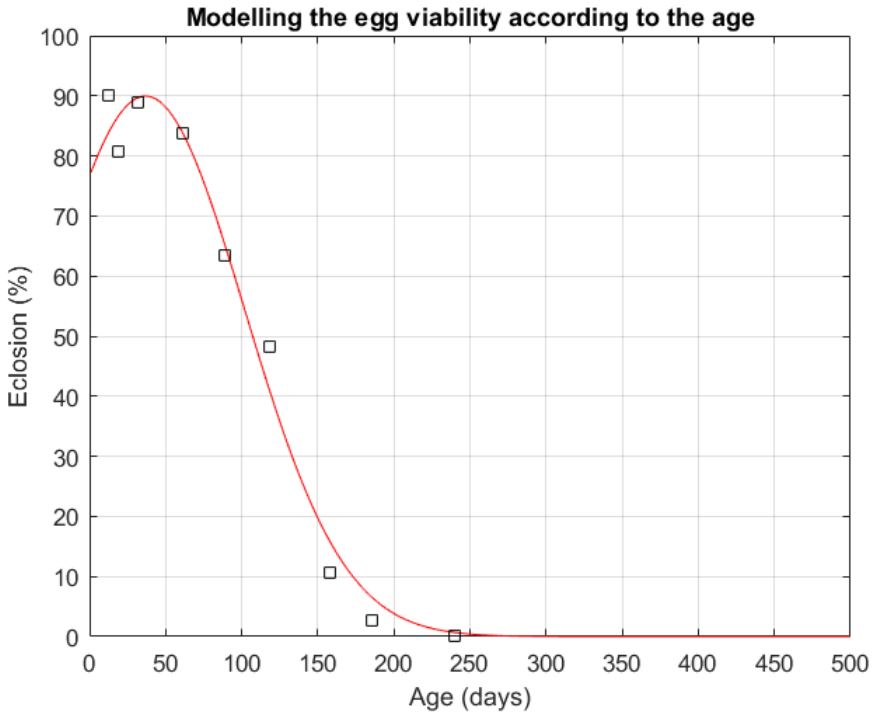

Figure 3.4: *Gaussian fitting for the viability sample from Soares-Pinheiro et al. (2017).*

than those stored in envelopes and plastic bags with their edges sealed (Soares-Pinheiro *et al.*, 2017).

We expected that the transition between quiescence and nonquiescence could be controlled by environmental conditions, which implies building a model with more inputs than the temperature (Schaeffer *et al.*, 2007).

Sample 3.9 (selected, as mentioned, from Table 3.4) is according to results from laboratory experiments performed in Brazil with *Ae. aegypti* reported in H. Silva and I. Silva (1999). The individuals were maintained at a temperature of 28 ± 1°C, over a relative humidity of 80 ± 5% and a photoperiod of 12 hours. Plus, eggs of different ages immersed for eight months had a viability period of up to 492 days, while they found higher hatching rates between three and 121 days (H. Silva and I. Silva, 1999).

Similarly, in Australia, the eggs remained viable for more than a year maintaining a hatching rate of approximately 2-15% (Faull and Williams, 2015). As for lower temperatures, a study performed experiments and an *Aedes aegypti* development over 1°C has been reported by Christophers (1960), but they concluded that, when the eggs hatched, the larvae were dead.

As described above, H. Silva and I. Silva (1999) obtained the biggest eclosion rates for groups of 3 to 121 days old quiescent eggs. This means that the quiescent eggs were stored for 3 to 720 days according to their oviposit colony and after this, they were exposed to favorable temperatures and water. Although the storage was for 4 months, they developed very well. However, lower rates were found for the 154 days old group and so on, which were similar to the results reported by Soares-Pinheiro *et al.* (2017).

The approach was convenient since they dried eggs by evaporation and stored them (H. Silva and I. Silva, 1999), which is a reasonable procedure if we compare it to the process in outdoor places. The available eggs were up to 720 days old, but they found a nonzero rate until the 492 days old group (H. Silva and I. Silva, 1999).

Therefore, both studies reported data about the quiescence ability and egg viability. However, while H. Silva and I. Silva (1999) kept the eggs dried for then to expose them to good environmental conditions, Soares-Pinheiro *et al.* (2017) developed another procedure that began by exposing the eggs for three days to the water stimulus, and after they maintained the eggs in containers where the environmental conditions were reduced to temperature and some air humidity, varying the type of container and the surroundings. The procedures were different, but the egg viability fluctuations had similar behavior.

The rates in Table 3.5 were adapted from H. Silva and I. Silva (1999) and H. Yang (2014). Both were calculated according to results obtained by H. Silva and I. Silva (1999).

Group	Quiescence age (days)	Eclosion (%)	*Per-capita* eclosion rate ($days^{-1}$)	*Per-capita* mortality rate ($days^{-1}$)	Mean eclosion ($days^{-1}$)
1	3	85.4	0.1067	0.0182	86.1
2	32	41.1	0.007593	0.0109	5.3
3	63	36.0	0.01092	0.0194	6.4
4	91	47.7	0.01640	0.0180	12.1
5	121	97.2	0.01762	0.00051	13.2
6	154	1.3	0.002	0.1518	1.6
7	273	4.3	0.01405	0.3127	8.6
8	337	0.3	0.00164	0.5439	1.0
9	427	10.9	0.00665	0.05437	5.6
10	462	0.5	0.00125	0.2488	1.0
11	492	0.2	0.000585	0.2922	1.0

Table 3.5: *Basic rates of Aedes aegypti.*

From Figure 3.5(a) we plot the data about quiescent egg age and *per-capita* eclosion. We analyze the column *per-capita* eclosion because it means the number of eggs per total eclosion rate. Also, by Figure 3.5(b), we have the percentage of eclosion according to the egg age group.

The laboratory experiments reflected how egg development happens during the quiescent period according to age, once they were carried out in a biological chamber (H. Silva and I. Silva, 1999). We pointed out that there are outliers, but in a general way, the viability was lower when the egg was older. Thus, we supported the hypothesis that age influences egg viability. Besides, through the data about egg eclosion and viability, we could model the way the quiescent egg turns into a nonquiescent one.

In a similar way, from Diniz, Melo-Santos, *et al.* (2015) the quiescent egg viability studied up to 180 days was around 70%. Before this, eggs stored for up to 150 days presented a viability rate of 80% (Diniz, Melo-Santos, *et al.*, 2015). Indeed, egg hatchability depends on many factors due to the influence of poor embryonal development and desiccation (H. Yang *et al.*, 2009).

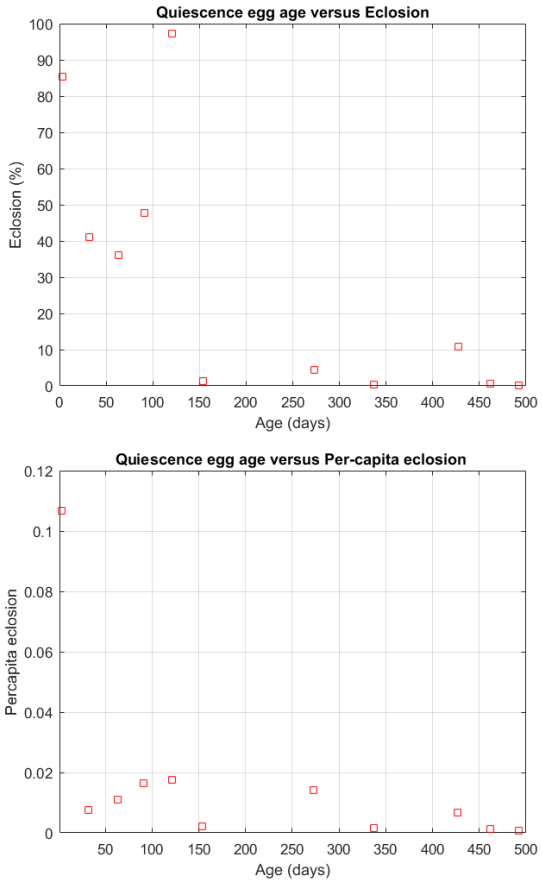

Figure 3.5: *Eclosion from then two calculations (H. Silva and I. Silva, 1999).*

After all, the success of the *Aedes aegypti* population is motivated by its hatchability and lifetime as an egg (Diniz, Albuquerque, *et al.*, 2017; Vieira, 2008; H. Silva and I. Silva, 1999). The stored eggs and hatchability are motivated by the past days' weather, such that we considered accumulated temperature and precipitation.

Although researchers such as Rossi, Ólivêr, *et al.* (2004) used the daily minimum, maximum, and mean temperatures to compose the inputs of dynamical systems, we assumed that applying daily mean temperature can provide enough information about the temperature influence over the *Aedes aegypti* life cycle (Lega *et al.*, 2017; Loncaric and Hackenberger, 2011; Rossi, Lopez, *et al.*, 2015; Yusoff *et al.*, 2012b; Yusoff *et al.*, 2012a).

Chapter 4

Model construction

We propose a structured matrix population model by age and stage, to investigate the behavior of *Aedes aegypti* population dynamics and to estimate its abundance for Brazilian municipalities.

4.1 Model assumptions and some considerations

This Section explains the assumptions established to build the mathematical model.

Age-structured models adapt to this approach since we built a single newborn class model where the offspring are born into the first age class only, similar to Leslie models (Cushing and Yicang, 1994). In this way, individuals in age-class i at time t can move to age-class $i + 1$ as a Leslie model (Cushing and Yicang, 1994), but they also can grow up, so it has the idea of an age and stage-structured model, i.e., generalized structured population models, where we assume some functions and parameters to represent the rates during the life cycle, composed of survival, age, growth, and birth.

For the next step, the individual can move to the next stage, or it remains the same for one more day. It does not need to finish the previous stage classes to move. Likewise, age means the time spent in each development stage, similar to Loncaric and Hackenberger (2011).

It is known that the older an individual gets, the higher the probability of moving to the next stage (Loncaric and Hackenberger, 2011). However, the relationship between age and growth is different for a quiescent egg.

Through the block structure, we represent the biological processes (Newman *et al.*, 2014). According to Newman *et al.* (2014), our model seems a BRS model because it includes growth (R), and also a BAS model because it includes age incrementation (A), both of them followed by survival (S) and birth (B).

Our system is a (time) variant. We can also classify it as dynamic because we are using entries from previous steps (precipitation and temperature). It is stochastic because we are

modeling some aleatory events, such as the probability of the quiescent egg turning into nonquiescent.

(i) The population has an age structure.

We consider the individual ages through classes once the biological conditions give a maximum life expectancy.

Secondly, age can restrict biological processes, such as the minimum age for larval and pupal development and the threshold for female fertility.

Finally, we have data about eggs accumulated up to 5 days old. Then, it is required information about the individuals in this age group, to compare the outputs of the respective five days with the real collected data. It means we do not have an egg storage measure, we only estimate the number of younger individuals.

(ii) We categorize the *Aedes aegypti* population into four compartments.

There exist quiescent eggs E^q, nonquiescent eggs E, the aquatic development D (larva and pupa), and adult female mosquito A, as illustrated in Figure 4.1. It produces a life cycle as Figure 4.2.

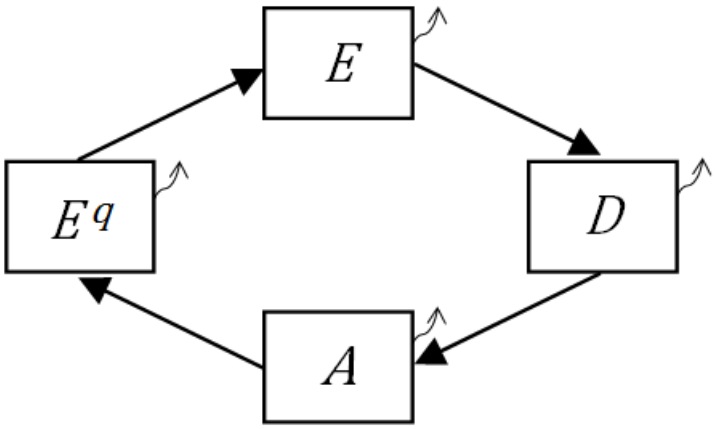

Figure 4.1: *Compartments of the model.*

(iii) We use one stage for quiescent eggs and assume eggs start with quiescence.

Ae. aegypti has embryonary quiescence (Diniz, Albuquerque, *et al.*, 2017). We know from Chapter 3 an *Aedes aegypti* quiescent egg is probably deposited above the water line, once it can be prompted immediately with the immersion into the water ((Denlinger *et al.*, 2012) apud (Diniz, Albuquerque, *et al.*, 2017)). However, eggs sometimes need more than one stimulus to hatch to larva (Diniz, Albuquerque, *et al.*, 2017).

The egg is the most resistant individual during the *Ae. aegypti* development (H. Yang, 2014). Although the serosal cuticle vulnerability during the first hours after the egg-

Figure 4.2: *Aedes aegypti life cycle. Adapted from* Ishikawa *(2012),* E. Souza *(n.d.),* Diáriogaúcho *(2015), and* Loyola *(2016).*

laying (Rezende *et al.*, 2008), the quiescence characteristic guarantees population maintenance.

The quiescent egg can turn into nonquiescent when the weather is good, which occurs quickly or not (H. Silva and I. Silva, 1999). It is possible because the egg has biological protection which provides enough food, depending on stored maternal reserves (Otero *et al.*, 2006; H. Yang, 2014).

The egg hatching rate depends on age as well as weather conditions since the hatching rate of a 121-day-old quiescent egg was greater than for a 427-day-old egg (H. Silva and I. Silva, 1999). While with 492 days the hatching rate was almost zero (H. Silva and I. Silva, 1999). However, the *Ae. aegypti* eggs from the same laying (at the same age) had different hatching rates along the quiescent period when maintained under the same environmental conditions (Diniz, Albuquerque, *et al.*, 2017).

After the first stimulus, when the embryo starts to develop itself, the weather helps it. Otherwise, there will be the probability that the egg will not be prompt, which persists over time (Dickerson, 2007; Maimusa *et al.*, 2016; H. Silva and I. Silva, 1999).

Then, we assumed the nonquiescent egg has a shorter maximum age than the quiescent egg, because of its faster development. Besides, we assumed the eggs have two stages because the development rates are different.

(iv) We considered the larval and pupal stages together as the aquatic development

stage.

Since they have a similar water dependence to survive and develop. Besides, we assume the transition and mortality functions proposed by H. Yang *et al.* (2009), which were together.

The data provides information about eggs and adults (Codeço *et al.*, 2015). Then, assuming only one stage, we now focus on the distribution of the population in these two steps of development.

(v) The availability of breeding sites depends on rainfall and temperature.

As well as in Rossi, Lopez, *et al.* (2015), the authors assumed both variables. However, from Otero *et al.* (2006), we found a model based on temperature, not on rainfall, because they explored regions where there was no dry season.

In Brazil, we assume that frequent rainfalls increase the abundance of breeding sites for the female mosquito to lay its eggs (Loncaric and Hackenberger, 2011).

We set the mean daily temperature of breeding sites as the same as the air (Otero *et al.*, 2006). That is, through the daily mean temperature data, we assume that atmospheric temperature provides an estimated temperature for the water.

(vi) Where there is water, there is enough food.

From item (iii), the egg has maternal reserves. Nevertheless, during the larval stage, the individual needs food. It can eat protozoa, bacteria, and fungi present in the water. In this way, larvae mortality is influenced by habitat desiccation (Schaeffer *et al.*, 2007) while pupae do not eat (Loncaric and Hackenberger, 2011; Otero *et al.*, 2006), but they breathe and need water.

On the other hand, the adult mosquito eats plants (A. P. d. Souza *et al.*, 2020) or blood, which doesn't depend immediately on water resources.

(vii) Desiccation is intrinsic to natural death.

We considered desiccation is not a mortality factor as Otero *et al.* (2006), based on the daily mean temperatures reported from the studied cities. Indeed, the hatching of mature eggs is greatly stimulated by the soaker, which means it is more common to occur after rainfall ((Christophers, 1960) apud (Otero *et al.*, 2006)).

(viii) Quiescent eggs can turn into nonquiescent after the needed temperature stimulus, even during the rain absence. The same occurs between nonquiescent egg to larvae.

The egg has maternal reserves (Otero *et al.*, 2006; H. Yang, 2014). It counts if they were exposed to the water in some previous days as quiescent eggs, or in a place where it developed through the evaporation process.

(ix) The quiescent period does not influence the time during larva and pupa stages, nor the female longevity.

We point out through biological experiments that groups of different quiescent days presented a similar number of days for aquatic stage development or female mosquito longevity (see Tables 3 and 4 from H. Silva and I. Silva (1999)).

(x) The gonotrophic cycle is periodic (Schaeffer *et al.*, 2007), and the availability of male mosquitoes is always enough.

In the breeding season, there are male mosquitoes available for copulation. The sperm is stored throughout the female's lifespan (H. Yang *et al.*, 2009). The eggs are fertilized when they are formed (H. Yang *et al.*, 2009) outside the female organs.

(xi) The adult female does not lay eggs at any age (Costa *et al.*, 2010; Maimusa *et al.*, 2016; H. Yang *et al.*, 2009).

Furthermore, similar to H. Yang *et al.* (2009) - where they assumed the mosquitoes copulated 24 hours after the emergence as an adult female -, we incorporate the first oviposit from the second day as an adult (Maimusa *et al.*, 2016). Around 50% of the females copulated, fed, and laid eggs one day after their emergence, while another 50% needed two days to lay eggs for the first time, during their third day.

There is a biological threshold of 2 up to 22 days old for female fertility (Maimusa *et al.*, 2016). Besides, adult females lay eggs every 2 days (see Table 3.1). It means we assume 11 cycles as the maximum for fertile females. In fact, *Aedes aegypti* reproduces 10.75 times in an average of 15.77 days (Maimusa *et al.*, 2016).

(xii) We have different daily survival and transition rates for eggs, aquatic development, and adult females.

Each stage is susceptible to stimuli. We set functions from literature (Section 3.2) and novel functions (Section 3.3).

(xiii) We propose a singular age and stage structure.

A second overview of the mosquito life cycle is shown in Figure 4.3. Through this is distinguished the individuals according to their stages as well as their age (see description on Table 4.1). Beyond this cycle, we consider the time spent in each stage, in the same way as developed by Loncaric and Hackenberger (2011) for *Aedes vexans*, because the individuals can move to the next stage before the end of its stage, as specified by Table 3.1.

(xiv) The rates can fluctuate while the weather provides different environmental conditions.

Summer, late Spring, and early Fall are the favorite periods for the breeding season.

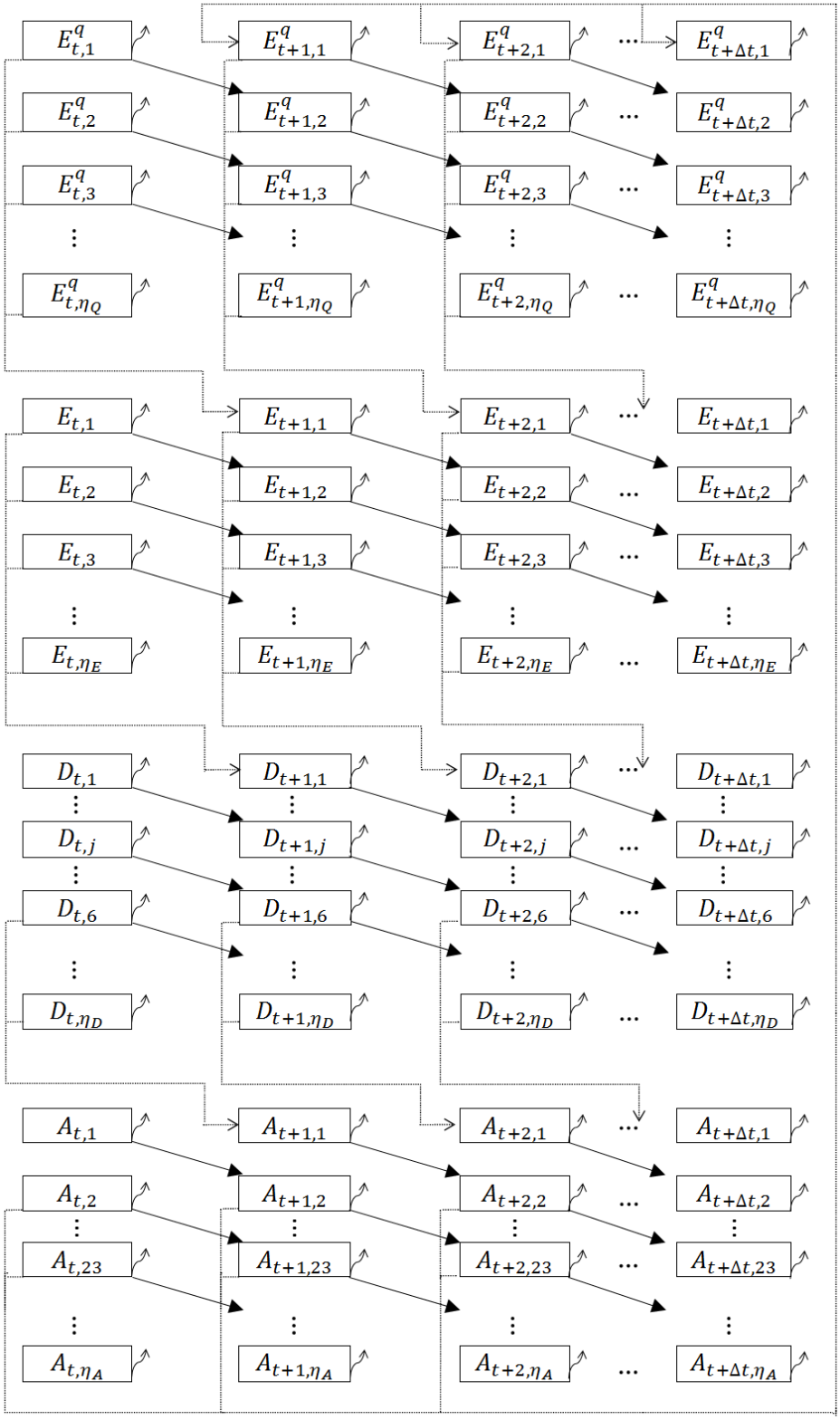

Figure 4.3: *The flow chart of mosquito's life cycle as established in the model.*

In this way, we consider a model where the quiescent eggs are the robust individuals who can survive over lower temperatures and rain absence.

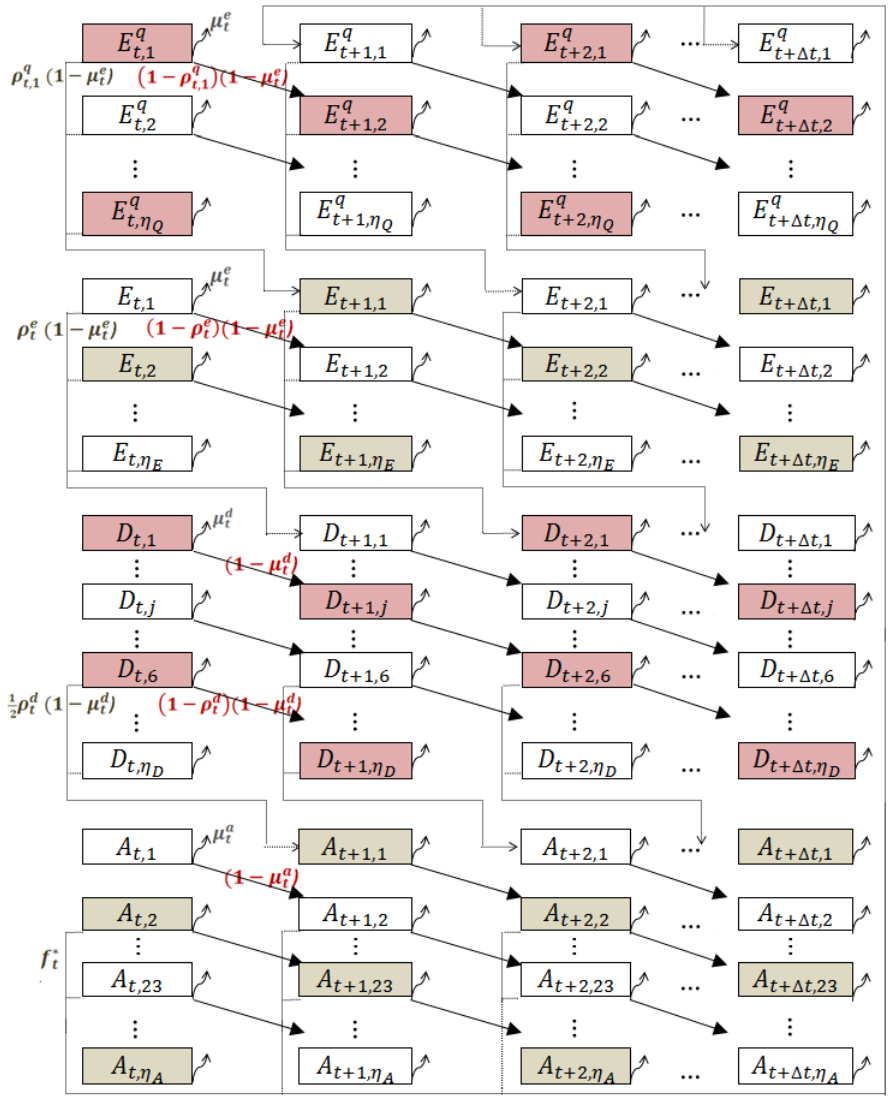

Figure 4.4: *The flow chart of mosquito's life cycle as established in the model. One color represents the path trends in the same class.*

About adult mosquitoes, the urban areas and the environmental conditions can increase the surrounding outdoor availability and the duration of the day when female mosquitoes bite most frequently (WHO, 2019). However, the indoor habitat is less susceptible to climatic variations and can increase the mosquitoes' longevity (WHO, 2019). Still, indoor environment specificities do not influence the model once we consider outdoor trap data.

(xv) It is a mid-term period when there is no migration.

(xvi) The model has a one-day projection interval, which means $\Delta t = 1$ day.

(xvii) The oviposition function considers temperature and precipitation dependence.

The biology of the adult female mosquito depends on the temperature to oviposit eggs (remember equation (3.4)).

Symbol	Definition
$E^q_{t,j}$	Representing the quiescent egg stage
	The number of j days old quiescent eggs on the day t.
$E_{t,j}$	Representing the nonquiescent egg stage
	The number of j days old nonquiescent eggs on the day t.
$D_{t,j}$	Representing the aquatic development stage - larval and pupal stages
	The number of j days old larvae and pupae on the day t.
$A_{t,j}$	Representing the adult female stage
	The number of j days old adult female mosquitoes on the day t.
η_Q	The maximum age reported for quiescent eggs.
η_E	The maximum age reported for nonquiescent eggs.
η_D	The number of days required for larvae and pupae development.
η_A	The maximum age reported for adult female mosquitoes.

Table 4.1: *Compartments description.*

Moreover, we represent a rain influence once that at the same temperature, in Costa *et al.* (2010), they verified that lower humidities increased the egg-laying.

4.2 Model development

The matrix P_t is called the population projection matrix associated with the model. Through the settings, we estimate the population number on the day t depending on the population on the day $t-1$. As the matrix entries change according to the environmental conditions, then P_t is weather-dependent.

The projection matrix is composed of the fertility F_t and transition T_t matrices, so it has a form $P_t = T_t + F_t$ and

$$M_{t+1} = P_t M_t\,, \tag{4.1}$$

with $M_0 \geq 0$. We organize the *Aedes aegypti* population as if each coordinate of the mosquito vector M_t represents the number of individuals in the current stage over the same age class, once the population stages can be organized in a vector according to the individuals' age.

There are four stages corresponding to the quiescent E^q_t and nonquiescent E_t eggs, the aquatic development D_t (larva and pupa), and the adult female mosquito A_t. For this approach, we consider $E^q_t = (E^q_{t,1}, E^q_{t,2}, \cdots, E^q_{t,\eta_Q})$, $E_t = (E_{t,1}, E_{t,2}, \cdots, E_{t,\eta_E})$, $D_t = (D_{t,1}, D_{t,2}, \cdots, D_{t,\eta_D})$ and $A_t = (A_{t,1}, A_{t,2}, \cdots, A_{t,\eta_A})$, where

$$M_t = (E^q_t,\, E_t,\, D_t,\, A_t)'.$$

For example, $E^q_{t,j}$ means the number of j days old quiescent egg on the day t, as well as the maximum age is η_Q days old, and so on (see Table 4.1). Thus, we set an η_Q, η_E, η_D, and η_A big enough, according to biological reports.

For this approach, we considered Table 4.2, and similar to Cushing and Yicang (1994)

we built the projection matrix

$$P_t = \begin{bmatrix} V_t & 0 & 0 & Z_t \\ S_t & X_t & 0 & 0 \\ 0 & W_t & Q_t & 0 \\ 0 & 0 & R_t & U_t \end{bmatrix}, \tag{4.2}$$

where $P_t \in \mathbb{R}^{m\times m}$ such that $m = \eta_Q + \eta_E + \eta_D + \eta_A$. The transition and the fertility matrices (Cushing and Yicang, 1994) are given by

$$T_t = \begin{bmatrix} V_t & 0 & 0 & 0 \\ S_t & X_t & 0 & 0 \\ 0 & W_t & Q_t & 0 \\ 0 & 0 & R_t & U_t \end{bmatrix} \quad \text{and} \quad F_t = \begin{bmatrix} 0 & 0 & 0 & Z_t \\ 0 & 0 & 0 & 0 \\ 0 & 0 & 0 & 0 \\ 0 & 0 & 0 & 0 \end{bmatrix}.$$

Symbol	Definition
P_t	The population projection matrix on the day t.
T_t	The transition matrix on the day t, consisting of the transition probabilities.
F_t	The fertility matrix on the day t is composed by the Z_t block.
M_t	The mosquito vector on the day t.
V_t	The daily survival transition of E_t^q.
X_t	The daily survival transition of E_t.
Q_t	The daily survival transition of D_t.
U_t	The daily survival transition of A_t.
S_t	The transition of quiescent egg that receives good environmental condition to become a nonquiescent egg.
W_t	The transition between nonquiescent egg and larval stages (hatching).
R_t	The transition between adult female that emerges from the pupa.
Z_t	The fertility matrix that represents the eggs laid by a fertile adult female mosquito.

Table 4.2: *Matrices blocks description.*

Thus, the system (4.1) is equivalent to

$$M_{t+1} = \begin{bmatrix} V_t & 0 & 0 & Z_t \\ S_t & X_t & 0 & 0 \\ 0 & W_t & Q_t & 0 \\ 0 & 0 & R_t & U_t \end{bmatrix} \begin{pmatrix} E_t^q \\ E_t \\ D_t \\ A_t \end{pmatrix} = \begin{pmatrix} V_t E_t^q + 0 + 0 + Z_t A_t \\ S_t E_t^q + X_t E_t + 0 + 0 \\ 0 + W_t E_t + Q_t D_t + 0 \\ 0 + 0 + R_t D_t + U_t A_t \end{pmatrix}.$$

Where the equations are

$$\begin{cases} E^q_{t+1} &= Z_{t_{[\eta_Q,\eta_A]}} A_{t_{[\eta_A,1]}} &+ V_{t_{[\eta_Q,\eta_Q]}} E^q_{t_{[\eta_Q,1]}} \\ E_{t+1} &= S_{t_{[\eta_E,\eta_Q]}} E^q_{t_{[\eta_Q,1]}} &+ X_{t_{[\eta_E,\eta_E]}} E_{t_{[\eta_E,1]}} \\ D_{t+1} &= W_{t_{[\eta_D,\eta_E]}} E_{t_{[\eta_E,1]}} &+ Q_{t_{[\eta_D,\eta_D]}} D_{t_{[\eta_D,1]}} \\ A_{t+1} &= R_{t_{[\eta_A,\eta_D]}} D_{t_{[\eta_D,1]}} &+ U_{t_{[\eta_A,\eta_A]}} A_{t_{[\eta_A,1]}} \end{cases} . \tag{4.3}$$

Compared to Schaeffer *et al.* (2007), they built a vector without coordinates related to age. Thus, one biological stage was composed of one entry, and the next entry represented the following stage.

Age coordinates configuration can limit life expectancy and determine high probabilities for biological processes, such as laying eggs and moving the individual to the next stage or remaining in the same but in the next class (as older).

Exceptions about the relationship between age and biological processes are found, once for the last stage the individual does not move to the next class, and for some instances of biological limitation, it dies. About eggs, the approach is very important once the egg hatching rate depends on its age as described in item (iii).

On the other hand, in Schaeffer *et al.* (2007) a constant value is used to move the individual over the stages, but recognizing it was a simple representation obtained through data modeling.

We assume a hypothesis about the movements among $E_t \to D_t$, $D_t \to A_t$ and $A_t \to E^q_t$ because we consider from some age, the individual is not age-dependent anymore and it matures and moves according to the environmental conditions. However, the relationship between $E^q_t \to E_t$ may be considered age-dependent (according to item (iii)) and we can find an expression to represent this behavior.

Likewise, we set $\rho^q_{t,j}$, $\rho^e_{t,j}$ and $\rho^d_{t,j}$, where $\rho^s_{t,j}$ is the transition rate for individuals in stage s to the next stage. It means the individual leaves the stage with a probability determined by $\rho^s_{t,j}$. Who remains in the same stage has probability represented by the complementary number, $(1 - \rho^s_{t,j})$.

Moreover, to deal with who survives, we set $(1 - \mu^s_t)$, and it is useful for both movement phenomena.

Through those settings and Table 4.3, we can build the main diagonal blocks of the transition matrix T_t to calculate the number of individuals that remain in the same stage, such as,

$$(1 - \rho^s_{t,j})(1 - \mu^s_t). \tag{4.4}$$

Otherwise, we set

$$\rho^s_{t,j}(1 - \mu^s_t), \tag{4.5}$$

for the individuals that grow up and move to the next stage, where $0 \leq \rho^s_{t,j} \leq 1$ and more strictly,

Symbol	Definition
μ_t^s	The daily mortality rate of individual in stage s on the day t.
$\mu_t^q = \mu_t^e$	The daily mortality rate of quiescent and nonquiescent egg on the day t.
μ_t^d	The daily mortality rate of larva and pupa on the day t.
μ_t^a	The daily mortality rate of adult female mosquito on the day t.
$\rho_{t,j}^s$	The daily transition on the day t of j days old individuals in stage s to the next stage, according to environmental conditions.
p_{ij}	Element of ith -row and jth-column of T_t on the day t.
$s_{1,j}$	Element of 1st-row and jth-column of S_t on the day t.
$w_{1,j}$	Element of 1st-row and jth-column of W_t on the day t.
$r_{1,j}$	Element of 1st-row and jth-column of R_t on the day t.
$z_{t,j}$	Nonzero element of jth-column of Z_t on the day t.
$v_{t,j}$	Nonzero element of jth-column of V_t on the day t.
$x_{t,j}$	Nonzero element of jth-column of X_t on the day t.
$q_{t,j}$	Nonzero element of jth-column of Q_t on the day t.
$u_{t,j}$	Nonzero element of jth-column of U_t on the day t.
f_t^*	The number of eggs laid by one each two fertile adult female mosquito on the day t according to temperature and precipitation.

Table 4.3: *Matrices entries and rates description.*

$$0 \ll \mu_t^s \leq 1\,. \tag{4.6}$$

Considering that the total population (100%) in each stage is represented by the probability 1. The range of μ_t^s is such that we guarantee the dissipative condition (Cushing and Yicang, 1994), that the sums of the columns of T_t are less than 1 (see more in Chapter 4).

The considerations above are enough to build the transition matrix T_t. The transitions are ruled according to the transition matrix T_t (Cushing and Yicang, 1994), which is basically composed of equations (4.4) and (4.5).

Indeed, the blocks from T_t represent who moves to the next stage (S_t, W_t and R_t) and who remains in the same stage adding one unit time to its age (V_t, X_t, Q_t and U_t), with a one-day projection interval. For this approach, we consider the descriptions in Table 4.2 and the matrices sparse configuration as (4.7) and (4.8). It consists of these transition probabilities. The blocks indicate who moves to the next age or to the next stage.

The question is how to consider $\rho_{t,j}^s$ and μ_t^s using temperature and, in some instances, age and precipitation.

In order to study the matrix F_t, we have a block composed of a time-dependent rate, which depends on temperature. Plus, breeding sites are more available after precipitation. Also, the matrix can depend on female feed, but we consider that the search for a blood meal needs one time lower than the time step, with the time step defined as a time lower than the minimum residence in any stage taking into account item (xvi) where $\Delta t = 1$ day. Then, we do not consider the search for a meal as a delay, in the same way as Schaeffer *et al.* (2007).

Thus, the mortality and the transition functions need to be functions such that the individual dies or moves to the next age/stage. The entries for the daily survival transition matrices are described in (4.7) and (4.8).

$$
\begin{aligned}
V_t &= \begin{bmatrix}
0 & 0 & \cdots & 0 & 0 \\
(1-\rho^q_{t,1})(1-\mu^e_t) & 0 & \cdots & 0 & 0 \\
0 & (1-\rho^q_{t,2})(1-\mu^e_t) & & 0 & 0 \\
\vdots & & \ddots & \vdots & \vdots \\
0 & 0 & \cdots & (1-\rho^q_{t,\eta_Q-1})(1-\mu^e_t) & 0
\end{bmatrix}, \\
X_t &= \begin{bmatrix}
0 & 0 & \cdots & 0 & 0 \\
(1-\rho^e_t)(1-\mu^e_t) & 0 & \cdots & 0 & 0 \\
0 & (1-\rho^e_t)(1-\mu^e_t) & & 0 & 0 \\
\vdots & & \ddots & \vdots & \vdots \\
0 & 0 & \cdots & (1-\rho^e_t)(1-\mu^e_t) & 0
\end{bmatrix}, \\
Q_t &= \begin{bmatrix}
0 & \cdots & 0 & 0 & \cdots & 0 & 0 \\
1-\mu^d_t & & 0 & 0 & \cdots & 0 & 0 \\
& \ddots & \vdots & \vdots & \ddots & \vdots & \vdots \\
0 & & 1-\mu^d_t & 0 & \cdots & 0 & 0 \\
0 & \cdots & 0 & (1-\rho^d_t)(1-\mu^d_t) & & 0 & 0 \\
\vdots & \ddots & \vdots & & \ddots & \vdots & \vdots \\
0 & \cdots & 0 & 0 & \cdots & (1-\rho^d_t)(1-\mu^d_t) & 0
\end{bmatrix}, \\
U_t &= \begin{bmatrix}
0 & 0 & \cdots & 0 & 0 \\
1-\mu^a_t & 0 & \cdots & 0 & 0 \\
0 & 1-\mu^a_t & & 0 & 0 \\
\vdots & & \ddots & \vdots & \vdots \\
0 & 0 & \cdots & 1-\mu^a_t & 0
\end{bmatrix}.
\end{aligned}
\tag{4.7}
$$

According to (4.7), the individual dies or moves to the next class due to its age, similar to Newman *et al.* (2014). The null last column of these matrices shows that we do not use the last vector entry now, because the remaining population will not be in the same stage

anymore.

Notice that, from $q_{2,1}, q_{3,2}$ till $q_{6,5}$, only the mortality is used, based on the literature (Table 3.1), once the individuals do not have sufficient age to maturate and move to the next stage, then all individuals continue as older, at the next class.

Referring to the entries of U_t, the pattern is due to there is no next stage because the adult female gets older and dies.

About V_t and X_t, the entries are almost the same, depending on the day t. However, while X_t does not depend on age, V_t depends on it.

The following matrices are able to describe how population growth happens concerning the movements of the stage.

$$
\begin{aligned}
S_t &= \begin{bmatrix} \rho^q_{t,1}(1-\mu^e_t) & \cdots & \rho^q_{t,\eta_Q-1}(1-\mu^e_t) & \rho^q_{t,\eta_Q}(1-\mu^e_t) \\ 0 & \cdots & 0 & 0 \\ \vdots & \ddots & \vdots & \vdots \\ 0 & \cdots & 0 & 0 \end{bmatrix}, \\
W_t &= \begin{bmatrix} \rho^e_t(1-\mu^e_t) & \cdots & \rho^e_t(1-\mu^e_t) \\ 0 & \cdots & 0 \\ \vdots & \ddots & \vdots \\ 0 & \cdots & 0 \end{bmatrix}, \\
R_t &= \begin{bmatrix} 0 & \cdots & 0 & \frac{1}{2}\rho^d_t(1-\mu^d_t) & \cdots & \frac{1}{2}\rho^d_t(1-\mu^d_t) \\ 0 & \cdots & 0 & 0 & \cdots & 0 \\ \vdots & \ddots & \vdots & \vdots & \ddots & \vdots \\ 0 & \cdots & 0 & 0 & \cdots & 0 \end{bmatrix}, \\
Z_t &= \begin{bmatrix} 0 & f^*_t & \cdots & f^*_t & 0 & \cdots & 0 \\ 0 & 0 & \cdots & 0 & 0 & \cdots & 0 \\ \vdots & \vdots & \ddots & \vdots & \vdots & \ddots & \vdots \\ 0 & 0 & \cdots & 0 & 0 & \cdots & 0 \end{bmatrix}.
\end{aligned} \tag{4.8}
$$

To build (4.8), we assume $s_{1,1}$ exists because $E^q_{t,1}$ can turn into $E_{t+1,1}$ as if the embryo is developed before its first 24 hours and it received enough stimulus during the first hours. Similarly, $w_{1,1}$ does exist because the individual can be a larva during its third day (according to Table 3.3).

On the other hand, from the aquatic development stage, we assume larvae and pupae need at least six days to become an adult mosquito, thus $r_{1,1} = \cdots = r_{1,5} = 0$, but $r_{1,6} \neq 0$ and so on.

Relative to R_t, we also note the proportion of half the population. Indeed, about the egg population (with quiescent or nonquiescent), we want to estimate the abundance of both sexes to compare with the trap data from Fiocruz (Codeço *et al.*, 2015). However, the adult traps only provide data about the female mosquito, so after the aquatic development

stage we consider half of the number of individuals who move to the adult stage, as a gender-limiting factor.

About the last entries, notice that s_{1,η_Q}, w_{1,η_E} and r_{1,η_D} can move a rate of the population while the remaining population is ignored. That is, the model considers the remaining individuals as unworthy, which works in some way different than the pattern found in the previous entries because the individuals are at the end of some stage. The end happens when they have the maximum age as the biological experiments attest (see Table 3.1). Thus, there is no way to continue in the same stage: they will die or mature. The assumption comes from the maximum age described in the literature and is included in Table 3.1.

Referring to ((xi)), we verify that the fertile females' threshold is 2 until 23 days old (Maimusa *et al.*, 2016). Then we have just $z_{1,2} = \cdots = z_{1,23} = f_t^* \neq 0$ (see more about it in equation (4.10)).

As the lifetimes spent in both stages are not short, there were individuals already dead according to the weather and the mortality function. Then the model discarded some remaining populations, which developed slowly once their biology was unsafe.

Since η_Q is big enough, s_{1,η_Q} represents a small probability that the egg with quiescence turns into nonquiescent. If the transition at η_Q age has not occurred, the egg can not hatch anymore, and it does not contribute to the population dynamics.

The matrices entries in (4.7) and (4.8) depend on age, temperature, and precipitation. Each definition is described in Table 4.3, and the respective function is described as follows. The general matrix setting is a sparse matrix.

$$\begin{bmatrix}
0 & \cdots & 0 & 0 & 0 & \cdots & 0 & 0 & 0 & \cdots & 0 & 0 & \cdots & 0 & 0 & 0 & * & \cdots & * & 0 & \cdots & 0 & 0 \\
* & \ddots & \vdots & \vdots & 0 & \cdots & 0 & 0 & 0 & \cdots & 0 & 0 & \cdots & 0 & 0 & 0 & 0 & \cdots & 0 & 0 & \cdots & 0 & 0 \\
0 & \ddots & 0 & 0 & 0 & \cdots & 0 & 0 & 0 & \cdots & 0 & 0 & \cdots & 0 & 0 & \vdots & \vdots & \ddots & \vdots & \vdots & \ddots & \vdots & \vdots \\
0 & & * & 0 & 0 & \cdots & 0 & 0 & 0 & \cdots & 0 & 0 & \cdots & 0 & 0 & 0 & 0 & \cdots & 0 & 0 & \cdots & 0 & 0 \\
* & \cdots & * & * & 0 & \cdots & 0 & 0 & 0 & \cdots & 0 & 0 & \cdots & 0 & 0 & 0 & 0 & \cdots & 0 & 0 & \cdots & 0 & 0 \\
0 & \cdots & 0 & 0 & * & \ddots & \vdots & \vdots & 0 & \cdots & 0 & 0 & \cdots & 0 & 0 & 0 & 0 & \cdots & 0 & 0 & \cdots & 0 & 0 \\
\vdots & \ddots & \vdots & \vdots & 0 & \ddots & 0 & 0 & 0 & \cdots & 0 & 0 & \cdots & 0 & 0 & 0 & 0 & \cdots & 0 & 0 & \cdots & 0 & 0 \\
0 & \cdots & 0 & 0 & 0 & & * & 0 & 0 & \cdots & 0 & 0 & \cdots & 0 & 0 & 0 & 0 & \cdots & 0 & 0 & \cdots & 0 & 0 \\
0 & \cdots & 0 & 0 & * & \cdots & * & * & 0 & \cdots & 0 & 0 & \cdots & 0 & 0 & 0 & 0 & \cdots & 0 & 0 & \cdots & 0 & 0 \\
0 & \cdots & 0 & 0 & 0 & \cdots & 0 & 0 & * & \ddots & \vdots & 0 & \cdots & 0 & 0 & 0 & 0 & \cdots & 0 & 0 & \cdots & 0 & 0 \\
0 & \cdots & 0 & 0 & 0 & \cdots & 0 & 0 & 0 & \ddots & 0 & 0 & \cdots & 0 & 0 & 0 & 0 & \cdots & 0 & 0 & \cdots & 0 & 0 \\
0 & \cdots & 0 & 0 & 0 & \cdots & 0 & 0 & 0 & \cdots & * & 0 & \cdots & 0 & 0 & 0 & 0 & \cdots & 0 & 0 & \cdots & 0 & 0 \\
0 & \cdots & 0 & 0 & \vdots & \ddots & \vdots & \vdots & 0 & \cdots & 0 & * & \ddots & \vdots & 0 & 0 & 0 & \cdots & 0 & 0 & \cdots & 0 & 0 \\
0 & \cdots & 0 & 0 & 0 & \cdots & 0 & 0 & 0 & \cdots & 0 & 0 & \ddots & 0 & 0 & 0 & 0 & \cdots & 0 & 0 & \cdots & 0 & 0 \\
0 & \cdots & 0 & 0 & 0 & \cdots & 0 & 0 & 0 & \cdots & 0 & 0 & & * & 0 & 0 & 0 & \cdots & 0 & 0 & \cdots & 0 & 0 \\
0 & \cdots & 0 & 0 & 0 & \cdots & 0 & 0 & 0 & \cdots & 0 & * & \cdots & * & * & 0 & 0 & \cdots & 0 & 0 & \cdots & 0 & 0 \\
0 & \cdots & 0 & 0 & 0 & \cdots & 0 & 0 & 0 & \cdots & 0 & 0 & \cdots & 0 & 0 & * & 0 & \cdots & 0 & 0 & \cdots & 0 & 0 \\
0 & \cdots & 0 & 0 & 0 & \cdots & 0 & 0 & 0 & \cdots & 0 & 0 & \cdots & 0 & 0 & 0 & * & \ddots & \vdots & 0 & \cdots & 0 & 0 \\
0 & \cdots & 0 & 0 & 0 & \cdots & 0 & 0 & 0 & \cdots & 0 & 0 & \cdots & 0 & 0 & 0 & 0 & \ddots & 0 & 0 & \cdots & 0 & 0 \\
0 & \cdots & 0 & 0 & 0 & \cdots & 0 & 0 & 0 & \cdots & 0 & 0 & \cdots & 0 & 0 & 0 & 0 & & * & 0 & \cdots & 0 & 0 \\
0 & \cdots & 0 & 0 & 0 & \cdots & 0 & 0 & \vdots & \ddots & \vdots & \vdots & \ddots & \vdots & \vdots & \vdots & \vdots & \ddots & 0 & * & \ddots & \vdots & \vdots \\
0 & \cdots & 0 & 0 & 0 & \cdots & 0 & 0 & 0 & \cdots & 0 & 0 & \cdots & 0 & 0 & 0 & 0 & \cdots & 0 & 0 & \ddots & 0 & 0 \\
0 & \cdots & 0 & 0 & 0 & \cdots & 0 & 0 & 0 & \cdots & 0 & 0 & \cdots & 0 & 0 & 0 & 0 & \cdots & 0 & 0 & & * & 0
\end{bmatrix}.$$

4.3 Composing all functions

Through this Section, we composed the functions that determine the flow of the *Aedes aegypti* population. More parameters and functions are described in Table 4.4.

Arriving at the fertility matrix Z_t, the entries configuration is very different from the transition matrix blocks, once the nonzero terms are all located at the first line of the matrix block.

As a first idea, let $r_f(t)$ be a rain factor, defined to represent the existence of a significant rainy days $r_d(t)$ during the present day t and the previous 2 days, which is similar to Lon-caric and Hackenberger (2011). Referring to that, in Loncaric and Hackenberger (2011) they used a rainfall dependence to determine the female fecundity, using the cumulative number of rainy days through an 8-day period, for another *Aedes aegypti* species cycle. In the same way, we adopt the function for *Ae. aegypti*, replacing the cumulative number of rainy days for 3 days, firstly based on Table 3.1 from where we see *Ae. aegypti* female mosquito often lays eggs every 2 days, and secondly because we consider that the humidity remains a few times after rain. Thus we set,

$$r_f(t) = \max\{r_d(t), r_d(t-1), r_d(t-2)\}. \tag{4.9}$$

Symbol	Definition
$f_{t,j}$	The number of eggs laid by only one j-days-old fertile adult female mosquito on the day t depending on temperature.
f_t^*	The number of eggs laid by one each two fertile adult female mosquito on the day t according to temperature, sanitation and precipitation.
t_p	The constant time between two ovipositions.
r_f	The rain factor is defined to represent the existence of significant rainy days during the present day t and the previous 2 days.
r_d	It indicates daily precipitation greater than a threshold referenced by q_a.
q_a	The city's historical annual mark of precipitation is divided by 365 days.
q_p	The precipitation on the day t, that is $q_p(t)$.
θ_m	An average of temperature about the present up to 21 previous days.
α_c	It measures the influence of the absence of precipitation during the past days for each city. It is an output of a fuzzy rule-based system.
$q_p^\dagger$	The indicator for accumulated precipitation of past days.
t_m	The number of previous days limited by the age of the individual where $0 \leq t_m \leq 21$.
q_{pm}	An average of precipitation of previous days limited by the age of the individual or $t_m + 2$.

Table 4.4: *Functions and parameters description.*

We calculate $r_d(t)$ through a sentence, such that it counts one when the precipitation on the day t is greater than the threshold given by q_a. The threshold q_a considers a historical amount of significant rain millimeters per day, such that its calculus is based on the city annual mark cited in Chapter 1, divided by 365 days so that it represents an average, but we take into account 75% of it. For both cities, we notice that $3mm < q_a < 6mm$. Then we have

$$r_d(t) = \begin{cases} 1, & \text{if } q_p(t) > 0.75\, q_a\,, \\ 0, & \text{otherwise.} \end{cases}$$

Notice that as the period is short for the female oviposition, we can consider any water level greater than 75% of the historical daily mean of precipitation, to compose the sum in (4.9). This accounts for the strength of the rainfall influence on the *Aedes aegypti* egg-laying.

The threshold above $1mm$ is because any rain level under $1mm$ is quickly absorbed or evaporated. Besides, the air humidity does not present a significant change. In fact, it is considered rain levels above $1mm$ as standard reporting threshold for airport METAR weather reports (Spark, n.d.[a]; Spark, n.d.[b]; Spark, n.d.[c]; Spark, n.d.[d]; Spark,

n.d.[e]).

Assuming a constant time t_p between two oviposition, where $t_p = 2$ days (Lega *et al.*, 2017; Yusoff *et al.*, 2012b), then we often find 5 - 7 cycles (Schaeffer *et al.*, 2007). About the first female egg-laying, we consider as in item (xi), that for 50% of them, it occurs for the first time during their second adult day, and for another part, it is during the third day as an adult.

As described in item (xi) and according to Maimusa *et al.* (2016), the females have up to 11 cycles, thus we assume that for the females which started to lay eggs on their second day, they lay eggs till their 22nd day. A similar assumption is about the female which started to oviposit on its third day, then the fertile period is until its 23rd day (Maimusa *et al.*, 2016).

Let $f_{t,j}$ be the number of eggs laid by only one j-days-old fertile adult female mosquito on the day t depending on temperature, $1 < j \leq 23 < \eta_D$. This term composes matrix Z_t. To obtain the number of eggs laid by all j-days-old fertile adult female mosquitoes on the day t, we multiply Z_t to the vector A_t from the system in equation (4.3).

Using the result from (3.4) to compose $f_{t,j}$, it yields a temperature-dependent polynomial, which in contrast does not vary on age j, for $1 < j \leq 23 < \eta_D$ and we can set $f_{t,j} = R_A^{Eq}(\theta)$, $1 < j \leq 23 < \eta_D$.

Further, *Ae. aegypti* is considered an urban mosquito (Barbosa *et al.*, 2019; Gama *et al.*, 2013; Soares *et al.*, 2008; WHO, n.d.[b]). The poor urban structure can provide breeding sites, especially in water collections in and around houses, such as drinking water containers, water tanks, discarded car tires, elevator shafts, and flower vases (Fiocruz, 2016; CW Morin *et al.*, 2015; WHO, 2020; WHO, n.d.[b]). When rainfall is absent for a long period, the females have nowhere to lay eggs (Loncaric and Hackenberger, 2011). Plus, if the females are living in unfavorable weather conditions, they decrease the fecundity in an attempt to increase their longevity (Beserra, Castro Jr., *et al.*, 2006).

Here, we include precipitation through $r_f(t)$. This option is justified by the fact that frequent rainfalls increase the abundance of breeding sites for the female mosquito to lay its eggs (as assumption (v)) (Loncaric and Hackenberger, 2011). The historical precipitation data often requires more than 3 days for the r_f function to be nonzero. However, even if there is no recent rain $r_f(t) = 0$, there are places where some females lay eggs, thus the fecundity cannot be zero.

The parameter rrf quantifies the minimum number of eggs that one female lays living in a period with a few rainy days. It is called by the authors the rest-rain fecundity, which was represented by the constant value 5 for other species in Loncaric and Hackenberger (2011). The reason to set this constant value is that even when the environmental conditions are extremely unfavorable, and there is no rain, there are places where some females lay eggs (Loncaric and Hackenberger, 2011). For now, we consider equation (4.11) where $rrf = 3$, is the minimum number of eggs per female for each oviposition, reported in Table 3.1. It means that over temperature and precipitation conditions, the females may have a different oviposition than in laboratory conditions. Thus, we build as fecundity

function,

$$z_{t,j} = f_t^* = \frac{1}{2}\left(3\ f_{t,j}\ r_f(t)\ \alpha_c\ rrf + 7\ \alpha_c\ rrf\right),\ 2 \leq j \leq 23 < \eta_A. \tag{4.10}$$

$$\Rightarrow z_{t,j} = f_t^* = \frac{3}{2}\ \alpha_c\ \left(3\, r_f(t)\ f_{t,j} + 7\right),\ 2 \leq j \leq 23 < \eta_A. \tag{4.11}$$

Therefore, as $z_{t,j}$ multiplies the number of fertile adult females with j age on the day t, we fix $1/2$ in (4.10) to represent that half of the females lay eggs in the present day, and the remaining females in the next, as previously remarked.

Proceeding to other matrix blocks, the behavior of the population over t is ruled according to equations (4.4) and (4.5). The transition between quiescent to nonquiescent egg is modeled taking into account that sometimes an egg needs more than a first stimulus to develop. Besides, according to Chapter 3, age strongly influences the eclosion rate.

First of all, we consider a transition related to age. Thus, we know from Soares-Pinheiro *et al.* (2017) if the eggs receive three days with water in a short period and after they were dried and stored, they may develop according to the age as modeled in (3.11).

The development depends on egg age but also temperature (see Figure 3.3). Thus, we build a function considering the equations (3.8) and (3.12), as well as the fact that the newborn is able to move for the next stage, the nonquiescent egg, if it receives a good temperature.

The temperature is considered during some couple of last days as alive because we consider they need approximately 44 days to hatch (see Table 3.3).

Thus, we assume the importance of the 22 previous days wherefore the egg feels enough stimulus to start the embryonic development, even with an average temperature around 10°C (following a probability according to the transition function). Notice that if the egg has an age lower than 22, we use the temperature information since the individual was born. It becomes to consider temperature about the present up to 21 previous days, which yields θ_m.

We know that the females recognize the promising places to lay eggs and that the eggs can develop through the air humidity. For this, we use precipitation to estimate the oviposition. Until now, we focused on temperature and age to compose this transition function.

We consider the daily precipitations, and if it rained more or equal to $24q_a$ millimeters over the 24 past days (the present and 23 previous days), then the indicator value $q_p^\dagger$ is 1, otherwise, it is zero. Hence, the precipitation indicator is replaced by α_c. We are using accumulated precipitation during 24 days once humidity influences the hatching rate (Costa *et al.*, 2010).

Even during periods of intermittent rainfall, there are urban places where some eggs can develop (Caprara *et al.*, 2009) apud (Novaes *et al.*, 2022). For this, we set a parameter α_c, where $0 \leq \alpha_c \leq \alpha_{fuzzy} = 0.5$, that is a rate to measure the influence of the absence of precipitation during past days for each city.

A value closer to 0 means that the sanitation panorama of the city is ideal, and the *Aedes aegypti* population development is limited, according to lower precipitation periods, i.e., water sources' lack. It is an output of a fuzzy rule-based system described in Chapter 2, which is also used to compose the aquatic development stage mortality and female fertility.

Based on the sanitation-related services situation in Brazilian regions, around 55% of the total population has wastewater collection and only 47% is treated (Novaes *et al.*, 2022). As well as for urban waste is not better since 92% of the population has a waste collection, but just 59% is disposed of adequately (Novaes *et al.*, 2022). We set $\alpha_{fuzzy} = 0.5$ as the maximum value, which varies according to the city sanitation's panorama.

Finally, we build

$$\rho^{q}_{t,j} \quad = \quad \left(R^{Et}_{Eq}(\theta_m)\, R^{Ej}_{Eq}(j)\right)\, \left(\alpha_c + (1-\alpha_c)\, q^{\dagger}_{p}\right), \tag{4.12}$$

in which θ_m and $q^{\dagger}_{p}$ are functions with argument t, once they depend on the weather on the day t and previous days.

Thus, θ_m is a medium accumulated temperature. We use information up to 22 previous days, but with double importance over the stimulus provided by the present day. It becomes,

$$\theta_m = \frac{\theta(t) + \theta(t-1) + \theta(t-2) + \cdots + \theta(t-t_m) \;+\; \theta(t)}{t_m + 2}, \tag{4.13}$$

while $j - t_m > 0$ and $0 \leq t_m \leq 21$. That is,

$$\theta_m = \frac{\theta(t) + \sum_{k=0}^{t_m} \theta(t-k)}{t_m + 2}, \tag{4.14}$$

such that $j - t_m > 0;\ 0 \leq t_m \leq 21$.

Similarly, $q^{\dagger}_{p}$ in (4.12) quantifies an indicator for accumulated precipitation of past days. It indicates the accumulated precipitation of two days more than for temperature, once we expect there is still humidity a few days after the rain because it is stored in containers, roofs, leaves, and so on, which contributes to the population dynamics. Hence, we assume the egg can receive humidity through precipitation of a recent day. Then we build the precipitation indicator,

$$q^{\dagger}_{p}(t) = \begin{cases} 1, & \text{if } q_{pm}(t) \geq q_a\,, \\ 0, & \text{otherwise}\,. \end{cases} \tag{4.15}$$

Upon we calculate an average of precipitation of previous days limited by the age of the individual, that is a mean of precipitation q_{pm} including the information of 2 previous

days more than the days considered in (4.14),

$$q_{pm}(t) = \frac{q_p(t) + q_p(t-1) + q_p(t-2) + \cdots + q_p(t-(t_m+2))}{t_m+3}. \tag{4.16}$$

Again, $j - t_m > 0$ and $0 \leq t_m \leq 21$. Hence,

$$q_{pm}(t) = \frac{\sum_{k=0}^{t_m+2} P(t-k)}{t_m+3}, \tag{4.17}$$

such that $j - t_m > 0;\ 0 \leq t_m \leq 21$.

When the indicator of $q_p^\dagger$ is zero, the parameter α_c of the city contributes to the model. Notice that $q_p^\dagger$ is an indicator function, from where we sum the precipitation during the past days and check if the sum is bigger than $24q_a\ mm$ to ensure the indicator receives 1, otherwise, it is zero.

It means that we use the temperature data since the egg was laid (limited by 21 previous days) and the precipitation data from 2 days earlier (limited by 23 previous days).

For this approach, if the environmental conditions do not provide the same laboratory conditions, then it is important to consider some restrictions on this population. Therefore, we are taking into account the age. After 492 days, we do not have reports to prove the egg can hatch as an alive larva. Thus, we consider time as a limiting factor assuming that a 500 days old quiescent egg does not interfere with the population dynamics anymore.

Indeed, through $R_{E^q}^{Ej}(j)$ in (4.12), the 500 or plus days-old eggs have a small percentage according to the function. When it is multiplied by the temperature function and the precipitation parameter, it is negligible. Hence, the last entry of the quiescent egg compartment ($M_t(500, 1)$) is ignored, i.e., it is not used for the calculus about the next time.

The mortality function for quiescent and nonquiescent eggs comes from (3.6), both depending on temperature. Thus,

$$\mu_t^q = \mu_t^e = R_{E^q}^0(\theta) = R_E^0(\theta). \tag{4.18}$$

After the egg is living as nonquiescent, it does not need more water for a few days, once it has some stored reserves and is more exposed to the temperature stimulus. With a good temperature, the egg may hatch.

Thereby, for the transition between nonquiescent egg and larva, following equation (3.5),

$$\rho_t^e = R_E^D(\theta) = 0.00764\ (\theta + 273)\ \frac{e^{40.55 - \frac{13094.10}{\theta+273}}}{1 + e^{92.501 - \frac{28169.2}{\theta+273}}}. \tag{4.19}$$

Then, we use (4.18) and (4.19) to replace into (4.20),

$$\begin{aligned} x_{t,j} &= (1-\rho_t^e)(1-\mu_t^e) \text{ for } 1 \leq j \leq \eta_E - 1 \text{ and} \\ w_{1,j} &= \rho_t^e (1-\mu_t^e), \text{ for } 1 \leq j \leq \eta_E. \end{aligned} \tag{4.20}$$

Regarding the mortality rate, it is classified as temperature-dependent by Lega *et al.* (2017) and assumes the function given by Rossi, Ólivêr, *et al.* (2004) described in (3.6),

$$\mu_t^e = 0.0731\,(\exp(0.0595\,\theta)). \tag{4.21}$$

We set this function although the authors established the mortality taking into account only one egg compartment, not two as in this work. In this case, we consider the same mortality function for quiescent and nonquiescent eggs (see Figure 3.2(b)). Besides, according to equations (4.18) and (4.21) we expect that older quiescent eggs (with more than 500 days old) do not contribute to the population dynamics, as v_{η_Q,η_Q} and s_{1,η_Q} determine in (4.7) and (4.8).

To improve the model we consider larvae and pupae stages together as an aquatic development stage, similar to H. Yang (2014) and H. Yang *et al.* (2009). For its mortality and transition rates, H. Yang *et al.* (2009) proposed parametrized functions that depend on the temperature as described in (3.1) and (3.2). Then, we build,

$$\begin{aligned} \mu_t^d &= 6.794\times10^{-6}\,\theta^4 - 6.778\times10^{-4}\,\theta^3 + 2.457\times10^{-2}\,\theta^2 \\ &\quad - 3.797\times10^{-1}\,\theta + 2.130\,, \\ \rho_t^d &= -3.420\times10^{-10}\,\theta^7 + 5.153\times10^{-8}\,\theta^6 - 3.017\times10^{-6}\,\theta^5 \\ &\quad + 8.723\times10^{-5}\,\theta^4 - 1.341\times10^{-3}\,\theta^3 + 1.164\times10^{-2}\,\theta^2 \\ &\quad - 5.723\times10^{-2}\,\theta + 1.310\times10^{-1}\,. \end{aligned} \tag{4.22}$$

However, we add the water abundance influence in this stage as an attempt to estimate the city maintenance when there are a few rain episodes. For this, we apply α_c and $r_f(t)$ again. Given $r_f(t) = 0$, i.e., if there was no significant rain level during the present day and two previous days, it yields greater mortality of the aquatic development stage, once it needs water for maturing,

$$\mu_t^d = \mu_t^d(1 + (\alpha_{fuzzy} - \alpha_c)) = R_D^0(\theta)(1.5 - \alpha_c)\,. \tag{4.23}$$

From equation (4.23), we notice that the larval and pupal development varies with the basic sanitation if there is no rain.

Therefore, we replace the transition and mortality functions as (4.22) to obtain

(4.24),

$$\begin{aligned} q_{t,j} &= (1-\rho_t^d)(1-\mu_t^d) \text{ for } 6 \leq j \leq \eta_D - 1\,, \text{and} \\ r_{1,j} &= \rho_t^d(1-\mu_t^d), \text{ for } 6 \leq j \leq \eta_D\,, \end{aligned} \tag{4.24}$$

considering only $(1-\mu_t^d)$ for those specific entries of Q_t where $j = 1, 2, \cdots, 5$. In this way, the functions do not depend on age, only temperature, and precipitation.

Finally, we have the adult female stage. For the mortality rate, we set a temperature-dependent function from H. Yang *et al.* (2009) given by (3.3) and we replace it to configure the matrix U_t, where $u_{t,j} = 1 - \mu_t^a$ is based on (4.25),

$$\begin{aligned} \mu_t^a = R_A^0(\theta) &= 3.809 \times 10^{-6}\,\theta^4 - 3.408 \times 10^{-4}\theta^3 + 1.116{\times}10^{-2}\,\theta^2 \\ &\quad - 1.590 \times 10^{-1}\,\theta + 8.692 \times 10^{-1}\,, \end{aligned} \tag{4.25}$$

for $1 \leq j \leq \eta_A - 1$.

Therefore, we built the whole model, as the matrix Z_t was already described (remember equation (4.11)).

We are not modeling the functions and parameters through the data provided by Fiocruz. Instead, we seek out biological experiments from the literature. The parameters can be difficult to determine over field conditions, due, for instance, to nutrient competition (Schaeffer *et al.*, 2007). These sensitive parameters can distort the model outputs (Schaeffer *et al.*, 2007). One way to set parameters and validate the model is to compare it with real data. The data helps us to catch the individual's fluctuations when we run the model, and compare the results. From then on, we improve the model by adding important variables.

4.4 System Structure

Structured population models denote classifications or cohorts of individuals and follow these groups in time (Cushing and Yicang, 1994). In fact, these models afford to consider the knowledge and data that biologists have amassed about the individuals (Cushing and Yicang, 1994).

When we run the model, P_t is different than P_{t-1} because the projection matrix depends on the weather in the present and previous days. Indeed, if we consider (4.2) through (4.7) and (4.8), we note that the calculations vary according to the day t.

Studying the model taking into account the equation (4.1), it becomes

$$M_{t+1} = P_t\, M_t = (T_t + F_t)\, M_t = T_t\, M_t + F_t\, M_t\,, \tag{4.26}$$

with $M_0 \geq 0$. Population amount is not negative, then we investigate the equilibrium solution and its stability (Cushing and Yicang, 1994).

Considering $M_{t+1} \approx M_t$, for a convergence problem with a fixed point method, we assume when it tends to the equilibrium, equation (4.26) yields

$$M_t = T_t M_t + F_t M_t \Rightarrow M_t - T_t M_t = F_t M_t$$
$$\Rightarrow (I - T_t) M_t = F_t M_t \Rightarrow M_t = (I - T_t)^{-1} F_t M_t \,. \tag{4.27}$$

And we can study the matrix $(I - T_t)^{-1} F_t$, instead of P_t. It provides results even in cases where we cannot find P_t eigenvalues, especially those analyzed over extreme conditions. After all, F_t includes a first line with values that used to be greater than 1, while T_t has entries non-negatives and smaller than one.

For the existence of $(I - T_t)^{-1}$, a sufficient condition is that each sum of the column of T_t is strictly less than 1 (Cushing and Yicang, 1994),

$$0 \leq \sum_{i=1}^{m} p_{ij} < 1 \,. \tag{4.28}$$

The sums of the columns of T_t are strictly less than 1, because we built the mortality functions such as the mortalities were never zero for any environmental conditions. It means there is a loss at each class over each time step, which implies the dissipative condition (Cushing and Yicang, 1994). It implies for the j-column, in general, we add $\rho^s_{t,j}(1 - \mu^s_t)$ to 0 or to $(1 - \rho^s_{t,j})(1 - \mu^s_t)$, from where we obtain

$$[(1 - \rho^s_{t,j}) + \rho^s_{t,j}](1 - \mu^s_t) = 1(1 - \mu^s_t).$$

By doing this, we guarantee a sufficient condition for the existence of $(I - T_t)^{-1}$, because as determined in equation (4.6), all the mortality functions yield $1 \geq \mu^s_t \gg 0$, besides $1 \geq \rho^s_{t,j} \geq 0$. Then according to Cushing and Yicang (1994), the product $(I - T_t)^{-1} F_t$ exists.

We set P_t as weather-independent P to study the stability of the model according to different scenarios. For this, we assume mean temperature and precipitation remain constant over the days, that is, $P = T + F$ is time-invariant. It is weather-independent when we build a linear autonomous structural model. In this case, we are able to apply some results found through the literature (Cushing and Yicang, 1994).

4.5 The theory behind general structured models

Structured population models designate classifications or clusters of individuals, following them in time (Cushing and Yicang, 1994). We discussed linear autonomous structured models for populations closed to immigration and emigration. For this, we supposed the matrix was constant over t, i.e., ignoring the day dependence in the model, as if the weather and sanitation were constant during the days.

Assume that individuals of a population are distributed into m classes. The number (or density) $M_i(t)$ in class i at time t is arranged in a class distribution vector $M(t)$.

Let $p_{ij} \in [0,\ 1]$ be the fraction of individuals in class j expected to shift to class i during one unit of time. It means that $0 \leq \sum_{i=1}^{m} p_{ij} \leq 1$, for $j = 1, 2, \cdots, m$. We denote by T the $m \times m$ transition matrix composed of these transition probabilities,

$$\begin{aligned} T &= (p_{ij}), & p_{ij} &\in [0,\ 1] \\ 0 \leq \sum_{i=1}^{m} p_{ij} &\leq 1, & j &= 1, 2, \cdots, m. \end{aligned} \tag{4.29}$$

Regarding the individuals in the population at time t, arranged in $M(t)$, when they survive to time $t + 1$, they are redistributed according to the vector $T\,M(t)$ (Cushing and Yicang, 1994).

Plus, let f_{ij} represent the expected number of i-class newborns per j-class individual alive at time $t + 1$. It comes from the births which occur during the time interval $(t, t + 1)$. Thus, F is the $m \times m$ fertility matrix

$$F = (f_{ij}) \geq 0, \quad f_{ij} \geq 0 \quad \text{and} \quad \sum_{i,j=1}^{m} f_{ij} \neq 0. \tag{4.30}$$

The vector of newborns at time $t + 1$ comes from $F\,M(t)$.

Considering both products, we calculate the distribution at time $(t + 1)$ through the matrix difference equation system

$$M(t + 1) = P\,M(t), \quad M(t_0) \geq 0, \quad t = t_0,\ t_0 + 1,\ t_0 + 2,\ \cdots \tag{4.31}$$

where the projection matrix P is given by

$$P = F + T \geq 0. \tag{4.32}$$

In this way, $M(t)$ is uniquely determined for all $t > t_0$ by recursive formula (4.31), once the initial population $M(t_0)$ is given.

First of all, we suppose that

the matrix P given by (4.32), (4.30) and (4.29) has a positive, simple, strictly dominant eigenvalue λ whose associated (right) eigenvector $v > 0$ is strictly positive. (4.33)

Sufficient for this assumption is that for $P = T + F$, we get $(I - T)^{-1}F$ non-negative, irreducible, and primitive (or equivalently, that some integer power of $(I - T)^{-1}F \geq 0$ is strictly positive. However, this is not necessary since we do not require that the left eigenvalue be strictly positive. Therefore, assumption 4.28 implies $(I - T)^{-1} = \sum_{k=0}^{\infty} T^k$, thus $(I - T)^{-1} \geq 0$ (Cushing and Yicang, 1994).

The dynamics of the model population (4.31) provide the analysis of the equilibrium (constant) solutions and the stability of the equilibrium.

The sum from (4.32) is expected to define the net reproductive number n for the matrix

P. This value allows studying the stability of the model, instead of calculating its eigenvalue λ. That is, we determine the eigenvalue of the matrix $(I-T)^{-1}F$ instead of the eigenvalue of the matrix P. The net reproductive number is easily calculated when T and F agree with the following assumptions.

First of all, we assume the inverse

$$(I-T)^{-1} = (e_{ij}) \text{ exists.} \tag{4.34}$$

The condition from equation (4.29) is necessary but making it more strict is a sufficient condition of existence. That means to guarantee that all of the column sums of T be strictly less than 1, such that

$$0 \leq \sum_{i=1}^{m} p_{ij} < 1, \qquad j = 1, 2, \cdots, m. \tag{4.35}$$

It produces some loss to each class over each time interval, which can be biologically seen as natural mortality.

The entry in (4.34), e_{ij}, gives the expected time spent in class i by an individual starting in class j during its lifetime (Cushing and Yicang, 1994). On the other hand, we consider $(I-T)^{-1}F = G = (g_{ij})$.

Thus, g_{ij} produces the expected number of i class offspring that an individual born into class j will produce over its life time (Cushing and Yicang, 1994).

Finally, the second assumption is about G, where

$$(I-T)^{-1}F \textit{ has a positive, simple, strictly dominant eigenvalue } n \textit{ whose right eigenvector } y > 0 \textit{ is strictly positive.} \tag{4.36}$$

A non-necessary but sufficient condition for this assumption is that $(I-T)^{-1}F$ is non-negative, irreducible, and primitive or, equivalently, that some integer power of $(I-T)^{-1}F \geq 0$ is strictly positive. We do not need to guarantee this condition since we do not require that the left eigenvalue be strictly positive. In fact, $F \geq 0$ by definition in (4.30). According to (4.35),

$$(I-T)^{-1} = \sum_{k=0}^{\infty} T^k,$$

therefore $(I-T)^{-1} \geq 0$.

Assume that F and T satisfy (4.34) and (4.36). Then n is named the net reproductive value for the model equation (4.31)–(4.32). (4.37)

4.5.1 Net reproductive number n

For Leslie's models, the newborns are always in the first age class, so the surviving individuals proceed to the next age class, which turns out that is easy to watch a cluster of individuals in time, with respect to their movements and reproductive activity. Hence the achievement of n in terms of the age-specific fertility and survival rates is quite simplified, which produces the expected number of offspring per individual over its lifetime (Cushing and Yicang, 1994).

In the general structured model described in (4.31), newborns are able to lie in any class, and individuals in one class can move to any other class in one unit of time.

For example, consider the newborn cohort produced by an adult population with $y > 0$, for y the positive eigenvector corresponding to n. For straightforwardness, we assume (4.35). Hence,

$$(I - T)^{-1} F\, y \;=\; n\, y \;\Rightarrow\; F\, y \;=\; n\,(I - T)\, y.$$

Considering a distribution where $b = Fy$, then $b = n(I - T)y$. We will watch a cohort in time and calculate the average number of offspring over the expected lifetime. After k time steps the distribution of this cohort b is $T^k b$, $k = 0, 1, \ldots$ In the same way, the offspring produced by this cohort is $FT^k b$. Therefore, the distribution of the total expected number of offspring produced by the cohort b along the time is

$$\sum_{k=0}^{\infty} FT^k b = F(I - T)^{-1} b = nb.$$

Analyzing a singular individual, we conclude that the expected number of offspring produced by one individual over its lifetime is the net reproductive number (Cushing and Yicang, 1994),

$$\frac{\sum_{i=1}^{m} nb_i}{\sum_{i=1}^{m} b_i} = n.$$

The net reproductive value n determines the stability of the trivial equilibrium in age-structured population models (Cushing and Yicang, 1994). For generalized structured population models, the net reproductive number is a generalization of that for the age model under assumptions (4.33), (4.34) and (4.36).

Lemma (for details see Cushing and Yicang (1994)). For a initial distribution $M(t_0) = M^o \geq 0$ $(\neq 0)$, n provides information about the population densities, where

(i) $n < 1$ implies $\lim_{t\to\infty} M_i(t) = 0$ for all $i = 1, 2, \ldots, m$.

(ii) $n > 1$ implies $\lim_{t\to\infty} M_i(t) = +\infty$ for all $i = 1, 2, \ldots, m$.

For $n = 1$ there exist positive equilibrium solutions $M = cv$ of the model equations.

Theorem (for details see Cushing and Yicang (1994)). Assume that P satisfies (4.33) and that F and T satisfy (4.34) and (4.36). Then $\lambda > 1$ (respectively $\lambda < 1$ of $\lambda = 1$) if and only if $n > 1$ (respectively $n < 1$ or $n = 1$).

Corollary ((Cushing and Yicang, 1994)). Let P satisfy (4.33). Then $n < 1 \Rightarrow\ n \leq \lambda \leq 1$ and $n > 1 \Rightarrow\ 1 \leq \lambda \leq n$.

4.5.2 Single Newborn Class Model

In this Section, we consider a general population model, but with an assumption: all newborns lie in the same class. Let class $i = 1$ as our model, without loss in generality.

An eigenvalue that carries biological information about the stability of the trivial equilibrium is the one associated with the system

$$(I - T)^{-1} F\, y \ = \ n\, y. \tag{4.38}$$

If n is positive, it is called the net reproductive number.

We expect a positive eigenpair to investigate population biology. Once the net reproductive number is the expected number of offspring per individual over its lifetime, and only for y strictly positive the initial assumption in equation 4.36 is valid.

The entries in the inverse $(I - T)^{-1} = (e_{ij})$, for $i, j = 1, \cdots, m$ are given by $e_{ij} = \frac{c_{ji}}{\det(I-T)}$, according to the transpose of the cofactors matrix, where c_{ji} is the cofactor of the $ji\text{-}th$ entry in $I - T$. Thus, we built

$$(I - T)^{-1} F = \frac{1}{det(I - T)} \begin{pmatrix} c_{11}\, f_{11} & c_{11}\, f_{12} & \cdots & c_{11}\, f_{1m} \\ c_{12}\, f_{11} & c_{12}\, f_{12} & \cdots & c_{12}\, f_{1m} \\ \vdots & \vdots & \ddots & \vdots \\ c_{1m}\, f_{11} & c_{1m}\, f_{12} & \cdots & c_{1m}\, f_{1m} \end{pmatrix}.$$

We highlight that each row is a scalar multiple of the first row in F, then 0 is an eigenvalue of multiplicity $m - 1$. The remaining eigenvalue and associated eigenvector for our single newborn class model, we calculated it by

$$n = \frac{1}{\det(I - T)} \sum_{k=1}^{m} f_{1k} c_{1k}\,. \tag{4.39}$$

It sweeps matrix columns because the model has a unique class of newborns. The entry f_{1k} is at the $k\text{-}th$ column and the first line of the fertility matrix. Here c_{1k} is the cofactor of the $1k\text{-}th$ entry of $(I - T)$ (Cushing and Yicang, 1994). It composes the y vector either, as $y = (c_{11}, c_{12}, \cdots, c_{1m})'$.

Biologically, n measures the expected number of offspring per individual over its lifetime (Cushing and Yicang, 1994). This number is used numerically to study the asymptotic dynamics of the population (Cushing and Yicang, 1994). It "can be used to determine the stability of the trivial equilibrium and hence the growth and survival or the decay and ultimate extinction of the population" (Cushing and Yicang, 1994).

We conclude the stability $n < 1$ or instability $n > 1$ of the trivial equilibrium. If $n = 1$,

then there exists a family of positive equilibria $x = cv$, where c is an arbitrary positive constant. Therefore, we conclude the trivial equilibrium is asymptotically stable if $n < 1$, and unstable for $n > 1$. Cushing and Yicang (1994) reported a patterned way to find n for general matrix models with a single newborn class. Thus, there are explicit algebraic formulas for n, which are often derivable, when no such formulas for λ are available (Cushing and Yicang, 1994).

Besides, a corollary guarantees that n provides a threshold for λ, such that $n \leq \lambda \leq 1$ or $1 \leq \lambda \leq n$.

If both n and λ are known, we calculate the mean generation time as

$$\gamma = \ln n / \ln \lambda,$$

where λ represents the growth rate of the population (Cushing and Yicang, 1994).

We expect zero to be stable in the case we have a matrix that represents bad weather, i.e., colder or warmer temperatures, and few precipitations. After all, different initial conditions still produce a decrease in the population. This tendency is reflected by $n < 1$, where the trivial equilibrium is stable.

Instead, good environmental surrounding improves a net reproductive number greater than 1, where any perturbation around the trivial equilibrium is unstable.

Note that the matrix F carries the biggest numbers of P. We study $(I - T)$ proprieties since this matrix is lower diagonal, where all entries are ranged between $[0, 1]$, which improves the mathematical tools concerning to determinant and cofactor matrix. In fact, as T has a null main diagonal, it implies that the determinant used to compose the net reproductive value is always 1. We perceive from mathematical simulations, that the matrix $(I - T)$ was better conditioned than P.

4.5.3 Structure example

We consider an example studied for the perennial plant *Dipsacus sylvestrix* Huds. They have a medicinal application for Lyme disease and a mathematical application for population projection matrix. Werner and Caswell (1977) categorized the plants into seven life cycle stages: seeds, 1-year dormant seeds, 2-year dormant seeds, small rosettes, medium rosettes, large rosettes, and flowering plants as Figure 4.5.

The fertility and transition matrices compose the projection matrix $P = T + F$, where its entries are given by

Figure 4.5: *Dipsacus sylvestrix. Source: the authors (Jul. 2020).*

$$P = T + F = \begin{bmatrix} 0 & 0 & 0 & 0 & 0 & 0 & 431 \\ 0.748 & 0 & 0 & 0 & 0 & 0 & 0 \\ 0 & 0.966 & 0 & 0 & 0 & 0 & 0 \\ 0.008 & 0.013 & 0.01 & 0.125 & 0 & 0 & 0 \\ 0.070 & 0.007 & 0 & 0.125 & 0.238 & 0 & 0 \\ 0.002 & 0.008 & 0 & 0.038 & 0.245 & 0.167 & 0 \\ 0 & 0 & 0 & 0 & 0.023 & 0.75 & 0 \end{bmatrix}.$$

The matrix T satisfies the dissipative condition Cushing and Yicang (1994), such that it consists of the sums of the columns of T that are less than 1 (the condition was mentioned in equation 4.6).

We know the fertility and transition matrices compose the projection matrix $P = T + F$, where its entries are given by

$$T = \begin{bmatrix} 0 & 0 & 0 & 0 & 0 & 0 & 0 \\ 0.748 & 0 & 0 & 0 & 0 & 0 & 0 \\ 0 & 0.966 & 0 & 0 & 0 & 0 & 0 \\ 0.008 & 0.013 & 0.01 & 0.125 & 0 & 0 & 0 \\ 0.070 & 0.007 & 0 & 0.125 & 0.238 & 0 & 0 \\ 0.002 & 0.008 & 0 & 0.038 & 0.245 & 0.167 & 0 \\ 0 & 0 & 0 & 0 & 0.023 & 0.75 & 0 \end{bmatrix}, \quad F = \begin{bmatrix} 0 & 0 & 0 & 0 & 0 & 0 & 431 \\ 0 & 0 & 0 & 0 & 0 & 0 & 0 \\ 0 & 0 & 0 & 0 & 0 & 0 & 0 \\ 0 & 0 & 0 & 0 & 0 & 0 & 0 \\ 0 & 0 & 0 & 0 & 0 & 0 & 0 \\ 0 & 0 & 0 & 0 & 0 & 0 & 0 \\ 0 & 0 & 0 & 0 & 0 & 0 & 0 \end{bmatrix}.$$

The formula from equation 4.39 can calculate the net reproductive number. As for the

fertility block we have only the non-null entry 431, then the formula becomes

$$n = \frac{1}{\det(I-T)} \sum_{k=1}^{7} f_{1k}\, c_{1k} \;\Rightarrow n = \frac{1}{\det(I-T)}\, f_{17}\, c_{17} \Rightarrow n = \frac{1}{\det(I-T)}\, 431\, c_{17}\,. \tag{4.40}$$

The entry f_{17} is at the 7-*th* column and the first line of the fertility matrix.

Here c_{17} is the cofactor of the 17-*th* entry of $(I-T)$. Thus, we disregarded the first column and line of the matrix, and calculated the determinant of the resulting 6×6 matrix, as

$$c_{17} = \begin{vmatrix} -0.748 & 1 & 0 & 0 & 0 & 0 \\ 0 & -0.966 & 1 & 0 & 0 & 0 \\ -0.008 & -0.013 & -0.01 & 0.875 & 0 & 0 \\ -0.070 & -0.007 & 0 & -0.125 & 0.762 & 0 \\ -0.002 & -0.008 & 0 & -0.038 & -0.245 & 0.833 \\ 0 & 0 & 0 & 0 & -0.023 & -0.75 \end{vmatrix} \Rightarrow c_{17} = 1.8525 \times 10^{-2}.$$

As $(I-T)$ is sparse, we easily calculate its determinant, where $\det(I-T) \approx 0.55541$. Therefore,

$$n \approx \frac{1}{0.55541} \cdot 431 \cdot 0.01825 \;\Rightarrow\; n \approx 14.376.$$

For this matrix model, we have $y = [0.5554\ 0.4154\ 0.4013\ 0.0158\ 0.0574\ 0.0229\ 0.0185]' > 0$. Therefore, $n > 1$ represents this population growing exponentially and the trivial equilibrium is unstable. The eigenvalue of the matrix P is given by $\lambda \approx 1.8842$. Then the mean generation time for this species is $\gamma = \ln n / \ln \lambda \Rightarrow \gamma = 4.207$.

Chapter 5

Numerical simulations

We present numerical simulations performed in Matlab and used to explore the fluctuations of *Aedes aegypti* population for a city over a year.

Additionally, we obtained results and compared them with the trap and weather data concerning 5 cities based on Spearman's and Pearson's correlation. The analysis includes the calculus of the net reproductive number for each city. Through simulations, we evaluated if the quiescent compartment and the derived functions could model a city scenario of *Aedes aegypti* fluctuation.

For each given municipality, Codeço *et al.* (2015) proposed and selected three areas with approximately $1km^2$ each and 2000 properties (as we presented in the map from Section 2.1). The surveillance was performed in different periods, and we used collected data from traps named BioGent-Sentinel and ovitraps, respectively, arranged in 5 mid-sized cities located in Brazil (Codeço *et al.*, 2015). The program was carried out from December 2009 to January 2012 (except for Nova Iguaçu, which occurred from July 2011 until June 2012) (Codeço *et al.*, 2015).

5.1 The cities' weather characteristics

- Campo Grande, state of Mato Grosso do Sul (Campogrande, n.d.[a]; Climate-Data, n.d.[a]; Codeço *et al.*, 2015; Spark, n.d.[a]): It has a highland tropical climate, with a dry and cold winter. The temperature range during the year varies more than in the other studied cities.

  April to October used to present a dry season.

  The annual mean temperature is around 23.4°C, and the mean total year precipitation is $1449mm$.

- Santarém, state of Pará (Adams *et al.*, 2006; Climate-Data, n.d.[d]; Codeço *et al.*, 2015; Spark, n.d.[e]): It has a tropical climate, with a monsoon season from January to May. High and variable precipitation throughout the year, mainly in March and April.

Some references consider there is no dry season, but the river level fluctuates 5 meters between the break of dry (July to December) and floating (January to June) seasons.

The annual mean temperature is around 26°C. The mean total year precipitation is 2150mm.

- Parnamirim, state of Rio Grande do Norte (Climate-Data, n.d.[b]; Codeço *et al.*, 2015; Spark, n.d.[d]): It has a tropical climate, with warm temperatures during the year, even in the winter.

  The precipitation reaches its maximum between April and May. October used to be a dry month. The rain absence period is from September to December.

  The annual mean temperature is around 25.6°C, while the mean total year precipitation is 1261mm.

- Duque de Caxias and Nova Iguaçu, state of Rio de Janeiro (Climate-Data, n.d.[c]; Codeço *et al.*, 2015; Spark, n.d.[b]; Spark, n.d.[c]): Both are adjacent cities that have a tropical climate. The high water marks occur during summer. The dry period occurs from April to October.

  The temperatures fall during the winter, especially in July.

  In Duque de Caxias, the annual mean temperature is around 23.2°C and the mean total year precipitation is 1299mm. Similarly, in Nova Iguaçu, the annual mean temperature is around 23.4°C, while precipitation is 1408mm.

5.2 Setting the initial conditions

According to Table 3.1, the life cycle in Figure 4.3, and the assumptions in items (iii)and (ix). We set $\eta_Q = 500$ days once H. Silva and I. Silva (1999) reported eclosion with 492 days, and they did not find eclosion up to 720 days. Besides, $\eta_E \ll \eta_Q$ where the maximum age is $\eta_E = 85$, and $\eta_D = 103$ days, respectively. About η_A, it was reported that the adult female mosquito can live around 57.8 ± 4.85, thus we consider $\eta_A = 63$. Likewise, the dimensions of each block of the projection matrix were determined based on the maximal time required to develop to the next stage.

In Schaeffer *et al.* (2007), the authors divided the model into two seasons. The first was concerned with the dry season, while the second was related to the wet season considering two peaks of accumulated rain (Schaeffer *et al.*, 2007). We assume only one model for fitting a year due to the similar photoperiod during the year for all municipalities and the weather influence over the model parameters.

We started running the model in the late overwintering period, or the start of breeding sites, depending on two weeks after the driest day, to provide the initial conditions. We highlight that the historical weather defined these days. The Weather Spark analyzed weather data from 1980 to 2016 period, to detect information that we describe in Table 5.1.

Brazilian Municipality	*Year's coldest day (day, °C)	Year's driest day (day, millimeter)	Drier Season (months, period)	♦Annual (millimeter)	†50% of that Annual for 24 days
Campo Grande	Jul. 19 (16)	Jul. 20 (26)	6.2 (Apr. 5-Oct. 10)	1449	47.64
Santarém	Jul. 11 (24)	Sep. 15 (20)	6.3 (Jun. 14-Dec. 25)	2150	70.68
Parnamirim	Jul. 31 (22)	Oct. 14 (4)	6.2 (Jul. 29-Feb. 4)	1261	41.46
Duque de Caxias	Jul. 20 (17)	Aug. 6 (29)	6.9 (Mar. 31-Oct. 27)	1299	42.71
Nova Iguaçu	Jul. 20 (16)	Aug. 6 (27)	6.7 (Apr. 2-Oct. 25)	1408	46.29

Table 5.1: *Critical days and characteristics (Climate-Data, n.d.[b]; Climate-Data, n.d.[c]; Climate-Data, n.d.[a]; Climate-Data, n.d.[d]; Spark, n.d.[a]; Spark, n.d.[b]; Spark, n.d.[c]; Spark, n.d.[d]; Spark, n.d.[e]). *Mean of the minimum daily temperature (average T_{min}, not average daily temperature). ♦The annual mean accumulated precipitation. †Half of the annual mean accumulated precipitation per 365 days multiplied by 24 days.*

Using weather data from the studied cities we define the coldest or driest day during the year, depending on the city's historical weather, which represents when the most unfavorable period ends and the breeding season starts, which we assume is the favorable period for *Aedes aegypti* development.

We start testing the mosquito breeding year through (two weeks after) the "Year's driest day", once it is right after the year's lowest chance of precipitation day, and the "Year's coldest day". Besides, the driest day is inside the "drier season" period, which implies we can expect the environmental conditions will start becoming better from the worse day.

In colder cities such as Campo Grande, where the adult population reaches its minimum after the coldest days of the year (Otero *et al.*, 2006), we also consider a critical day set by the driest day of the year, which occurred after the coldest.

Then we estimate the individual's proportion of younger eggs and fertile females according to the data. As we mentioned in item (i), we have information about five accumulated days about eggs while we know a unique day per month about female mosquitoes.

For the adults, BG-Sentinel collects the females searching for a blood meal (Codeço *et al.*, 2015). As they located the traps in strategic places near electric power, we assumed they were fertile females searching for breeding sites.

We use the scheme from Figure 5.1 to obtain the model output due to the egg density for about 5 consecutive days. On day $t + 4$ we kept the information since the day t, supposing the ovitrap was exposed on the day t. Then we use the information of the newborns in day t and what happened with them over the next four days as well as what happened with the new newborns during this period.

Since ovitraps stuck the quiescent egg with adhesive, and they counted 5 days of accumulated eggs per month (Codeço *et al.*, 2015), even those dead, we consider a scheme similar to the tree of possibilities from Figure 5.1. Thus, the young individual could develop till day $t + 4$ if it would not be stuck.

Our approach compares the number of eggs collected during the day t up to $t + 4$, which were counted even dead, to the individuals that could be alive during these 5 days according to the weather data, but without considering the natural mortality. It means

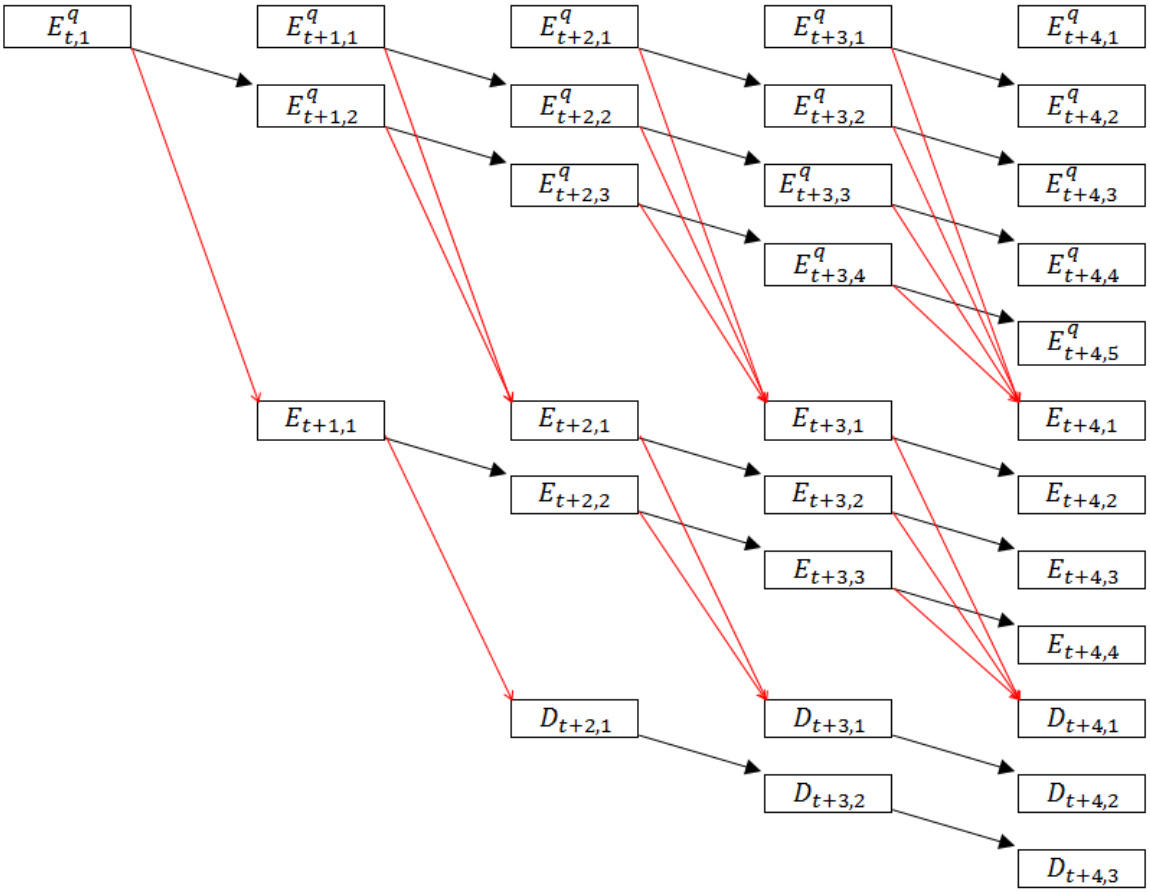

Figure 5.1: *Scheme for identifying the individuals that sum a total of 5 days old on the day $t + 4$ from day t.*

the individual could be already dead in the outputs of the model, and it composed an auxiliary variable to simulate what hypothetically would happen to it if it was alive, during a maximum of 5 days after its death.

Concerning that tree (Figure 5.1), the absence of natural mortality implies that the number of five-day-old individuals on the day $t + 4$ has the same value if we sum the one-day-old quiescent eggs in days $t, t + 1, \ldots, t + 4$.

It implies that the number of 5-day-old alive individuals is always lower than the number of individuals that we are assuming as output and comparing with the ovitrap data.

About the initial condition, but now referring to the aquatic development stage, we use a number between eggs and mosquitoes to represent the total number of individuals living in this stage.

Similarly, for the ages of quiescent and nonquiescent eggs, and the aquatic development, we use the same number of individuals for the initial condition. On the other hand, we use a lower value for the adult mosquito.

Therefore, the initial condition vector for the five cities was the same, given by =

$(E^q, E, D, A)'$ where the entries of E^q, E, D were 50000, while $A = (1000, ..., 1000)'$. We assumed an initial condition based on the real number in nature, instead of using the first data.

In fact, we set at the start there were more eggs than other individuals, once there are more coordinates for egg vectors (remember matrices sizes), following (Schaeffer *et al.*, 2007), and the collected data tendency. Indeed, at first, Schaeffer *et al.* (2007) assumed there were only immature eggs at time 0 into tree holes, because they modeled *Aedes furcifer* and *africanus* that live in forests.

We chose not to calculate a particular initial condition for each city. From our point of view, the system feeds itself, and when we start the comparisons with the data, the "initial condition" was absorbed by the dynamics of the model. That is why we do not compare the correlation during the first months of simulation due to the fluctuation. We concluded through a sensibility analysis that the results were not significantly influenced by the initial condition.

5.3 Data, model simulation, and discussion

The Brazilian institution Fiocruz collected data about surveillance schemes using traps for adults and eggs, named BioGent-Sentinel and ovitraps, respectively, arranged in 5 mid-sized cities (Codeço *et al.*, 2015). For a municipality, Codeço *et al.*, 2015 purposed and selected three areas, with approximately $1km^2$ each and 2000 properties.

The ovitraps were exposed during five consecutive days of each month. Referring to the BG-Sentinel, the exposition happened during one day. Both were located in three neighborhoods from each city, once they were arranged in urban regions with 1 km^2 of the area each.

BioGent-Sentinel (BG-Sentinel) is a bucket. There is an artificial wind produced by electric power to collect the mosquito flying near to the surface Codeço *et al.*, 2015. There is a white gauze covering. In the middle of this cover, there is a black tube from where a flow is created by an exhauster fan that captures mosquitoes flying. 24 BG-Sentinels were installed for 24 hours per 1km^2 area (monthly). They were placed indoors due to their energy requirement.

Ovitraps are containers filled with 300ml of hay infusion and with wooden paddles (Codeço *et al.*, 2015). They exposed 120 traps per 1 km^2 area, for 5 days (monthly) (Codeço *et al.*, 2015).

To install the traps, researchers needed to select houses, and a random set of geographical coordinates was taken and once in the field, the closest house was chosen (Codeço *et al.*, 2015).

The number of traps installed per km^2 was different between trap types, according to manufacturer's or literature recommendations (Codeço *et al.*, 2015). We included the data for each city, obtained from the surveillance schemes.

Figure 5.2: *BG-Sentinel and ovitrap used by* Codeço *et al. (2015).*

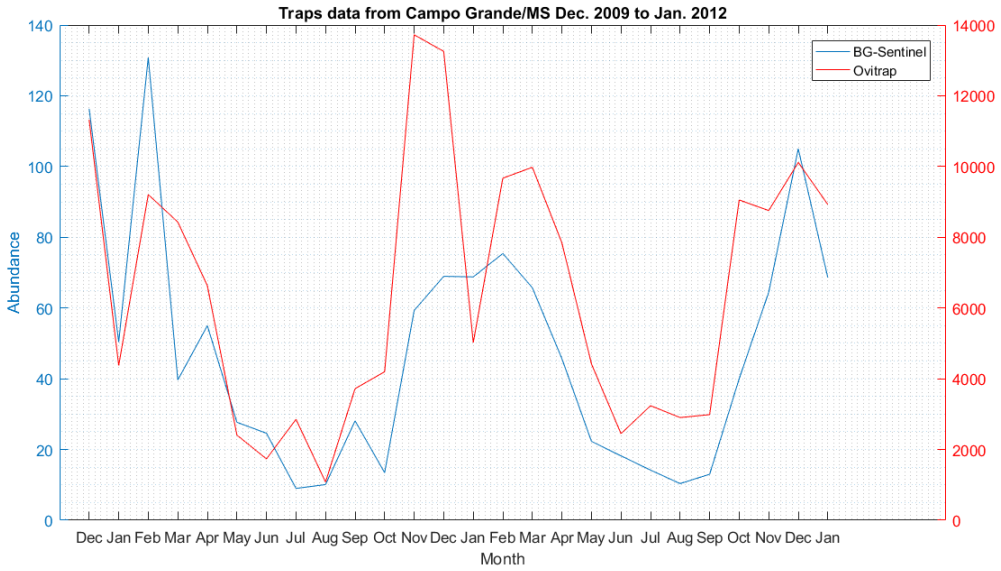

Figure 5.3: *Campo Grande's BG and ovitrap data for the surveillance period. The red line represents ovitrap data, while the blue line is for BG-Sentinel data.*

As we described before (see Figure 5.1), the Scheme sums the newborns that we kept alive and simulates what happens with them according to the transition matrix. While "Newborns up to 5" represents the alive individuals up to 5 days old as a total age. We organized the simulations considering Table 5.2.

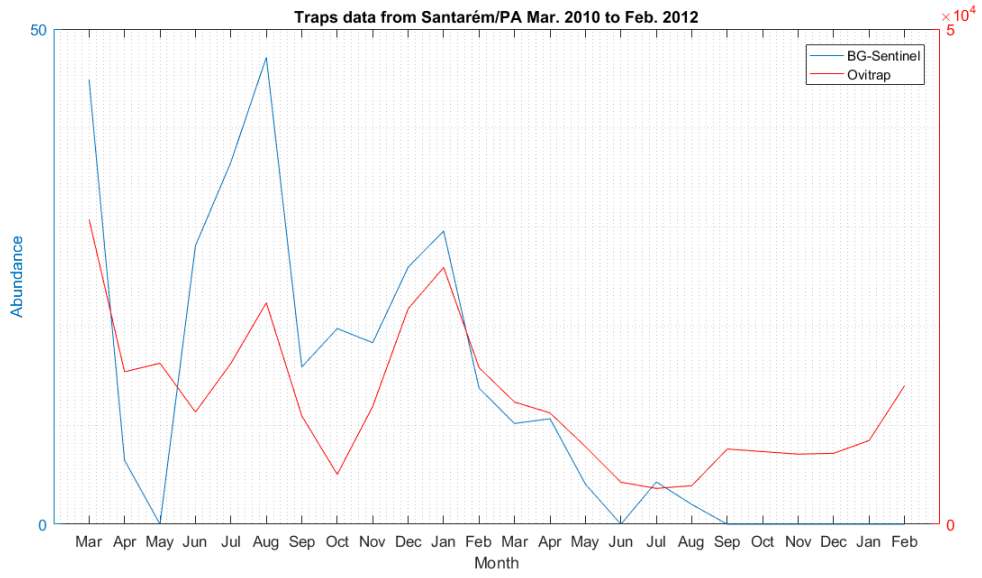

Figure 5.4: *Santarém's BG and ovitrap data for the surveillance period. The red line represents ovitrap data, while the blue line is for BG-Sentinel data.*

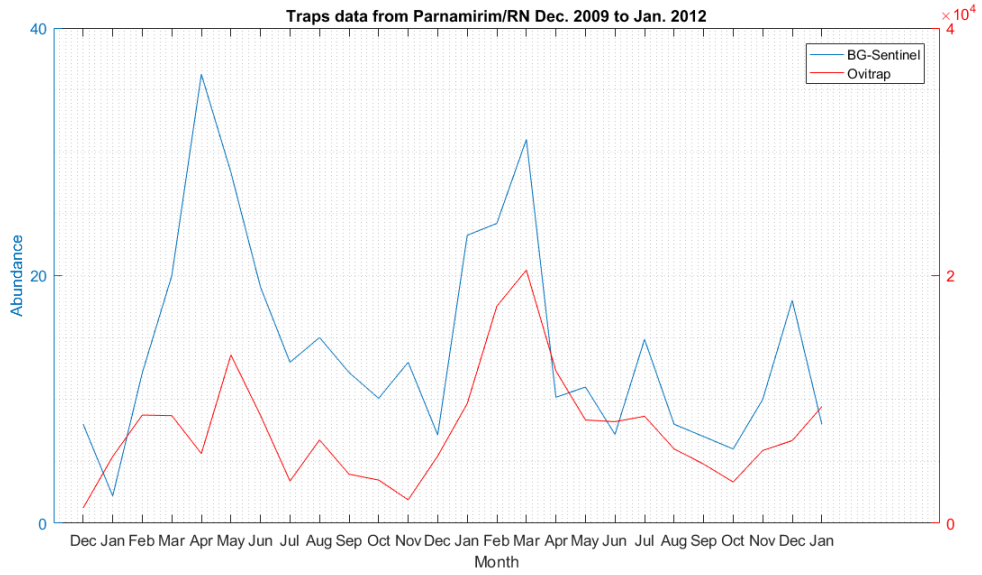

Figure 5.5: *Parnamirim's BG and ovitrap data for the surveillance period. The red line represents ovitrap data, while the blue line is for BG-Sentinel data.*

5.4 Population dynamics for Duque de Caxias/RJ

The surveillance in this city occurred from November 2009 to October 2010, and the trap data collected is shown in Figure 5.7.

Through the data, we concluded there were newborns and mosquitoes in Duque de Caxias because the traps registered data nonzero during a one-year surveillance program.

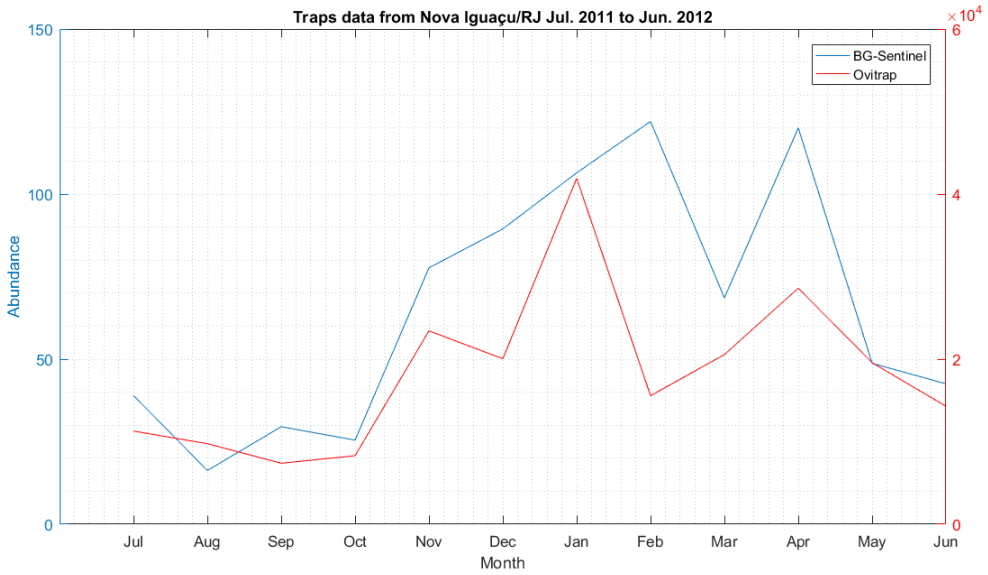

Figure 5.6: *Nova Iguaçu's BG and ovitrap data for the surveillance period. Instead of July to June, as BG was collected on June, 29th, in June 2012 they did not collect ovitrap, and it was collected lately, on July, 3rd. The red line represents ovitrap data, while the blue line is for BG-Sentinel data.*

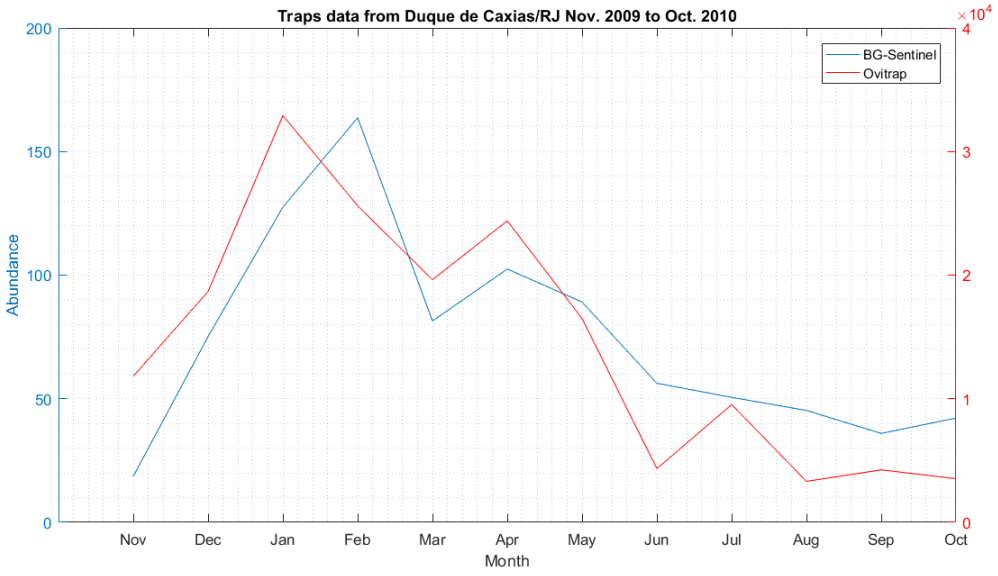

Figure 5.7: *Duque de Caxias's BG and ovitrap data for the surveillance period. The red line represents ovitrap data, while the blue line is for BG-Sentinel data.*

We built a vector composed of information about the days which we got data from Duque, adding all of its three neighborhood data, in comparison with a second vector composed of the outputs of the model for the respective days.

We use this methodology once ovitraps were exposed on the same day over the three neighborhoods, as well BG-Sentinel traps were exposed over the three neighborhoods on the same day (Nov. 17th for ovitrap and Nov. 13th for BG). Therefore, we built a vector

Symbol	Definition
MQE	Representing the model output about the total number of quiescent eggs.
MNE	Representing the model output about Nonquiescent eggs.
MQN	Representing the model output about quiescent new eggs.
MFI	Representing the model output about five-day-old individuals considering the mortality.
MDT	Representing the model output about the aquatic development stage (larva and pupa).
MAF	Representing the model output about adult females.
MFF	Representing the model output about fertile adult females.
MNS	Representing the model output about new individuals as determined by Scheme, i.e., the five-day-old individuals without considering the mortality.
DAF	Representing the data from BG-Sentinel about the adult female mosquito.
DOV	Representing the data from ovitraps about the five-day-old individuals.

Table 5.2: *Organizing data, inputs, and outputs of the model.*

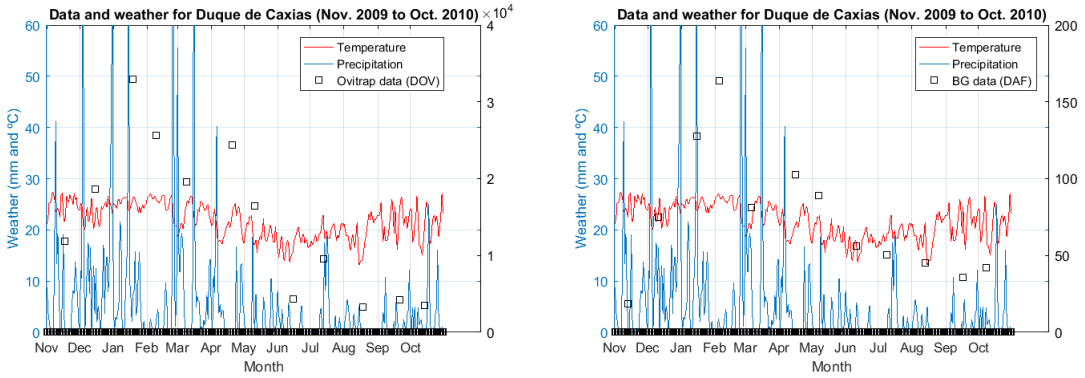

Figure 5.8: *Weather, ovitrap and BG-Sentinel data over Nov. 2009 to Oct. 2010 in Duque de Caxias.*

with nonzero data in different coordinates for BG and ovitrap.

From Chapter 2, we run the model with α_c determined according to the fuzzy rule-based system output. It produced $\alpha_c = \alpha_{DC} = 0.142$ for Duque de Caxias, and we obtained plots in Figure 5.9.

Through the first plot in Figure 5.9, we realized that the initial condition provides intense fluctuation during the starting days. From our point of view, the system feeds itself, and when we start the comparisons with the data, the "initial condition" was absorbed by the dynamics of the model. That is why we do not compare the correlation during the first months of the simulation.

In general, the simulation collected the trap fluctuations, as we compared in Figure 5.10.

We evaluated the correlation between the model outputs and the data through Pearson's and Spearman's correlations to study the model accuracy according to the real data. The relationships between data and the numerical results are presented in Figure 5.11.

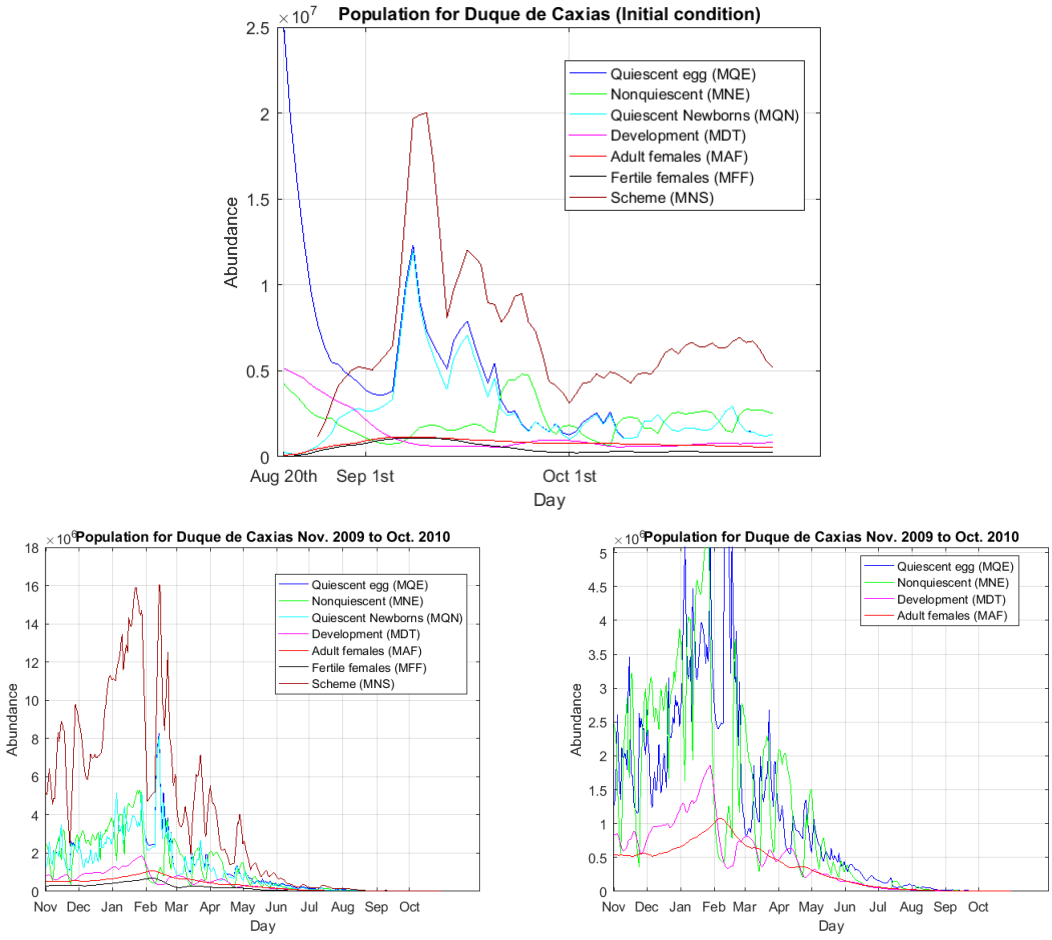

Figure 5.9: *Aedes aegypti population dynamics for Duque de Caxias.*

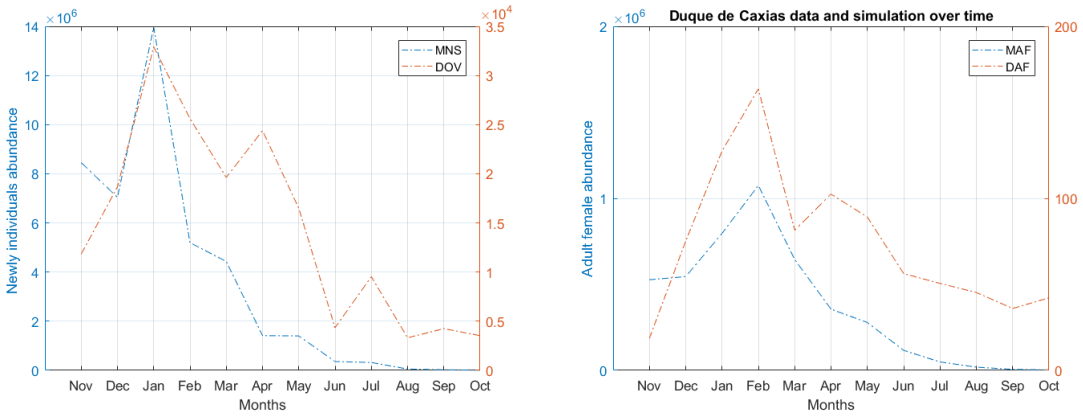

Figure 5.10: *Model output and trap data along the year. The red lines represent the data, and the blue lines are the model output. While the first plot is about new individuals, the second one is about adult females.*

.

We obtained a strong correlation with an adequate p-value for Spearman and Pearson's correlation. For ovitrap, we found a Spearman correlation of 0.818, with p-value = 0.002,

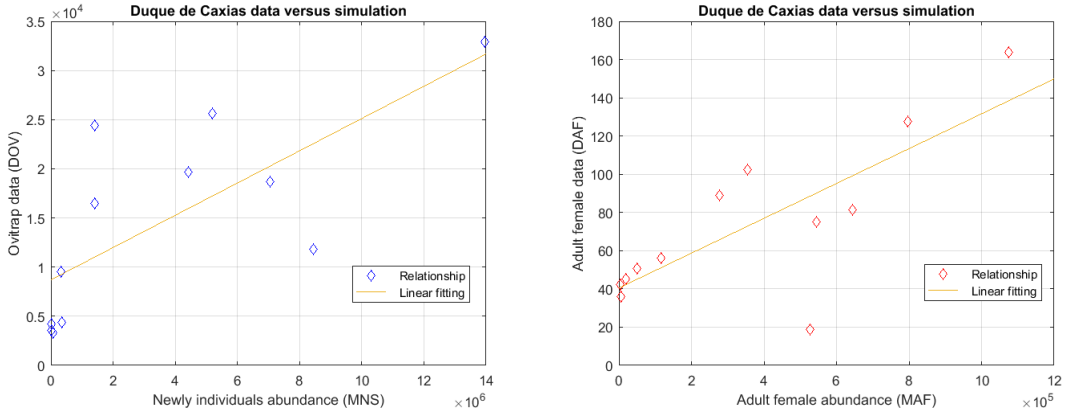

Figure 5.11: *Dependence between variables.*

while for BG-Sentinel, compared to all females, the Spearman's correlation was 0.713, with p-value = 0.012. Related to BG and fertile females, the correlation was 0.6154 (with p-value= 0.037). For Pearson's correlation, we got 0.728 for ovitrap (with p-value = 0.007), and better results for BG, around 0.7714 (with p-value= 0.003) referring to all females and 0.7709 (with p-value= 0.0033) for fertile females.

5.5 Population dynamics for Parnamirim/RN

The surveillance in this city occurred from December 2009 to January 2012, and the trap data collected was presented in Figure 5.5.

Through the data, we concluded there were newborns and mosquitoes in Parnamirim because the traps registered data during a surveillance program of 26 months.

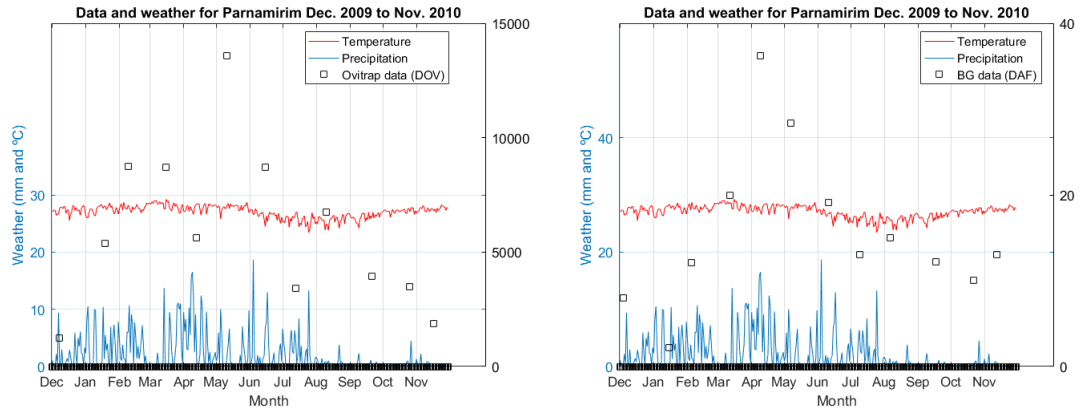

Figure 5.12: *Weather, ovitrap and BG-Sentinel data over Dec. 2009 to Nov. 2010 in Parnamirim.*

We built a vector composed of information about the days which we got data from Parnamirim, adding all of its three neighborhood data, in comparison with a second vector composed of the outputs of the model for the respective days.

We used this methodology once ovitraps were exposed on the same day over the three neighborhoods.

However, BG-Sentinel traps were exposed over the three neighborhoods on the same day except for January and April 2010. In April BG data was provided on days 9 or 10 for its three areas. In January 2010, Emaus neighborhood BG data was zero. Therefore, we calculate correlation and plots comparing the simulation of a sum of two neighborhoods, and also without computing this month.

The first days of the collection were Dec.8th for ovitrap and Dec.4th for BG. Therefore, similar to Duque de Caxias, we built a vector with nonzero data in different coordinates for BG and ovitrap for comparisons.

From Chapter 2, we run the model with α_c determined according to the fuzzy rule-based system output. It produced $\alpha_c = \alpha_{PA} = 0.182$ for Parnamirim, and we obtained plots in Figure 5.13.

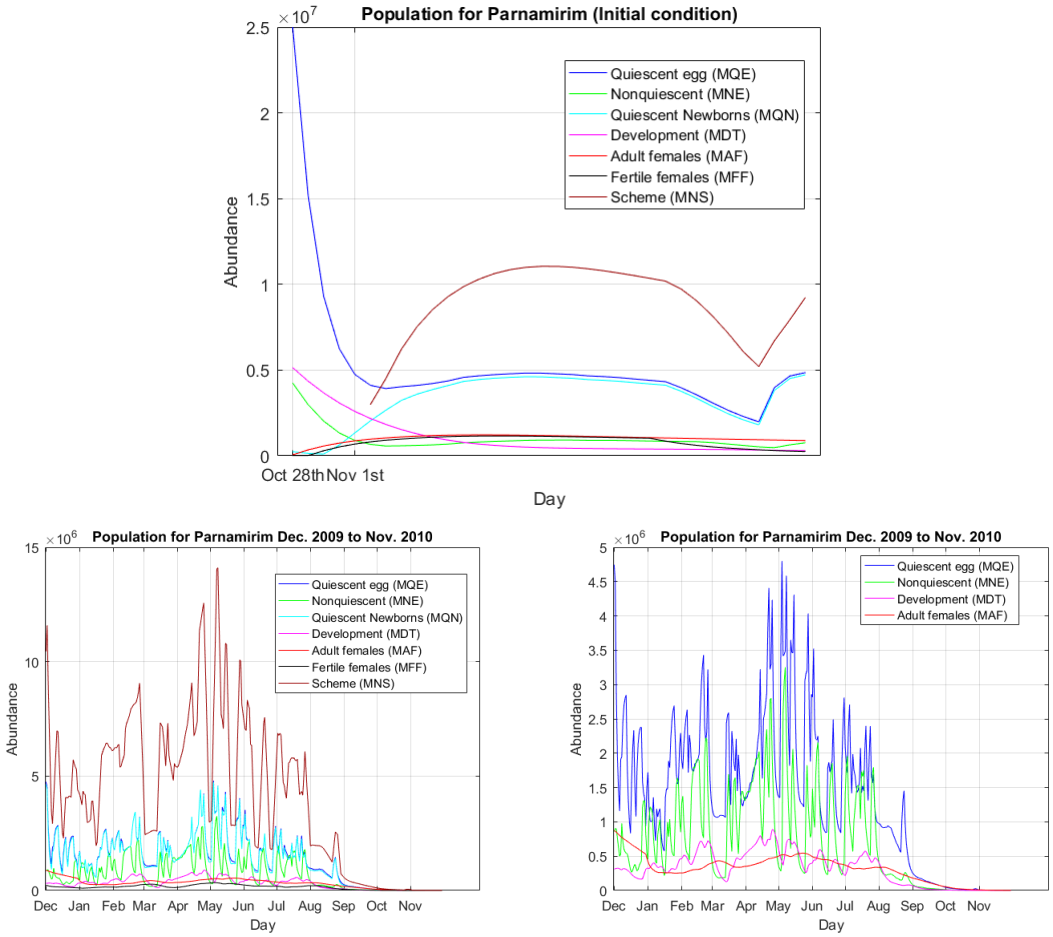

Figure 5.13: *Aedes aegypti population dynamics for Parnamirim.*

The first plot in Figure 5.13 showed that the initial condition provided intense fluctuation during the starting days. That is why we compared the correlation with and without the first month of the simulation (December 2009).

From the correlation's value and plot behavior, we concluded that comparisons after February were better than with December.

The simulation collected the trap fluctuations, as we compared in Figure 5.14.

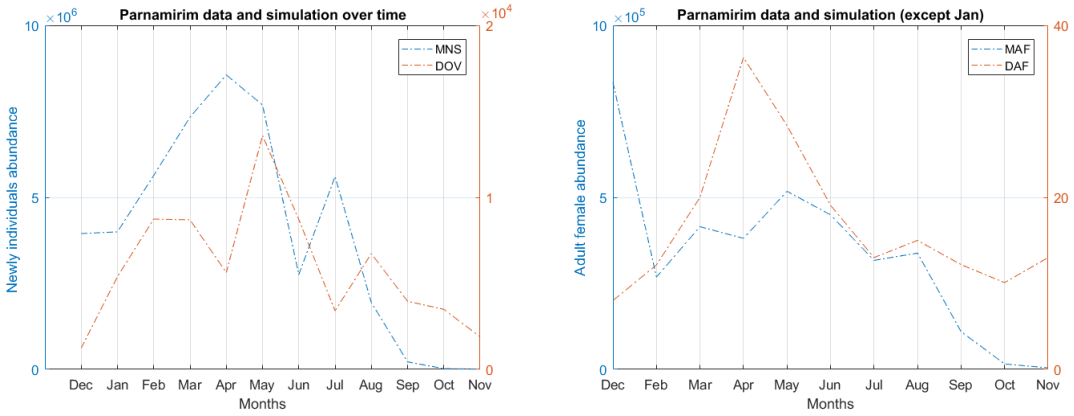

Figure 5.14: *Model output and trap data along the year. The red lines represent the data, and the blue lines are the model output. While the first plot is about newly individuals, the second one is about adult females.*

We evaluated the correlation between the model outputs and the data through Pearson's and Spearman's correlations to study the model accuracy according to the data.

The relationship between data and the numerical results is presented in Figure 5.15.

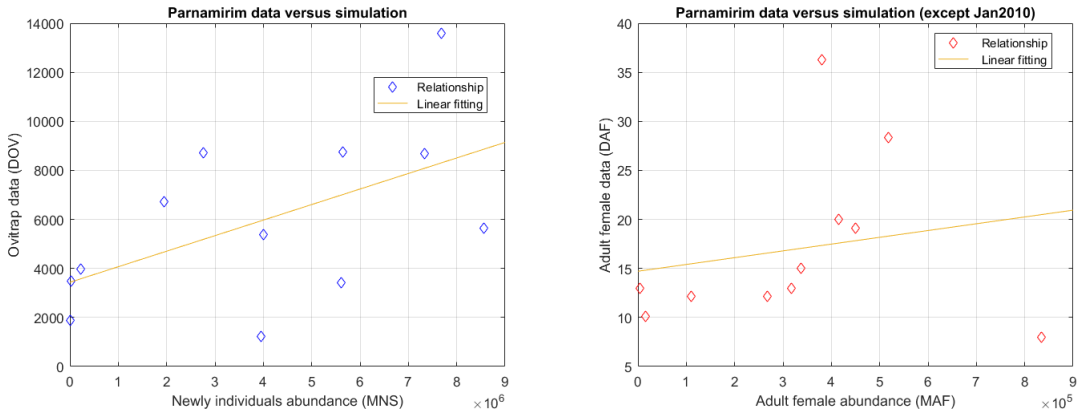

Figure 5.15: *Dependence between variables for Parnamirim results.*

We calculated the correlation and p-value for Spearman and Pearson's correlation. We found a Spearman's correlation for ovitrap and the model output scheme of 0.5385, with p-value = 0.075.

Between BG-Sentinel and fertile females, Spearman's correlation was 0.6923, with p-value = 0.016, while we included January 2010. When we did not include it, we got 0.700, p-value of 0.021. Related to all females, the correlation was lower, around 0.44, which we justified according to the location of the traps, once fertile females fly near breeding sites.

For Pearson's correlation, we got 0.5476 for ovitrap (with p-value = 0.065). Related to BG, we got the Pearson's correlation of 0.525 (with p-value= 0.0797) with fertile females

(December to November including January), but weak results referring to BG and total females, of 0.2136 with January, or 0.256 without January (with p-value= 0.448).

We highlighted that from February to November (months 3 to 12) Pearson's correlation was stronger, about 0.645 for BG and fertile according to Pearson (p-value 0.04), and even better for Spearman (for fertile females was 0.782 while for all females was 0.8303, with p-value 0.0056).

In December 2009, the correlation may be weak due to the proximity of the initial condition.

If we consider fertile females only, Pearson's correlation also became stronger, about 0.525 with p-value = 0.0797 with January, or 0.5605 without January, as well as 0.646, p-value = 0.044 from February 2010 to November 2010.

5.6 Population dynamics for Campo Grande/MS

In the capital city of the state of Mato Grosso do Sul, Campo Grande/MS, the total area was around 8100 km^2 while the urban area was around 332 km^2 (Campogrande, n.d.[b]). For urban and total population information remember the IBGE numbers in Section 2.1.

The surveillance in this city occurred from December 2009 to January 2012, and the trap data collected is in Figure 5.3.

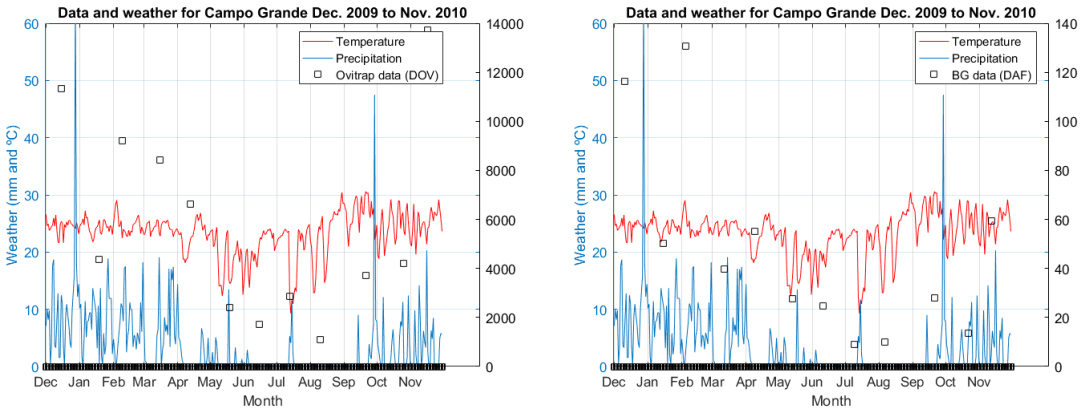

Figure 5.16: *Weather, ovitrap and BG-Sentinel data over Dec. 2009 to Nov. 2010 in Campo Grande.*

Through the data, we concluded there were newborns and mosquitoes for Campo Grande because the traps registered data nonzero during the surveillance program, except a few non-data neighborhoods (about both traps in Carlota on Jan/2010, and one zero data about ovitrap on Jan/2011 in Guanandi, as well there was null BG information of Planalto in Mar/10, Guanandi in Oct/2010, and Carlota in Sep/2011).

We built a vector composed of information about the days which we have data from Campo Grande (adding its three neighborhoods), in comparison with a second vector composed of the output of the model for the respective days.

We used this methodology once ovitraps were exposed on the same day over the three neighborhoods. On the other hand, BG-Sentinel traps were exposed over the three neighborhoods on the same day, but it used to be a different day than the ovitraps exposure, which implied we built a vector with nonzero data in different coordinates for BG and ovitrap.

We ran the model from Chapter 2 with α_c determined according to the fuzzy rule-based system output. It produced $\alpha_{CG} = 0.0861$ for Campo Grande.

Firstly, we simulated a one-year period between December 2009 and November 2010 5.17.

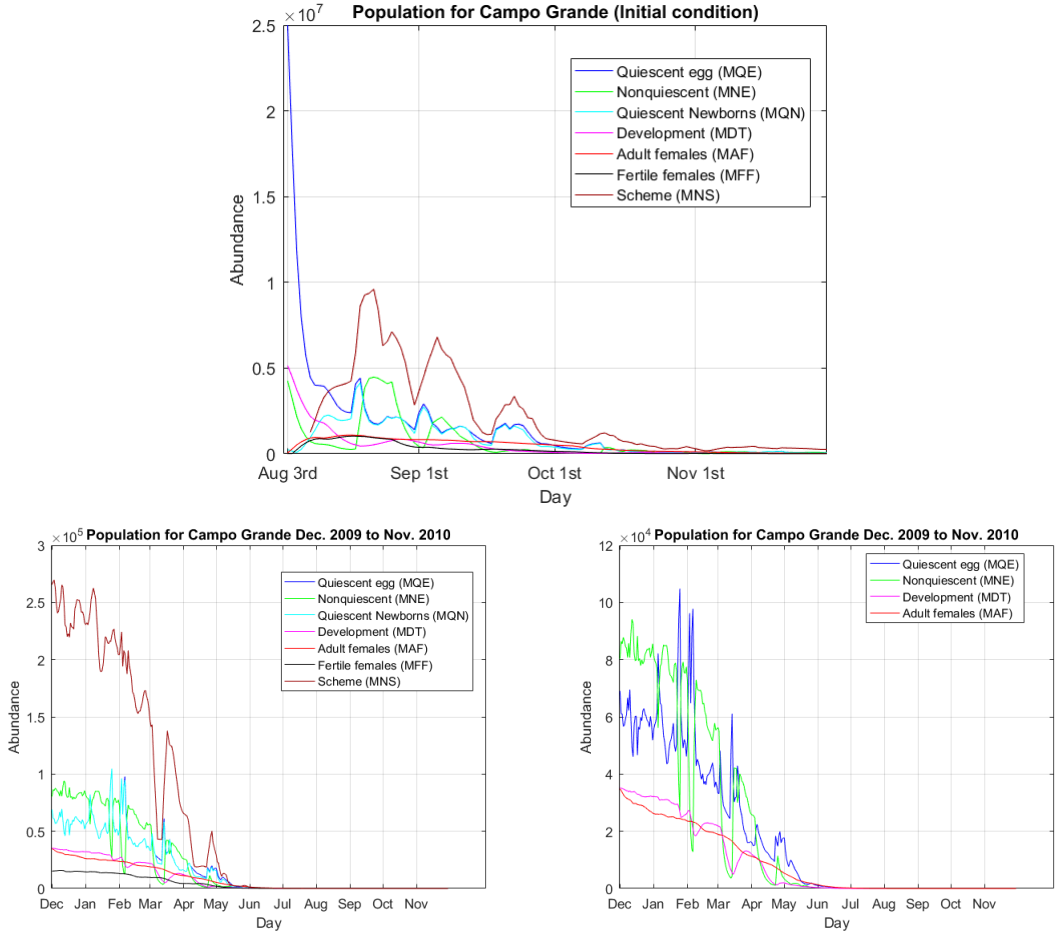

Figure 5.17: *Aedes aegypti population dynamics for Campo Grande.*

The dynamic for this period was compared for twelve months period, producing a weaker correlation than the one produced through the vectors without considering the months where a neighborhood presented null data.

For the results between the model outputs for females and the data through Pearson's correlation, while we did not take into account January/2010, March/2010, and October/2010 due to the BG null information, we got 0.9153, p-value=0.0005. Plus, 0.45 (p-value=0.23) for Spearman's correlation, therefore it was weak.

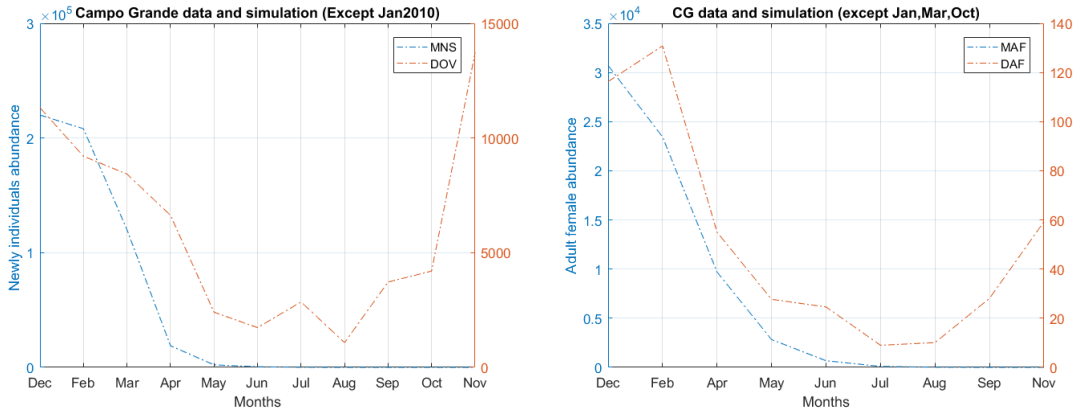

Figure 5.18: *Model output and trap data along the year. The red lines represent the data, and the blue lines are the model output. While the first plot is about newly individuals, the second one is about adult females.*

However, for fertile females, Pearson's correlation was 0.927, p-value=0.0003. Spearman's correlation was weak (0.45 p-value=0.223).

For ovitrap, we ignored only January 2010 and obtained a Pearson's correlation of 0.585 p-value=0.0586. On the other hand, we did not get a correlation for Spearmann (only 0.2455). Therefore, we obtained a significant correlation with adequate p-value with Pearson.

One year of intermittent data we found in Duque de Caxias for example, but not for Campo Grande during the surveillance program Dec. 2009-Jan. 2012. Pearson's correlation for 12 months was 0.787 (p-value 0.0024) between BG and fertile females, 0.793 (0.0021) for BG and total females. In spite of this, we got a weak correlation for ovitrap, 0.447 (p-value 0.1451). For Spearman's, the null information produced weaker correlations through the year, about 0.5175 (0.0887) for BG and fertile females, also 0.5175 between BG and all females, while for ovitrap 0.3007 (p-value 0.3475).

It means the data was limited and its effects of making decisions without a month of comparisons can produce consequences, which can be better if we consider only the nine months with all data, as we agree in the model results.

The relationship between data and the numerical results is presented in Figure 5.19.

5.7 Population dynamics for Nova Iguaçu/RJ

In the second city of Rio de Janeiro, the surveillance program occurred for one year, but later, from July 2011 to June 2012. Nova Iguaçu is located 15 km in the Northwest direction of Duque de Caxias (Cidade-Brasil, 2021). Nova Iguaçu is not the capital city of the state of Rio de Janeiro, nor Duque de Caixas. Its total area was around 521.3 km^2 with a density of 1575 inhabitants/km^2 (Cidade-Brasil, 2021). For urban and total population information remember the IBGE numbers in Section 2.1.

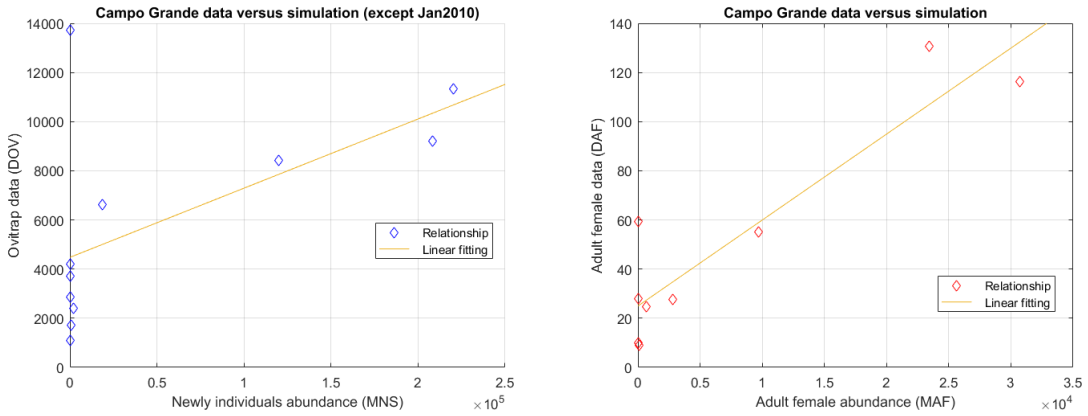

Figure 5.19: *Dependence between variables for Campo Grande results.*

The surveillance in this city occurred during a leap year, which was considered for the temporal scale, and the trap data collected is in Figure 5.6. We plot together the data with daily mean temperature and precipitation (see Figure 5.20).

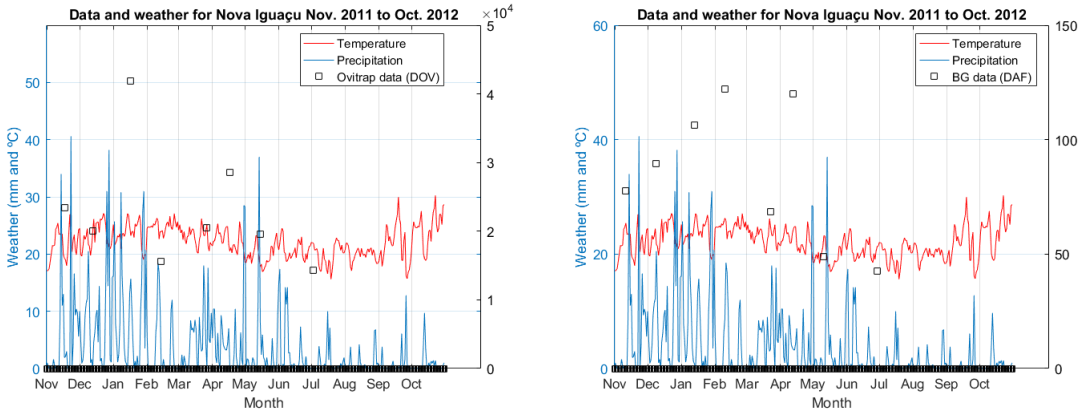

Figure 5.20: *Weather, ovitrap, and BG-Sentinel data for Nov, 2011 to Oct, 2012 in Nova Iguaçu.*

Through the data, we concluded there were newborns and mosquitoes because the traps registered data nonzero during the surveillance program, except for the special case of June 2012. An interesting fact is that instead of announcing July to July, in June they did not collect ovitrap, it was collected at the start of July*, 3rd. Only BG was collected on June, 29th. It was considered in the temporal vector, as we confirm through the plots 5.20.

We used this methodology once traps were exposed on the same day over the three neighborhoods. On the other hand, BG-Sentinel traps were exposed over the three neighborhoods on the same day, but it used to be a different day than the ovitraps exposure, which implied we built a vector with nonzero data in different coordinates for BG and ovitrap.

We ran the model with $\alpha_{NI} = 0.147$ determined according to the fuzzy rule-based system output (remember Table 2.3).

As the historical driest day occurs in August (remember Table 5.1), we started simula-

tions in August, for a fixed initial condition, and compared correlation during the periods of November to June* in Figure 5.21.

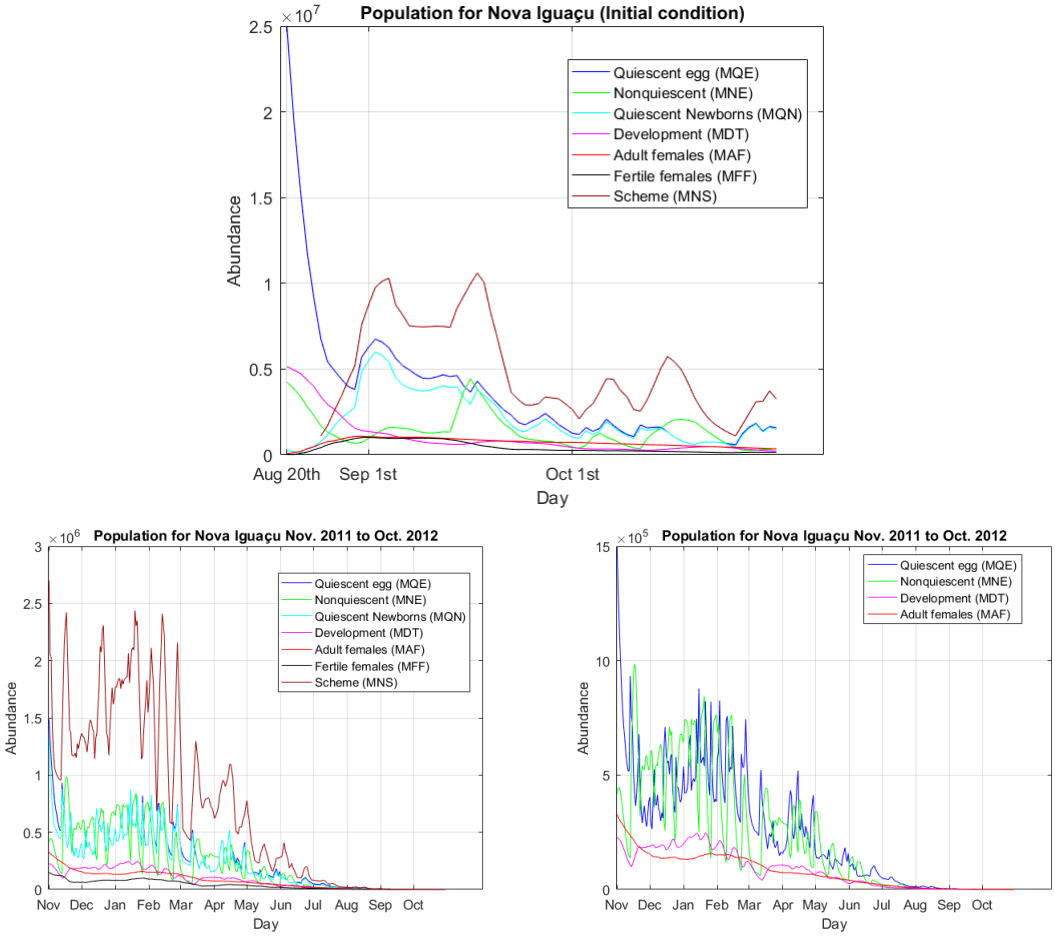

Figure 5.21: *Aedes aegypti population dynamics for Nova Iguaçu.*

The dynamic for this period was compared for an eight-month period, producing a correlation between adult females and the Scheme representing younger individuals. A linear dependence is better represented in Figure 5.22.

From Figure 5.22, we see in November the tendency of the data is different from the model. If we have data and use it as an initial condition in the model, the first month of forecasting can be improved. We ran a fixed initial condition for all cities after the worst period, trying not to influence the results, that is, trying to look at the abundance even given a not realistic initial condition.

For the results between the model outputs for females and the BG data, Spearman's correlation was strong (LaMorte, 2021) for fertile females, 0.691 (p-value= 0.069), but not for all females 0.571 (p-value= 0.151). On the other hand, Pearson's correlation produced high p-values and weaker correlation. It was 0.516 (p= 0.19) for fertile, while 0.406 for all females (p-value= 0.318).

For ovitrap, we obtained a Pearson's correlation of only 0.401, with inadequate p-value=0.324. Similarly, we got a correlation for Spearman around 0.429, with inadequate

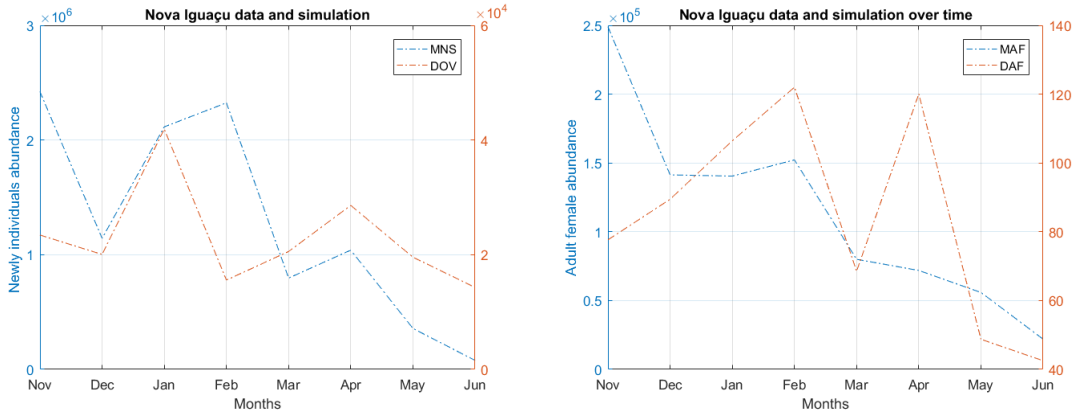

Figure 5.22: *Model output and trap data along the year. The red lines represent the data, and the blue lines are the model output. While the first plot is about newly individuals, the second one is about adult females.*

p-value=0.299.

It means we are not able to accurately forecast this city. It could be improved if we get more data collected, that is, if the data was not limited to one year, and starting in the unfavorite period (July and August). The effects of making decisions without a year of comparisons can not be evaluated.

The relationship between data and the numerical results is presented in Figure 5.23.

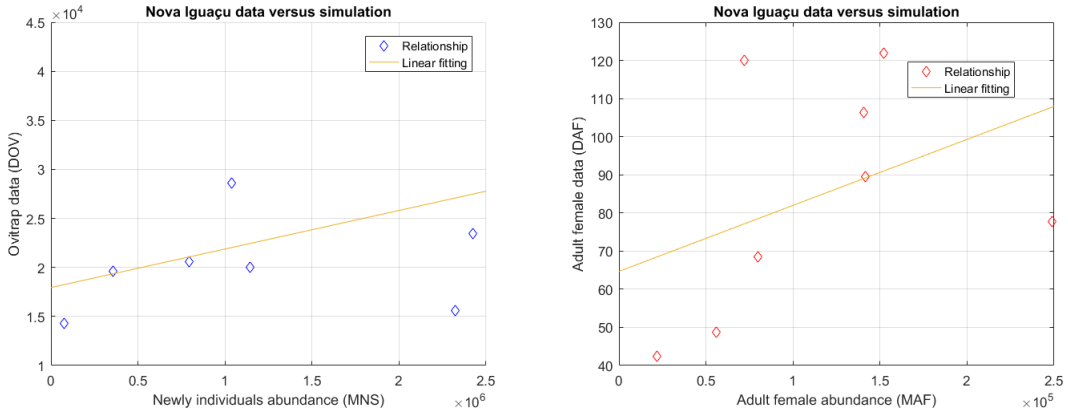

Figure 5.23: *Dependence between variables for Nova Iguaçu results.*

5.8 Discussion for Santarém/PA

The surveillance in this city occurred from March 2010 to February 2012 and the trap data collected was shown in Figure 5.4.

Through the data, we concluded there were newborns in Santarém, but the traps registered data zero during the second year of the surveillance program (Codeço *et al.*, 2015).

According to Codeço *et al.* (2015), "the two years of study were very similar in climate but very different in mosquito abundance". There was the implementation of a new vector control program during the second year, which caused significantly fewer mosquitoes than the first year. Besides, the neighborhoods presented non-data during some months. Their findings produced a negative correlation Codeço *et al.*, 2015, and also in our model the null data did not help in getting results, once we analyzed the correlation. In Rossi, Ólivêr, *et al.* (2004), they also used Spearman's correlation to evaluate the outputs of the model.

5.9 Weather scenarios and extreme conditions

One way to validate the model is by studying it over extreme conditions. For this, we set different scenarios corresponding to extreme temperatures and constant rainfall. Therefore, we analyzed the population behavior and the weather influence over n by setting different scenarios concerning mean temperatures and frequencies of rainy episodes. The simulation started with a fixed initial condition.

It can help to evaluate the contribution of precipitation to population maintenance. Besides, extreme temperatures for *Aedes aegypti* shall provide a slower development or even population extinction.

The weather was accessed daily and accumulated because we used a historical sample of precipitation and temperature to compute an indicator of past rainy days and the average temperature during the previous days, respectively.

The initial condition is the same for both sets, where it is given as an attributed population in each stage and age. Also, the parameter α_c is constant for a city, in order to analyze only weather influence, where $\alpha_c = 0.0$ would represent the output of the fuzzy rule-based system for a city with better sanitation panorama than Campo Grande.

We built scenarios considering the cities' basic sanitation panorama without climate fluctuations. We analyzed the population behavior and the weather influence over the stability through the calculus of the largest eigenvalue of P_t and $(I - T)^{-1}F$, given by the λ and the net reproductive number n, respectively. The parameter γ is the mean generation time, as we mentioned in Subsection 4.5.1.

For numerical analysis, according to different scenarios, we highlighted that over extreme conditions (drier or hotter days), the net reproductive number was easily obtained due to the matrix $(I - T)^{-1}F$ being well conditioned, even when the bigger eigenvalue of $P = T + F$ could not be quickly numerically calculated. For short and long periods of the year, weather and sanitation produced an impact on the population fluctuations.

The procedure is fast as P_t is sparse. While we ran the model, the infinity norm of T_t gave a number lower than 1. That is, as the functions are such that the separate sum of each column of T_t is lower than 1, then $(I - T_t)^{-1}$ exists and the system is stable.

The scenarios concerned constant mean temperature and daily precipitation for a city with a basic sanitation panorama similar to the studied cities. The simulation started with a fixed initial condition.

For cities with annual mean precipitation and basic sanitation similar to Duque de Caxias, which means a medium sanitation panorama, where $\alpha_c = 0.142$, we built Table 5.3 for daily precipitations of 1 or 7mm per day, over temperatures of 15, 16, 21, 22, 28, 33, and 34°C.

According to Tables 5.3 and 5.4, we note the weather impact on the net reproductive number and the increasing or decreasing trend of population densities. It varies according to n and λ. Although the sparse matrix P, several weather conditions produced a slow rate

θ	15	16	16	21	21	22	22	28	28	33	33	34
q_p	7.0	7.0	1.0	7.0	1.0	7.0	1.0	7.0	1.0	7.0	1.0	7.0
n	0.282	0.477	0.125	1.107	0.133	1.226	0.124	1.823	0.085	0.502	0.018	0.232
λ	0.977	0.985	0.963	1.004	0.942	1.007	0.937	1.025	0.919	0.975	Error	0.951
γ	53.82	48.76	55.84	28.78	33.75	27.37	32.09	24.72	29.20	27.75	-	29.20

Table 5.3: *Net reproductive number n, growth rate λ and mean generation time γ for daily temperature (θ in °C) and precipitation (q_p in mm) for Duque de Caxias scenarios.*

of *Aedes aegypti* population maintenance.

There was a case over warm temperature and a few rain millimeters, where we obtained only the calculus of the largest eigenvalue of $(I - T)^{-1}F$.

Thus, the Error entry means that using *eigs* function for sparse matrices in Matlab we could not calculate the eigenvalue of P to adequate accuracy. Therefore, the net reproductive number gave information about the population, while an error was found over a warm temperature $\theta = 33$°C and few rainfalls q_p =1mm, and the system reported that it did not find any eigenvalues of P to sufficient accuracy.

We highlight that for an adequate temperature $\theta = 28$°C but few rainfalls, q_p =1mm, the mean generation time of 29.2 days for *Aedes aegypti* development was the same as over a warm temperature $\theta = 33$°C with significant rainfalls q_p =7mm.

Consider a pair of plots as it appears in the sequence in Figure 5.24. From the first and second pairs, we highlighted that over temperatures of 22, and 28°C, and frequent rainy episodes of 7mm, the population increased at all stages. However, even at a good temperature of 28°C, the population decreased quickly because of rain absence and the adequate sanitation panorama of the city. Concerning the plots from the first and second pairs, we note that even at a good mean temperature, precipitation was necessary to maintain the population of this city. Constant and significant rain episodes, together with standard temperatures, could provide adequate environmental conditions for breeding sites, increasing the population.

The first pair from Figure 5.25 showed that even over rainy days, the warmer mean temperature had a negative effect on population dynamics. A warmer mean temperature is not adequate for *Aedes aegypti* development, and we noticed that larvae and pupae are alive for a few days. Without larvae, the whole population was decreasing. Without rain, it decreased even earlier.

Even though, from Figure 5.25, the plots suggest a cold period has a negative influence over the *Aedes aegypti* population. The population was getting older and dying.

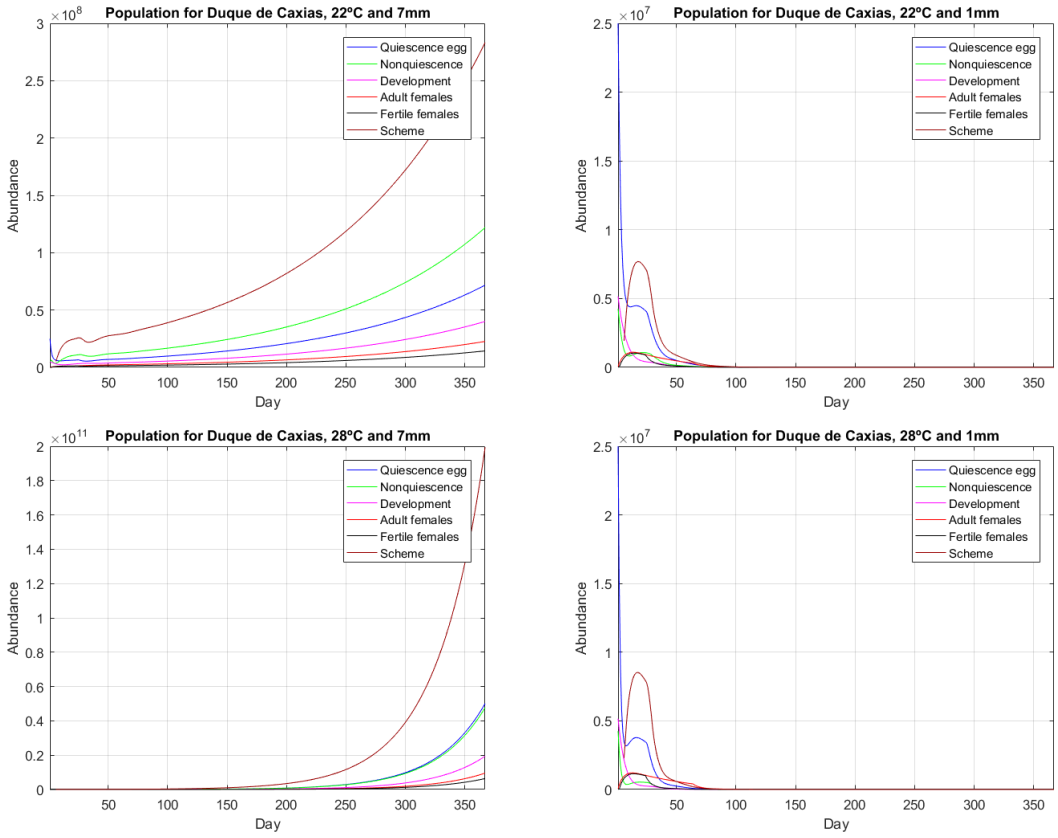

Figure 5.24: *Aedes aegypti population dynamics over extreme constant conditions in Duque de Caxias.*

From sets of cold or warmer mean temperatures, we noticed they were not adequate for *Aedes aegypti* development, and larvae and pupae were alive for a few days. Without larvae, the whole population is decreasing. Without rain, it decreased even earlier. After some months the population could be extinct.

For 16°C, the population had a smooth decrease. For 15°C, the development was even slower.

A warmer temperature of around 34°C also produced a negative behavior (see Figure 5.25). If there was more rain, the decrease in the population was slower than for an insignificant amount.

An overview of the plots from the frame of Figures 5.24 and 5.25 suggested a consistent relationship between mean temperature, precipitation, and mosquito abundance. The mean generation time increases as long as we approximate the 16°C. A better panorama involves temperatures near 21°C to 28°C, with frequent rainy episodes.

On the other hand, for cities with inadequate basic sanitation, such as Santarém, where $\alpha_C = 0.25$, we found that the mean temperature of 33°C together with significant rain still produces a good habitat for *Aedes aegypti*. Despite the panorama for Duque de Caxias, the same weather produced an immediate decreasing effect.

Although the sparse matrix P, several weather conditions produced a slow rate of *Aedes aegypti* development. For this city, Matlab routine was able to calculate the eigenvalue of

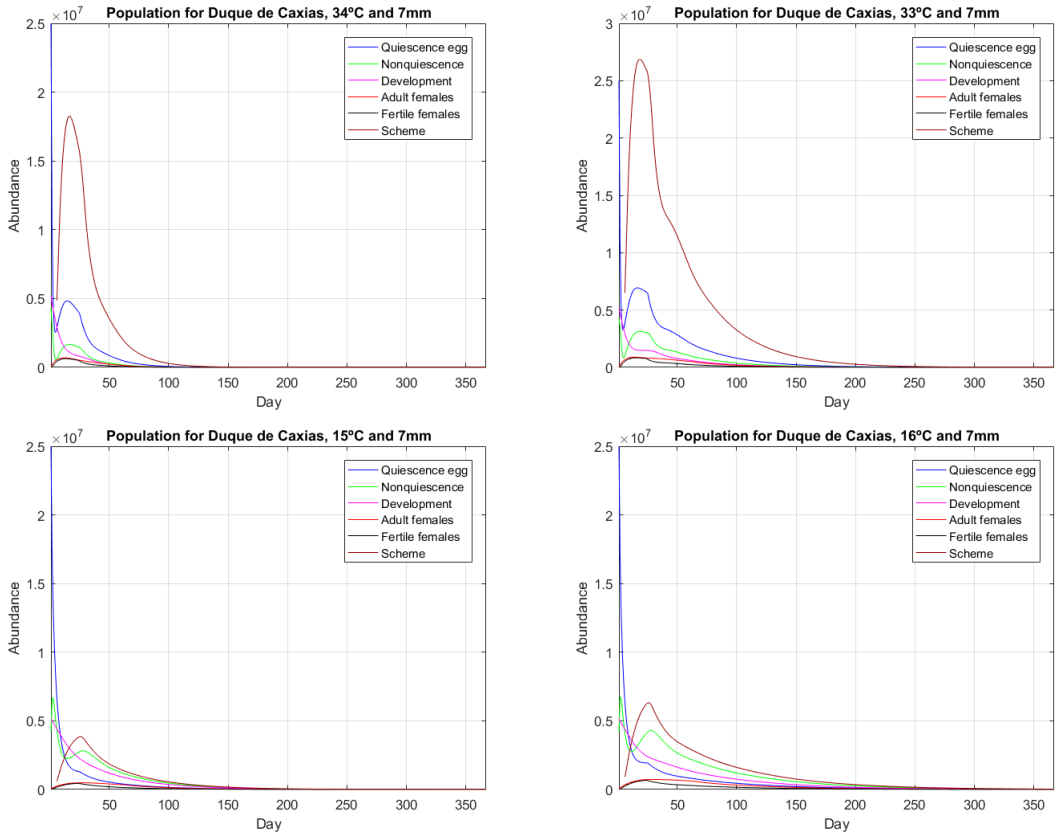

Figure 5.25: *Aedes aegypti population dynamics over extreme weather constant conditions in Duque de Caxias.*

θ	16	16	21	21	22	22	28	28	33	33	34
q_p	1.0	7.0	1.0	7.0	1.0	7.0	1.0	7.0	1.0	7.0	7.0
n	0.330	0.840	0.368	1.949	0.348	2.158	0.254	3.209	0.057	0.884	0.409
λ	0.978	0.996	0.969	1.024	0.966	1.030	0.952	1.050	0.913	0.995	0.969
γ	50.81	45.75	31.57	27.77	30.16	26.47	27.73	23.97	31.55	26.71	27.97

Table 5.4: *Net reproductive number n, growth rate λ and mean generation time γ for daily temperature (θ in ºC) and precipitation (q_p in mm) for Santarém scenarios.*

P using the *eigs* function for sparse matrices, due to the poor sanitation conditions helped the *Aedes aegypti* development.

Consider a pair of plots as it appeared in the sequence in Figure 5.26. From the first and second pairs, we highlighted that over good temperatures of 22, and 28ºC, and frequent rainy episodes of 7mm, the population increased at all stages. However, even at a good temperature of 28ºC, the population decreased because of rain absence. It decreased slowly if we compare it to Duque de Caxias, due to the inadequate sanitation panorama of Santarém.

Similar conclusions from Duque de Caxias simulations, we can validate for Santarém, once we note that even at a good mean temperature, precipitation is necessary to maintain the population of this city. Constant and significant rain episodes, together with standard

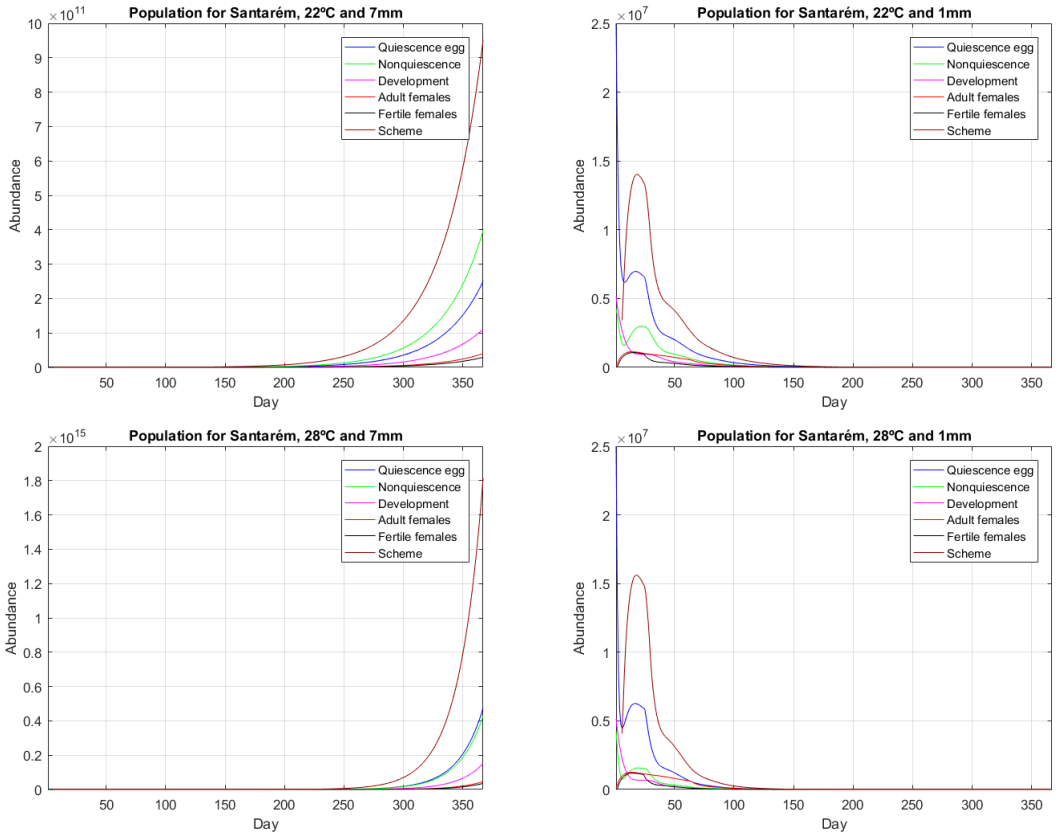

Figure 5.26: *Aedes aegypti population dynamics over extreme constant conditions in Santarém.*

temperatures, provide adequate environmental conditions for breeding sites, increasing the population.

The first pair from Figure 5.27 reflects that even over rainy days, the warmer mean temperature had a negative effect on population dynamics. A warmer mean temperature is not adequate for *Aedes aegypti* development, but we noticed that the inadequate sanitation panorama helped the population at the start, and continuously provided environmental conditions, so the population was not extinct.

Even though, from Figure 5.27, the plots suggest that a cold period had a negative influence over the *Aedes aegypti* population. For 16°C, the population had a slow decrease.

Even over inadequate mean temperatures for *Aedes aegypti* development (21 and 22°C), in the presence of significative precipitation, we conclude $n > 1$ and the population grows.

From sets of cold or warmer mean temperatures, we noticed they were not adequate for *Aedes aegypti* development, and larvae and pupae were alive for a few days. Without larvae, the whole remaining population decreased. Without rain, it decreased earlier. The population could be extinct some months later.

A warmer temperature of around 34°C also produced a negative behavior (see Figure 5.27). If there was more rain, the decrease in the population was slower than for an insignificant amount.

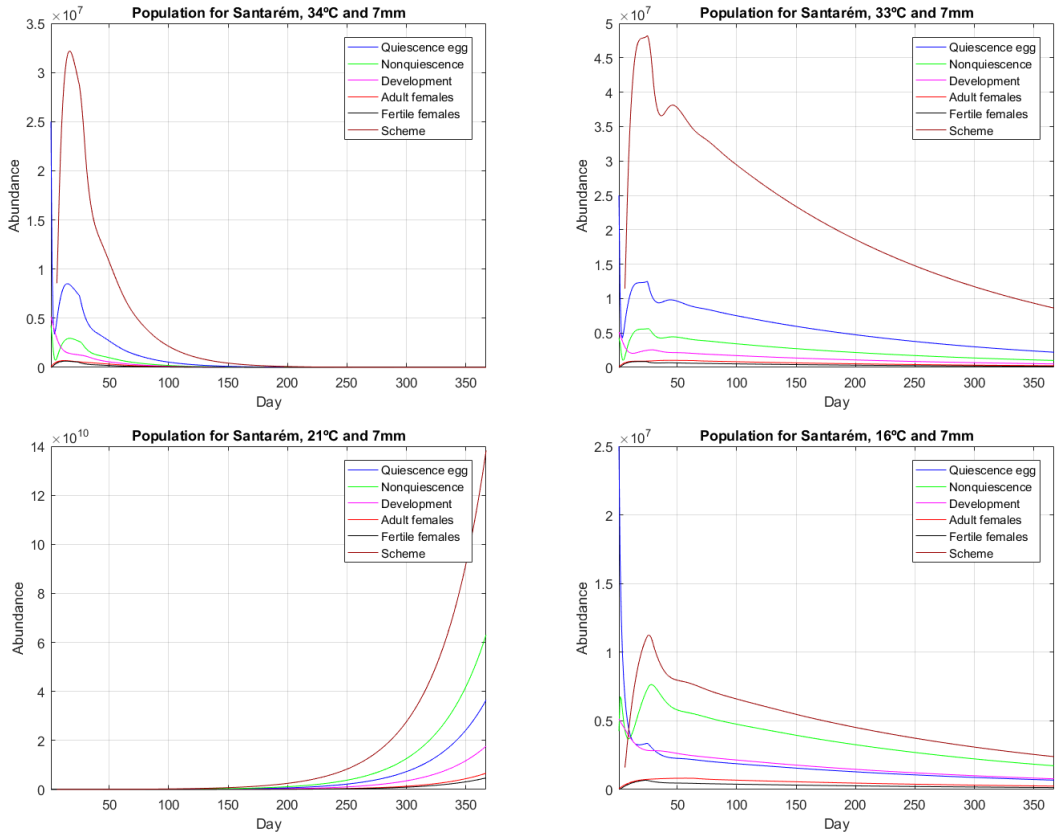

Figure 5.27: *Aedes aegypti population dynamics over extreme constant conditions in Santarém.*

An overview of the plots from the frame of Figures 5.26 and 5.27 suggested a consistent relationship between mean temperature, precipitation, and mosquito abundance.

On the other hand, for cities with inadequate basic sanitation, we found that the mean temperature of 33°C, with significant rain, still produced an adequate habitat for *Aedes aegypti*, in spite of the panorama for Duque de Caxias, where it produced an immediate decreasing effect.

5.10 Sensitivity analysis for the basic sanitation parameter α_c

We established comparisons among different basic sanitation characteristics, considering the same weather constant panorama, but analyzing the α_c parameter.

The results from Table 5.5 showed the net number varying according to the basic sanitation of the city. That influence was represented in Figures 5.28 and 5.29.

An overview of the plots from the frame of Figures 5.28 and 5.29 suggested a consistent relationship between basic sanitation and mosquito abundance. After all, the fluctuations for Santarém showed slower mortality during rain absence, which is a result of breeding site conditions over inadequate sanitation. Similarly, there was a faster development of rain abundance.

	$\alpha_c = 0.25$ (Santarém)	$\alpha_c = 0.142$ (Duque de Caxias)
θ=16, q_p=7	0.84	0.48
θ=22, q_p=7	2.16	1.23
θ=28, q_p=7	3.21	1.82
θ=33, q_p=7	0.88	0.50
θ=33, q_p=1	0.06	0.02
θ=28, q_p=1	0.25	0.08
θ=22, q_p=1	0.35	0.12

Table 5.5: *The net reproductive number n, for a fixed daily temperature (θ in °C) and precipitation (q_p in mm for Duque de Caxias and Santarém basic sanitation panorama.*

5.11 What if Brazilian policies for sanitation are achieved?

The national policies for basic sanitation called "Marco legal do saneamento básico" has a goal of 99% of the population being served with a water supply and intermittent services until 2033 (Brasil, 2020a). Also, it requires that 90% be served with sewerage services (Brasil, 2020a).

We recognized there were challenges to control *Aedes aegypti* abundance and providing the quality of the basic sanitation services to the population. However, these services are not free and the service companies can reinvest in structure maintenance and improvements.

This mark would improve public health by decreasing *Aedes aegypti* population according to the scenarios for all the studied cities.

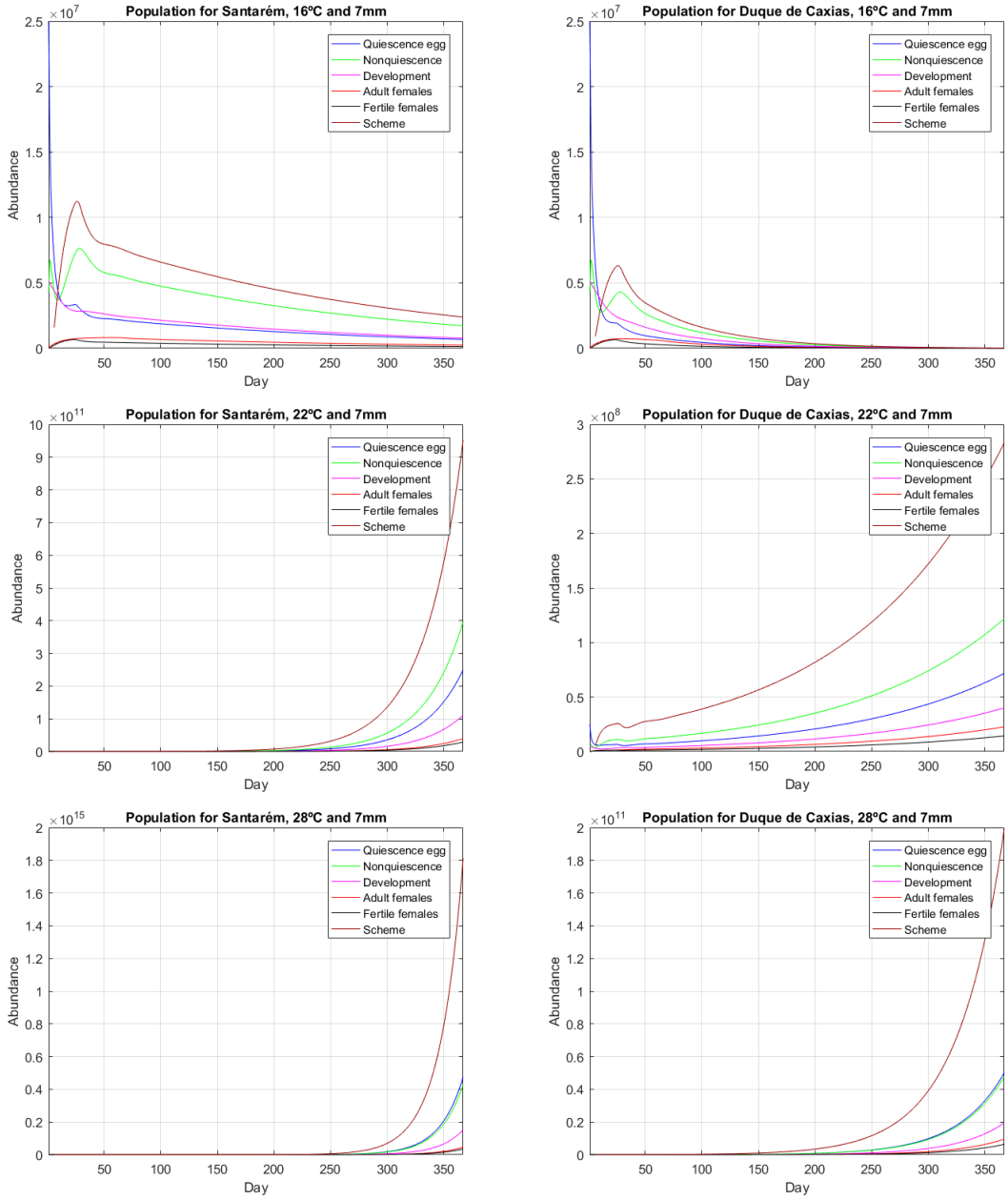

Figure 5.28: *Aedes aegypti population dynamics over extreme constant conditions for different basic sanitation panoramas. We selected Santarém (first column) and Duque de Caxias (second column).*

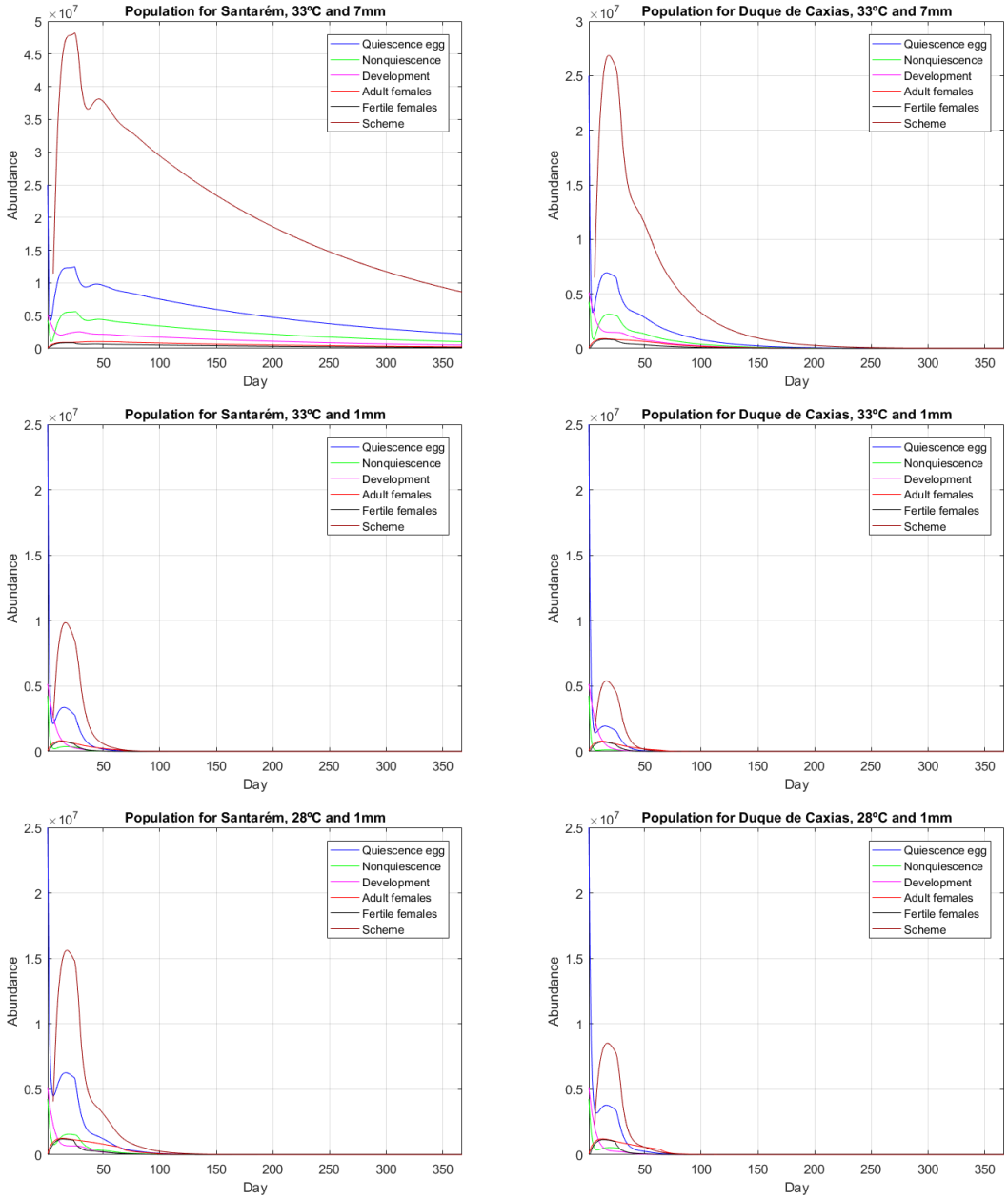

Figure 5.29: *Aedes aegypti population dynamics over extreme constant conditions for different basic sanitation panoramas. We selected Santarém (first column) and Duque de Caxias (second column).*

Chapter 6

Final considerations

Our model simulations assessed the impact of basic sanitation improvements on *Aedes aegypti* population development and the importance of collecting trap data monthly from urban endemic regions to encourage and support continuous surveillance schemes.

We pointed out that the matrix model could provide a powerful tool for forecasting different endemic regions, and was sensitive to the *Aedes aegypti* fluctuations. The model provided a tool to investigate peaks in the *Aedes aegypti* population and its dynamics in Brazilian municipalities.

We organized functions from several papers and used biological experiments to create novel functions for *Aedes aegypti* development. We found temperature, precipitation, and sanitation functions that connected the population data to the surrounding variables. The contribution of our model's approach was that we related weather with the city's sanitation characteristics and the *Aedes aegypti* population's biological stages. The model considered the basic sanitation panorama as an output of a fuzzy system and worked using development stages that combine quiescent egg characteristics, besides weather data, temperature, and precipitation on a daily average and accumulated.

These findings help in building a model that can capture the population dynamics for cities in different regions, only calculating the parameter related to the basic sanitation characteristics of the city and the mean of the annual rainfalls in millimeters. Thus, we input the historical and forecasting weather and the sanitation percentages reported by the national system. This powerful tool can be improved by using real data collected to feed the system inputs. Together, we can promote warnings of outbreaks in the medium-term period.

Data and forecasting can provide a guide to detect potential breeding sites, endemic regions, and periods accessing possible outbreaks to intervene. It is possible to couple the model with predictive models of diseases spread by *Aedes aegypti*. After all, by predicting the abundance of females, it is possible to study the transmission dynamics of the diseases they cause.

Unfortunately, human efforts can not directly change the weather, while basic sanitation can be evaluated and improved. In this way, public health does not need to be considered

when we identify a problem, if we can predict an outbreak and act before it happens. Famous minds studied ways to enhance public health through basic sanitation improvements (Kone, 2021).

However, in Brazil, the surveillance programs are sporadic. Plus, the Brazilian system of basic sanitation just recently organized information from all states in an online platform. We noticed limitations for forecasting, due to missing data, and also some data that reflected contrasts between small towns and big cities, especially if we take into consideration the Northern and Northeastern regions.

By improving sanitation services, sanitation data online system, government policies, surveillance, and human actions, we may improve public health. With the mathematical tool, we can obtain the contribution from a city's data and forecast guiding periods in which Brazilian sanitary systems can use technologies and governmental policies in order to bring about population control for *Aedes aegypti*. This mark would improve public health by decreasing *Aedes aegypti* population according to the scenarios for all the studied cities. There are measures that the government policies, the sanitation system, and the population can take to avoid the worst-case scenarios for *Aedes aegypti* and related diseases in Brazil. Also, there are initiatives and projects, such as the "Marco legal do saneamento básico" (national policies for basic sanitation) that we can follow in an attempt to improve scenarios (Brasil, 2020a), which includes using technologies, mathematical models to purpose govern interventions, and investments to provide health quality.

References

[Adams *et al.* 2006] C Adams, R Murrieta, and WA Neves. *Sociedades Caboclas Amazônicas: Modernidade E Invisibilidade*. Annablume, 2006. ISBN: 9788574196442. URL: https://books.google.ca/books?id=K0o9YHG6ti8C (cit. on pp. 17, 73).

[Ahumada *et al.* 2004] JA Ahumada, D Lapointe, and MD Samuel. "Modeling the population dynamics of *Culex quinquefasciatus* (diptera: culicidae), along an elevational gradient in hawaii". In: *J Med Entomol* 6.41 (Nov. 2004), pp. 157–70. URL: https://doi.org/10.1603/0022-2585-41.6.1157 (cit. on p. 1).

[Almeida *et al.* 2020] Ls Almeida, ALS Cota, and. "Sanitation, arboviruses, and environmental determinants of disease: impacts on urban health". In: *Ciênc. saúde coletiva* 25.10 (2020). URL: https://doi.org/10.1590/1413-812320202510.30712018 (cit. on p. 5).

[Barbosa *et al.* 2019] GL Barbosa *et al.* "Influence of strategic points in the dispersion of *Aedes aegypti* in infested areas". In: *Rev Saúde Pública [Internet]* 53.29 (2019), pp. 1–12. URL: https://doi.org/10.11606/S1518-8787.2019053000702 (cit. on p. 59).

[Barrera *et al.* 2014] R Barrera, M Amador, V Acevedo, RR Hemme, and G Félix. "Sustained, area-wide control of *Aedes aegypti* using cdc autocidal gravid ovitraps". In: *The American journal of tropical medicine and hygiene* 91.6 (2014), pp. 1269–1276. URL: https://doi.org/10.4269/ajtmh.14-0426 (cit. on p. 2).

[Barros and R. Bassanezi 2006] LC Barros and RC Bassanezi. *Tópicos de lógica fuzzy e biomatemática*. Unicamp/IMECC, 2006. URL: https://www.researchgate.net/profile/Rodney-Bassanezi/publication/256373655_Topicos_de_Logica_Fuzzy_e_Biomatematica/links/00b7d5225f8c99730a000000/Topicos-de-Logica-Fuzzy-e-Biomatematica.pdf (cit. on pp. 5, 15, 16, 19, 20, 22).

[B. Bassanezi *et al.* 2011] BSB Bassanezi, AG Oliveira Filho, and A Udelsmann. "Construção de um modelo matemático fuzzy para predizer o risco de vômitos pós-operatórios numa população pediátrica oncológica a partir da determinação dos fatores de risco". PhD thesis. Campinas, São Paulo: Faculdade de Ciências Médicas, Universidade Estadual de Campinas, 2011 (cit. on p. 20).

[R. Bassanezi 2012] RC Bassanezi. *Temas & Modelos*. Santo André, SP. UFABC, 2012. URL: https://gradmat.ufabc.edu.br/livros/Temas%20&%20Modelos-%20o%20livro.pdf (cit. on p. 37).

[Bassani 2016] LT Bassani. "Sistema de base de regras fuzzy como método alternativo para avaliar o risco de doenças cardiovasculares". MA thesis. Campinas, Brasil: Instituto de Matemática e estatística, Universidade de Campinas, 2016 (cit. on p. 22).

[Bernardelli 2010] MLFH Bernardelli. "Contribuição ao debate sobre o urbano e o rural". In: *Cidade e campo: relações e contradições entre urbano e rural*. Ed. by MEB Sposito and AM (Org.) Whitacker. 2nd ed. Expressão popular, São Paulo, 2010, pp. 33–52 (cit. on p. 13).

[Beserra, Castro Jr., *et al.* 2006] EB Beserra, FP Castro Jr., JW Santos, TS Santos, and CRM Fernandes. "Biologia e exigências térmicas de *Aedes aegypti* (l.) (diptera: culicidae) provenientes de quatro regiões bioclimáticas da paraíba". In: *Neotropical Entomology* 35.6 (2006), pp. 853–860. URL: https://doi.org/10.1590/S1519-566X2006000600021 (cit. on pp. 28, 29, 59).

[Beserra, Fernandes, *et al.* 2009] EB Beserra, CRM Fernandes, SAO Silva, LA Silva, and JW Santos. "Efeitos da temperatura no ciclo de vida, exigências térmicas e estimativas do número de gerações anuais de *Aedes aegypti* (diptera, culicidae)". In: *Iheringia* 99.2 (June 2009). Série Zoologia [Internet], pp. 142–148. URL: https://doi.org/10.1590/S0073-47212009000200004 (cit. on pp. 28, 29).

[BRASIL 2007] BRASIL. *Lei n 11.445, de 5 de janeiro de 2007*. Accessed in Apr. the 6th, 2020. 2007. URL: https://www.planalto.gov.br/ccivil%5C_03/%5C_ato2007-2010/2007/lei/l11445.htm (cit. on pp. 6, 7).

[BRASIL 2010] BRASIL. *Lei nº 12.305, de 2 de agosto de 2010*. Accessed in Jun. the 2nd, 2020. 2010. URL: http://www.planalto.gov.br/ccivil%5C_03/%5C_ato2007-2010/2010/lei/l12305.htm (cit. on pp. 6, 9).

[Brasil 2011] Brasil. *Plano Nacional de Saneamento Básico - PLANSAB - (Proposta de Plano)*. Acessed in Jun. the 4th, 2020. 2011. URL: http://www.cidades.gov.br/plansab (cit. on pp. 7–9).

[Brasil 2012] Brasil. *Sistema Nacional de Informações sobre Saneamento: diagnóstico dos serviços de água e esgotos – 2010*. Brasília: MCIDADES.SNSA, 2012 (cit. on p. 8).

[Brasil 2013a] Brasil. "Anexo - módulo 4: novos paradigmas tecnológicos para a concepção de projetos em saneamento básico." In: *Planos municipais de saneamento básico*. Ed. by JR Gimenez, VE Schneider, and SF (Org.) Tieppo. ISBN 978-85-7958-050-5. Brasília: Capacidades. Ministério das Cidades, Secretaria Nacional de Saneamento, 2013 (cit. on pp. 9, 10).

[Brasil 2013b] Brasil. "Módulo 1: planos de saneamento básico". In: *Planos municipais de saneamento básico*. Ed. by JR Gimenez, VE Schneider, and SF (Org.) Tieppo. ISBN 978-85-7958-050-5. Brasília: Capacidades. Ministério das Cidades, Secretaria Nacional de Saneamento, 2013. Chap. 1 (cit. on pp. 6, 8–10).

[Brasil 2013c] Brasil. "Módulo 4: estudos para a elaboração do diagnóstico". In: *Planos municipais de saneamento básico*. Ed. by JR Gimenez, VE Schneider, and SF (Org.) Tieppo. ISBN 978-85-7958-050-5. Brasília: Capacidades. Ministério das Cidades, Secretaria Nacional de Saneamento, 2013. Chap. 4 (cit. on pp. 6, 9, 11, 14).

[Brasil 2014] Brasil. *OMS: Para cada dólar investido em água e saneamento, economiza-se 4,3 dólares em saúde global*. Access in Oct. the 8th, 2023. 2014. url: https://brasil.un.org/pt-br/55290-oms-para-cada-d%C3%B3lar-investido-em-%C3%A1gua-e-saneamento-economiza-se-43-d%C3%B3lares-em-sa%C3%BAde-global (cit. on p. 7).

[Brasil 2019a] Brasil. *Curso de autoinstrução introdução à coleta de dados do SNIS Água e Esgotos: Módulo 1: O SNIS*. Capacidades, Ministério do Desenvolvimento Regional, Brasília, 2019 (cit. on p. 7).

[Brasil 2019b] Brasil. *Curso de autoinstrução introdução à coleta de dados do SNIS Água e Esgotos: Módulo 11: Formulário de pesquisa simplificada*. Capacidades, Ministério do Desenvolvimento Regional, Brasília, 2019 (cit. on pp. 9, 10).

[Brasil 2019c] Brasil. *Curso de autoinstrução introdução à coleta de dados do SNIS Água e Esgotos: Módulo 2: O SNIS - Coleta de dados*. Capacidades, Ministério do Desenvolvimento Regional, Brasília, 2019 (cit. on pp. 7, 10).

[Brasil 2019d] Brasil. *Curso de autoinstrução introdução à coleta de dados do SNIS Água e Esgotos: Módulo 4: Dados gerais*. Capacidades, Ministério do Desenvolvimento Regional, Brasília, 2019 (cit. on p. 7).

[Brasil 2019e] Brasil. *Curso de autoinstrução introdução à coleta de dados do SNIS Água e Esgotos: Módulo 6: Dados de água*. Capacidades, Ministério do Desenvolvimento Regional, Brasília, 2019 (cit. on p. 8).

[Brasil 2019f] Brasil. *Curso de autoinstrução introdução à coleta de dados do SNIS Água e Esgotos: Módulo 7: Dados de esgotos*. Capacidades, Ministério do Desenvolvimento Regional, Brasília, 2019 (cit. on p. 9).

[Brasil 2019g] Brasil. *Documento em revisão submetido à apreciação dos conselhos nacionais de saúde, recursos hídricos e meio ambiente*. Acessed in Aug. the 8th, 2023. 2019. url: https://www.gov.br/mdr/pt-br/assuntos/saneamento/plansab/Versao_Conselhos_Resoluo_Alta__Capa_Atualizada.pdf (cit. on p. 9).

[Brasil 2020a] Brasil. *Lei Nº 14.026, de 15 de Julho de 2020*. Access in Oct. the 8th, 2023. 2020. url: https://www.planalto.gov.br/ccivil_03/_ato2019-2022/2020/lei/l14026.htm (visited on 10/08/2023) (cit. on pp. 9, 98, 102).

[Brasil 2020b] Brasil. *Ranking do saneamento 2020*. Accessed in Jun. the 24th, 2020. 2020. url: http://tratabrasil.org.br/images/estudos/itb/ranking_2020/Tabela_100_cidades_Ranking_Saneamento_4.pdf (cit. on p. 10).

[Campogrande n.d.(a)] Campogrande. *A cidade: Clima*. Accessed in Feb. the 18th, 2019. n.d. url: http://campogrande.net/a-cidade/clima (cit. on p. 73).

[Campogrande n.d.(b)] Campogrande. *A cidade: Geografia*. Accessed in Feb. the 18th, 2019. n.d. url: http://campogrande.net/a-cidade/geografia (cit. on p. 86).

[Caprara *et al.* 2009] A Caprara *et al.* "Irregular water supply, household usage and dengue: a bio-social study in the brazilian northeast". In: *Cadernos de Saúde Pública* 25.1 (2009), pp. 125–136. url: https://doi.org/10.1590/S0102-311X2009001300012 (cit. on p. 60).

[Carneiro *et al.* 2009] PLS Carneiro *et al.* "Curva de crescimento em caprinos, da raça mambrina, criados na caatinga (growth curve in mambrina goats raised in caatinga)". In: *Rev. Bras. Saúde Prod. An.* 10.3 (2009), pp. 536–545. url: https://www.researchgate.net/publication/285099679 (cit. on p. 38).

[Castanho 2005] MJP Castanho. "Construção e avaliação de um modelo matemático para predizer a evolução do câncer de próstata e descrever seu crescimento utilizando a teoria dos conjuntos fuzzy". PhD thesis. Campinas, São Paulo: Faculdade de Engenharia Elétrica e de Computação, Universidade Estadual de Campinas, 2005 (cit. on p. 16).

[Castree *et al.* 2013] N Castree, R Kitchin, and A Rogers. *A dictionary of human geography*. 1st ed, 581 p. Oxford: Oxford University Press, 2013 (cit. on p. 13).

[Chen *et al.* 2007] CD Chen *et al.* "Comparative oviposition preferences of *Aedes (Stegomyia) aegypti (L.)* to water from storm water drains and seasoned tap water". In: *Dengue Bulletin* (2007), pp. 124–130. url: https://apps.who.int/iris/handle/10665/170366 (cit. on pp. 29, 34).

[Christophers 1960] R Christophers. Aedes aegypti *(L.), The Yellow Fever Mosquito*. Cambridge Univ. Press., Cambridge, 1960 (cit. on pp. 29, 39, 46).

[Cidade-Brasil 2021] Cidade-Brasil. *Município de Nova Iguaçu*. Access in Oct. the 29th, 2023. 2021. url: https://www.cidade-brasil.com.br/municipio-nova-iguacu.html (visited on 04/08/2021) (cit. on p. 88).

[Climate-Data n.d.(a)] Climate-Data. *Clima Campo Grande*. Access in Mar. the 13th, 2020. n.d. url: https://pt.climate-data.org/america-do-sul/brasil/mato-grosso-do-sul/campo-grande-3912/ (cit. on pp. xi, 73, 75).

[Climate-Data n.d.(b)] Climate-Data. *Clima Parnamirim*. Accessed in Jul. the 12th, 2019. n.d. url: https://pt.climate-data.org/america-do-sul/brasil/rio-grande-do-norte/parnamirim-42745/ (cit. on pp. xi, 74, 75).

[Climate-Data n.d.(c)] Climate-Data. *Clima Rio de Janeiro*. Accessed in Mar. the 13th, 2020. n.d. URL: https://pt.climate-data.org/america-do-sul/brasil/rio-de-janeiro-208/ (cit. on pp. xi, 74, 75).

[Climate-Data n.d.(d)] Climate-Data. *Clima Santarém*. Accessed in Mar. the 13th, 2020. n.d. URL: https://pt.climate-data.org/america-do-sul/brasil/para/santarem-4512/ (cit. on pp. xi, 73, 75).

[Codeço *et al.* 2015] CT Codeço *et al.* "Surveillance of *Aedes aegypti*: comparison of house index with four alternative traps". In: *PLoS Neglected Tropical Diseases* 9.2 (2015), pp. 1–23. URL: https://doi.org/10.1371/journal.pntd.0003475 (cit. on pp. vii, viii, 2, 10, 11, 46, 55, 73–75, 77, 78, 91, 92).

[Costa *et al.* 2010] EAPA Costa, EMM Santos, JC Correia, and CMR Albuquerque. "Impact of small variations in temperature and humidity on the reproductive activity and survival of *Aedes aegypti* (diptera, culicidae)". In: *Rev Bras entomol [Internet]* 54.3 (2010), pp. 488–93. URL: https://doi.org/10.1590/S0085-56262010000300021 (cit. on pp. 47, 50, 60).

[Couret and Benedict 2014] J Couret and MQ Benedict. "A meta-analysis of the factors influencing development rate variation in *Aedes aegypti* (diptera: culicidae)". In: *BMC Ecol* 14.3 (2014), pp. 1–15. URL: https://doi.org/10.1186/1472-6785-14-3 (cit. on p. 28).

[Cushing and Yicang 1994] JM Cushing and Z Yicang. "The net reproductive value and stability in matrix population models". In: *Natural Resource Modeling* 8.4 (1994), pp. 297–333 (cit. on pp. 1, 2, 43, 50, 51, 53, 64–71).

[Denlinger *et al.* 2012] D Denlinger, G Yocum, and Rinehart J. "10- hormonal control of diapause." In: *Insect Endocrinology*. Ed. by L.I. (Ed.) Gilbert. Academi Press, 2012. Chap. 10, pp. 430–463 (cit. on pp. 28, 44).

[DL Denlinger and Armbruster 2014] DL Denlinger and PA Armbruster. "Mosquito diapause". In: *Annual review of entomology* 59 (2014), pp. 73–93. URL: https://doi.org/10.1146/annurev-ento-011613-162023 (cit. on pp. 2, 27, 28).

[Diáriogaúcho 2015] Diáriogaúcho. *Aedes aegypti: saiba como o mosquito mais temido da atualidade surgiu no Brasil*. Accessed in Mar. the 7th, 2024. 2015. URL: https://diariogaucho.clicrbs.com.br/dia-a-dia/noticia/2015/12/aedes-aegypti-saiba-como-o-mosquito-mais-temido-da-atualidade-surgiu-no-brasil-4928429.html (cit. on pp. viii, 45).

[Dickerson 2007] CZ Dickerson. "The Effects of Temperature and Humidity on the Eggs of *Aedes aegypti* (L.) and *Aedes albopictus* (Skuse) in Texas". MA thesis. Texas, Estados Unidos: Texas A&M University, Dec. 2007 (cit. on p. 45).

[Diniz, Albuquerque, *et al.* 2017] DFA Diniz, CMR Albuquerque, LO Oliva, MAV Melo-Santos, and CFJ Ayres. "Diapause and quiescence: dormancy mechanisms that contribute to the geographical expansion of mosquitoes and their evolutionary success". In: *Parasites & Vectors* 10.310 (2017). URL: https://doi.org/10.1186/s13071-017-2235-0 (cit. on pp. 27–29, 41, 44, 45).

[Diniz, Melo-Santos, *et al.* 2015] DFA Diniz, MAV Melo-Santos, *et al.* "Fitness cost in field and laboratory *Aedes aegypti* populations associated with resistance to the insecticide temephos". In: *Parasites & Vectors* 8.662 (2015). URL: https://doi.org/10.1186/s13071-015-1276-5 (cit. on p. 40).

[DIVE 2022] DIVE. *Boletim Epidemiológico n° 09/2022 Vigilância entomológica do* Aedes aegypti *e situação epidemiológica de dengue, chikungunya e zika vírus em Santa Catarina*. Accessed in Jun. the 23th, 2022. 2022. URL: https://www.dive.sc.gov.br/phocadownload/doencas-agravos/Dengue/Boletins/Boletim-Dengue09-08-04-2022.pdf (cit. on p. 3).

[Endlich 2010] AM Endlich. "Perspectivas sobre o urbano e o rural". In: *Cidade e campo: relações e contradições entre urbano e rural*. Ed. by MEB Sposito and AM (Org.) Whitacker. 2nd ed. Expressão Popular, São Paulo, 2010, pp. 11–31 (cit. on p. 13).

[Farnesi *et al.* 2009] LC Farnesi, AJ Martins, DC Valle, and GL Rezende. "Embryonic development of *Aedes aegypti* (diptera: culicidae): influence of different constant temperatures". In: *Mem Inst Oswaldo Cruz* 104.1 (2009), pp. 124–126. URL: https://doi.org/10.1590/S0074-02762009000100020 (cit. on pp. viii, x, 28, 34–37).

[Faull and Williams 2015] KJ Faull and CR Williams. "Intraspecific variation in desiccation survival time of *Aedes aegypti* (l.) mosquito eggs of australian origin". In: *Journal of vector ecology* 40.2 (2015), pp. 292–300. URL: https://doi.org/10.1111/jvec.12167 (cit. on p. 39).

[Fiocruz 2016] Fiocruz. *Quais os principais criadouros do mosquito 'Aedes aegypti'?* Accessed in Jan. the 10th, 2023. 2016. URL: https://portal.fiocruz.br/pt-br/quais-os-principais-criadouros-do-mosquito-aedes-aegypti (cit. on pp. 8, 59).

[Fiocruz 2017] Fiocruz. *Conheça semelhanças e diferenças entre mosquitos transmissores da febre amarela*. Accessed in Jun. the 24th, 2020. 2017. URL: https://portal.fiocruz.br/noticia/conheca-semelhancas-e-diferencas-entre-mosquitos-transmissores-da-febre-amarela (cit. on p. 8).

[Freitas 2005] AR Freitas. "Growth curves in animal production". In: *R. Bras. Zootec* 34.3 (2005), pp. 786–795. URL: https://doi.org/10.1590/S1516-35982005000300010 (cit. on p. 38).

[G1 2019] G1. *Saneamento básico: maior parte das grandes cidades reinveste menos de 30% do que arrecada.* Accessed in Jun. the 15th, 2020. 2019. URL: https://g1.globo.com/economia/noticia/2019/07/23/saneamento-basico-maior-parte-das-grandes-cidades-reinveste-menos-de-30percent-do-que-arrecada.ghtml (cit. on pp. 6, 9, 10).

[Gama *et al.* 2013] ZP Gama, N Nakagoshi, and M Islamiyah. "Distribution patterns and relationship between elevation and the abundance of *Aedes aegypti* in mojokerto city 2012". In: *Journal of Animal Sciences* 3.4A (2013), pp. 11–16. URL: http://dx.doi.org/10.4236/ojas.2013.34A1003 (cit. on p. 59).

[Gould and Solomon 2008] EA Gould and T Solomon. "Pathogenic flaviviruses". In: *Lancet* 371.9611 (2008), pp. 500–509. URL: https://doi.org/10.1016/S0140-6736(08)60238-X (cit. on pp. 1, 27).

[GOV 2024] GOV. *Capacidades: conhecer para desenvolver: Cursos.* URL: https://www.capacidades.gov.br/cursos/ (visited on 03/03/2024) (cit. on p. 6).

[Gov 2020] Gov. *Secretaria da Saúde alerta para o aumento de casos de dengue no Estado.* Accessed in Jun. the 17th, 2020. 2020. URL: https://www.sc.gov.br/noticias/temas/saude/secretaria-da-saude-alerta-para-o-aumento-de-casos-de-dengue-no-estado (cit. on p. 3).

[IBGE 2014] IBGE. *Manual da base territorial.* Rio de Janeiro: IBGE, 2014 (cit. on p. 14).

[IBGE 2017] IBGE. *Estudos e Pesquisas Informação Geográfica número 11: Classificação e caracterização dos espaços rurais e urbanos do Brasil - Uma primeira aproximação.* Accessed in Jun. the 3rd, 2020. Rio de Janeiro: IBGE, 2017. URL: https://biblioteca.ibge.gov.br/visualizacao/livros/liv100643.pdf (cit. on pp. 12–14).

[IBGE 2019] IBGE. *Estimativas da população residente no Brasil e unidades da federação com data de referência em 1º de julho de 2019.* access in Jan. the 10th, 2023. 2019. URL: https://biblioteca.ibge.gov.br/visualizacao/livros/liv100643.pdf (cit. on p. 10).

[Ishikawa 2012] Walther Ishikawa. *Espécies.* Planeta intervertebrados. Accessed in Mar. the 7th, 2024. 2012. URL: http://www.planetainvertebrados.com.br/index.asp?pagina=especies_ver&id_categoria=28&id_subcategoria=&com=1&id=157&local=2 (cit. on pp. viii, 45).

[Jerônimo *et al.* 2011] GT Jerônimo, GM Speck, MM Cechinel, ELT Gonçalves, and ML Martins. "Seasonal variation on the ectoparasitic communities of nile tilapia cultured in three regions in southern brazil". In: *Brazilian Journal of Biology* 71.2 (2011), pp. 365–373. URL: https://dx.doi.org/10.1590/S1519-69842011000300005 (cit. on p. 2).

[Johansson *et al.* 2009] MA Johansson, F Dominici, and GE Glass. "Local and global effects of climate on dengue transmission in puerto rico". In: *Plos Neglected Tropical Diseases* 3.2 (2009). URL: https://doi.org/10.1371/journal.pntd.0000382 (cit. on p. 2).

[Klafke *et al.* 2023] F Klafke, VG Barros, and E HenningView. "Solid waste management and aedes aegypti infestation interconnections: a regression tree application". In: *WM&R* 41.11 (2023). URL: https://doi.org/10.1177/0734242X23116431 (cit. on p. 5).

[Kone 2021] D Kone. *Why focus on water, sanitation, and hygiene?* Access in Aug. the 10th, 2023. 2021. URL: https://www.gatesfoundation.org/our-work/programs/global-growth-and-opportunity/water-sanitation-and-hygiene (cit. on p. 102).

[Kraemer *et al.* 2019] MUG Kraemer, RC Reiner, and OJ et al Brady. "Past and future spread of the arbovirus vectors *Aedes aegypti and Aedes albopictus*". In: *Nat Microbiol* 4 (2019), pp. 854–863. URL: https://doi.org/10.1038/s41564-019-0376-y (cit. on pp. 3, 14).

[Laboissière 2016] P Laboissière. *Sterile* Aedes aegypti *production to begin by September*. Accessed in Jan. the 6th, 2022. 2016. URL: https://agenciabrasil.ebc.com.br/node/1002809 (cit. on p. 28).

[LaMorte 2021] Wayne W. LaMorte. *The Correlation Coefficient*. Access in Oct. the 29th, 2023. 2021. URL: https://sphweb.bumc.bu.edu/otlt/MPH-Modules/PH717-QuantCore/PH717-Module9-Correlation-Regression/PH717-Module9-Correlation-Regression4.html (visited on 04/21/2021) (cit. on p. 90).

[Lega *et al.* 2017] J Lega, HE Brown, and R Barrera. "*Aedes aegypti* (diptera culicidae) abundance model improved with relative humidity and precipitation-driven egg hatching". In: *Journal of Medical Entomology* 54.5 (2017), pp. 1375–1384. URL: https://doi.org/10.1093/jme/tjx077 (cit. on pp. 2, 30, 41, 59, 63).

[Loncaric and Hackenberger 2011] ZK Loncaric and B Hackenberger. "Stage and age structured *Aedes vexans and Culex pipiens (Diptera: Culicidae)* climate-dependent matrix population model". In: *Theoretical Population Biology* 83 (2011), pp. 82–94. URL: https://doi.org/10.1016/j.tpb.2012.08.002 (cit. on pp. 1, 28, 30, 41, 43, 46, 47, 57, 59).

[Loyola 2016] Gilmar Loyola. *Mosquito da dengue botando ovos*. Youtube. Accessed in Mar. the 7th, 2024. 2016. URL: https://www.youtube.com/watch?v=UwM8E-avlk0 (cit. on pp. viii, 45).

[Maimusa *et al.* 2016] HA Maimusa, AH Ahmad, NFA Kassim, and J Rahim. "Age-stage, two-sex life table characteristics of *Aedes albopictus and Aedes Aegypti* in penang island, malaysia". In: *Journal of the American Mosquito Control Association* 32.1 (2016), pp. 1–11. URL: https://doi.org/10.2987/moco-32-01-1-11.1 (cit. on pp. 30, 45, 47, 56, 59).

[Morin and Ebi 2018] C Morin and KL Ebi. *Forecasting and Modeling Techniques to Study Climate's Impact on Public Health*. 2018. URL: https://sinews.siam.org/Details-Page/forecasting-and-modeling-techniques-to-study-climates-impact-on-public-health (cit. on p. 1).

[CW Morin *et al.* 2015] CW Morin, AJ Monaghan, MH Hayden, R Barrera, and K Ernst. "Meteorologically driven simulations of dengue epidemics in san juan, pr". In: *PLOS Neglected Tropical Diseases* 9.8 (2015). URL: https://doi.org/10.1371/journal.pntd.0004002 (cit. on pp. 30, 59).

[Nakhapakorn and Tripathi 2005] K Nakhapakorn and NK Tripathi. "An information value based analysis of physical and climatic factors affecting dengue fever and dengue hemorrhagic fever incidence". In: *International Journal of Health Geographics* 4.13 (2005). URL: https://doi.org/10.1186/1476-072X-4-13 (cit. on p. 28).

[Nations 2010] United Nations. *Resolution adopted by the General Assembly on 28 July 2010*. Access in Apr. the 16th, 2020. 2010. URL: https://undocs.org/A/RES/64/292 (cit. on p. 6).

[Newman *et al.* 2014] KB Newman *et al. Modelling Population Dynamics: Model Formulation, Fitting and Assessment using State-Space Methods*. Methods in Statistical Ecology, Springer, 2014 (cit. on pp. 1, 43, 54).

[Novaes *et al.* 2022] C Novaes, PF Silva, and RC Marques. "*Aedes Aegypti* - insights on the impact of water services". In: *GeoHealth* 6 (2022). URL: https://doi.org/10.1029/2022GH000653 (cit. on pp. 60, 61).

[Otero *et al.* 2006] M Otero, HG Solari, and N Schweigmann. "Stochastic population dynamics model for *Aedes Aegypti*: formulation and application to a city with temperate climate". In: *Bulletin of mathematical biology* 68.8 (2006), pp. 1945–1974. URL: https://doi.org/10.1007/s11538-006-9067-y (cit. on pp. 28, 45, 46, 75).

[Pedrycz and Gomide 2007] W Pedrycz and F Gomide. *Fuzzy systems engineering toward human-centric Computing*. Hoboken, NJ, EUA: IEEE Press/John Wiley & Sons, 2007, p. 544 (cit. on p. 15).

[Pener 1992] MP Pener. "Environmental cues, endocrine factors, and reproductive diapause in male insects". In: *Cronobiology international* 9.2 (1992), pp. 102–113. URL: https://doi.org/10.3109/07420529209064521 (cit. on p. 28).

[R *et al.* 2014] Barrera R *et al.* "Use of the cdc autocidal gravid ovitrap to control and prevent outbreaks of *Aedes aegypti* (diptera: culicidae)". In: *Journal of medical entomology* 51.1 (2014), pp. 145–154. URL: https://doi.org/10.1603/me13096 (cit. on p. 2).

[Reisen *et al.* 2008] WK Reisen *et al.* "Impact of climate variation on mosquito abundance in California". In: *Journal of Vector Ecology* 33.1 (2008), pp. 89–98. URL: https://doi.org/10.3376/1081-1710(2008)33[89:iocvom]2.0.co;2 (cit. on p. 2).

[Rezende *et al.* 2008] GL Rezende *et al.* "Embryonic desiccation resistance in *Aedes aegypti* presumptive role of the chitinized serosal cuticle". In: *BMC developmental biology* 8.82 (2008). URL: https://doi.org/10.1186/1471-213X-8-82 (cit. on pp. 28, 45).

[Ribeiro 2023] R Ribeiro. *Lula revoga dois decretos sobre saneamento básico.* Accessed in Aug. the 9th, 2023. 2023. URL: https://agenciabrasil.ebc.com.br/radioagencia-nacional/politica/audio/2023-07/lula-revoga-dois-decretos-sobre-saneamento-basico (cit. on p. 9).

[Rosa and Ferreira 2010] LR Rosa and DAO Ferreira. "As categorias rural, urbano, campo, cidade: a perspectiva de um continuum". In: *Cidade e campo: relações e contradições entre urbano e rural.* Ed. by MEB Sposito and AM (Org.) Whitacker. 2nd ed. Expressão popular, São Paulo, 2010, pp. 187–204 (cit. on p. 13).

[Rossi, Lopez, *et al.* 2015] MM Rossi, LF Lopez, and E Massad. "The dynamics of temperature-and rainfall-dependent dengue transmission in tropical regions". In: *Ann Biom Biostat* 2.2 (2015). URL: https://www.researchgate.net/publication/287215347_The_Dynamics_of_Temperature-_And_Rainfall-Dependent_Dengue_Transmission_in_Tropical_Regions (cit. on pp. 30, 34, 41, 46).

[Rossi, Ólivêr, *et al.* 2004] MM Rossi, L Ólivêr, and E Massad. "Modelling the implications of temperature on the life cycle of *Aedes aegypti* mosquitoes". In: *Ecological Modelling Applied to Entomology.* Ed. by Ferreira C and Godoy W. Entomology in Focus, vol 1. Springer International Publishing, 2004. Chap. 4, pp. 81–107 (cit. on pp. 33, 34, 41, 63, 92).

[Sardão 2016] T Sardão. *Dengue e zika: ABES alerta sobre a importância do saneamento básico no combate às doenças.* Access in Oct. the 8th, 2023. 2016. URL: https://abes-dn.org.br/922/ (visited on 04/02/2016) (cit. on p. 8).

[Schaeffer *et al.* 2007] B Schaeffer, B Mondet, and S Touzeau. "Using a climate-dependent model to predict mosquito abundance: application to *Aedes (Stegomyia) africanus and Aedes (Diceromyia) furcifer* (diptera: culicidae)". In: *Infect Genet Evol.* 8.4 (2007), pp. 422–432. URL: https://doi.org/10.1016/j.meegid.2007.07.002 (cit. on pp. 1, 28, 39, 46, 47, 52, 54, 59, 64, 74, 77).

[H. Silva and I. Silva 1999] HHG Silva and IG Silva. "Influência do período de quiescência dos ovos sobre o ciclo de vida de *Aedes aegypti* (linnaeus, 1762) (diptera, culicidae) em condições de laboratório". In: *Rev. Soc. Bras. Med. Trop.* 32.4 (1999). URL: https://doi.org/10.1590/S0037-86821999000400003 (cit. on pp. viii, 27–30, 38–41, 45, 47, 74).

[J. Silva and Machado 2018] JCBD Silva and CJS Machado. "Associations between dengue and socio-environmental variables in capitals of the Brazilian northeast by cluster analysis". In: *Ambient soc* 21 (2018). URL: https://doi.org/10.1590/1809-4422asoc0133r2vu18L4TD (cit. on pp. 5, 8, 11).

[M. R. d. Silva 2022] Monalisa R da Silva. "Modelagem de técnicas de controle populacional do mosquito *Aedes aegypti*". PhD thesis. Juiz de Fora, Minas Gerais: Universidade Federal de Juiz de Fora, 2022 (cit. on pp. 1, 28–30).

[M. R. d. Silva *et al.* 2022] Monalisa R da Silva, Pedro H G Lugão, Fábio Prezoto, and Grigori Chapiro. "Modeling the impact of genetically modified male mosquitoes in the spatial population dynamics of aedes aegypti". In: *Sci Rep* 12.9112 (2022). url: https://doi.org/10.1038/s41598-022-12764-7 (cit. on p. 30).

[Siraj *et al.* 2017] AS Siraj *et al.* "Temperature modulates dengue virus epidemic growth rates through its effects on reproduction numbers and generation intervals". In: *PLOS Neglected Tropical Diseases* 11.7 (2017), pp. 1–19. url: https://doi.org/10.1371/journal.pntd.0005797 (cit. on p. 30).

[SNSA n.d.] SNSA. *Ministério das Cidades: Série Histórica - Sistema Nacional de Informações sobre Saneamento (SNIS)*. Secretaria Nacional de Saneamento Ambiental. Accessed in Mar. the 4th, 2020. n.d. url: http://app4.mdr.gov.br/serieHistorica/# (cit. on pp. x, 9, 10, 12, 16, 17).

[Soares *et al.* 2008] VARC Soares, WC Rodrigues, and MMO Cabral. "Estudo de áreas e depósitos preferenciais de *Aedes albopictus* (skuse, 1894) e *Aedes aegypti* (linnaeus, 1762) no município de paracambi - rio de janeiro". In: *EntomoBrasilis* 1.3 (2008), pp. 63–68. url: https://doi.org/10.12741/ebrasilis.v1i3.30 (cit. on p. 59).

[Soares-Pinheiro *et al.* 2017] VC Soares-Pinheiro, W Dasso-Pinheiro, JM Trindade-Bezerra, and WP Tadei. "Eggs viability of *Aedes aegypti Linnaeus (Diptera, Culicidae)* under different environmental and storage conditions in manaus, amazonas". In: *Braz. J. Biol.* 77.2 (2017), pp. 396–401. url: https://doi.org/10.1590/1519-6984.19815 (cit. on pp. viii, x, 28, 36–40, 60).

[A. P. d. Souza *et al.* 2020] Antonio Pancracio de Souza *et al. Aedes aegypti: mitos verdades*. Ponta Grossa, PR: Atena, 2020, 2020. isbn: 978-65-5706-335-4 (cit. on p. 46).

[C. Souza *et al.* 2015] CMN Souza, AM Costa, LRS Moraes, and CM Freitas. *Saneamento: promoção da saúde, qualidade de vida e sustentabilidade ambiental*. Editora Fiocruz, Rio de Janeiro, 2015. url: https://www.academia.edu/19748251/Saneamento_Promo%C3%A7%C3%A3o_da_Sa%C3%BAde_qualidade_de_vida_e_sustentabilidade_ambiental (cit. on p. 6).

[E. Souza n.d.] EAB Souza. *Biologia do vetor Aedes aegypti*. Accessed in Mar. the 7th, 2024. n.d. url: https://slideplayer.com.br/slide/385777/ (cit. on pp. viii, 45).

[L. Souza, Caires, *et al.* 2010] LA Souza, DN Caires, PLS Carneiro, CHM Malhado, and R Martins Filho. "Curvas de crescimento em bovinos da raça indubrasil criados no estado do sergipe (growth rate curves of indubrasil cattle raised at sergipe state)". In: *Rev. Ciênc. Agron.* 41.4 (2010), pp. 671–676. url: https://doi.org/10.1590/S1806-66902010000400022 (cit. on p. 38).

[L. Souza, Carneiro, *et al.* 2011] LA Souza, PLS Carneiro, *et al.* "Curvas de crescimento em ovinos da raça morada nova criados no estado da bahia". In: *R. Bras. Zootec.* 40.8 (2011), pp. 1700–1705. URL: https://doi.org/10.1590/S1516-35982011000800011 (cit. on p. 38).

[S. Souza *et al.* 2010] SS Souza, IG Silva, and HHG Silva. "Associação entre incidência de dengue, pluviosidade e densidade larvária de *Aedes aegypti*, no estado de goiás". In: *Revista da Sociedade Brasileira de Medicina Tropical* 43.2 (2010), pp. 152–155. URL: https://www.scielo.br/j/rsbmt/a/Wy57cBsYYHwLvdQ8QymQqxc/?format=pdf&lang=pt (cit. on p. 2).

[Spark n.d.(a)] Weather Spark. *Condições meteorológicas médias de Campo Grande.* Accessed in Mar. the 13th, 2020. n.d. URL: https://pt.weatherspark.com/y/29530/Clima-caracter%5C%C3%5C%ADstico-em-Campo-Grande-Brasil-durante-o-ano (cit. on pp. xi, 17, 58, 73, 75).

[Spark n.d.(b)] Weather Spark. *Condições meteorológicas médias de Duque de Caxias.* Accessed in Mar. the 13th, 2020. n.d. URL: https://pt.weatherspark.com/y/30577/Clima-caracter%5C%C3%5C%ADstico-em-Duque-de-Caxias-Brasil-durante-o-ano (cit. on pp. xi, 17, 58, 74, 75).

[Spark n.d.(c)] Weather Spark. *Condições meteorológicas médias de Nova Iguaçu.* Accessed in Mar. the 13th, 2020. n.d. URL: https://pt.weatherspark.com/y/30570/Clima-caracter%5C%C3%5C%ADstico-em-Nova-Igua%5C%C3%5C%A7u-Brasil-durante-o-ano (cit. on pp. xi, 17, 58, 74, 75).

[Spark n.d.(d)] Weather Spark. *Condições meteorológicas médias de Parnamirim.* Accessed in Mar. the 13th, 2020. n.d. URL: https://pt.weatherspark.com/y/31426/Clima-caracter%5C%C3%5C%ADstico-em-Parnamirim-Brasil-durante-o-ano (cit. on pp. xi, 17, 58, 74, 75).

[Spark n.d.(e)] Weather Spark. *Condições meteorológicas médias de Santarém.* Accessed in Mar. the 13th, 2020. n.d. URL: https://pt.weatherspark.com/y/29537/Clima-caracter%5C%C3%5C%ADstico-em-Santar%5C%C3%5C%A9m-Brasil-durante-o-ano (cit. on pp. xi, 17, 58, 73, 75).

[Tracey 2019] WD Tracey. "The taste of water: female mosquitos require a specific ion-channel protein to sense the presence of fresh water in which they can lay their eggs". In: *elife* 27.8 (2019). URL: https://doi.org/10.7554/eLife.48654 (cit. on pp. 28, 29).

[Trpis 1972] M Trpis. "Dry season survival of *Aedes aegypti* eggs in various breeding sites in the dar es salaam area, tanzania". In: *Bulletin of the World Health Organization* 47.3 (1972), pp. 433–437. URL: https://www.ncbi.nlm.nih.gov/pmc/articles/PMC2480724/ (cit. on p. 2).

[Usher 1966] MB Usher. "A matrix approach to the management of renewable resources, with special reference to selection forests". In: *Journal of Applied Ecology* 3.2 (Nov. 1966), pp. 355–367. URL: https://www.jstor.org/stable/2401258 (cit. on p. 1).

[Vieira 2008] G Vieira. *A dengue em números: ovos*. Accessed in Jul. the 6th, 2022. 2008. URL: http://www.fiocruz.br/ioc/cgi/cgilua.exe/sys/start.htm?infoid=573%5C&sid=32 (cit. on pp. 2, 8, 27, 28, 41).

[Werner and Caswell 1977] P Werner and H Caswell. "Population growth rates and age versus stage-distribution models for teasel (dipsacus sylvestris huds.)" In: *Ecology* 58 (Sept. 1977), pp. 1103–1111. DOI: 10.2307/1936930 (cit. on pp. 1, 70).

[WHO 2019] WHO. *Dengue control: the mosquito*. Accessed in Mar. the 13th, 2020. 2019. URL: http://www.who.int/denguecontrol/mosquito/en/ (cit. on p. 49).

[WHO 2020] WHO. *Water sanitation hygiene: Where is the risk of dengue fever most acute and what should be done?* Accessed in Apr. the 16th, 2020. 2020. URL: https://www.who.int/water_sanitation_health/emergencies/qa/emergencies_qa13/en/ (cit. on pp. 5, 8, 11, 59).

[WHO n.d.(a)] WHO. *Humanitarian Health Action: Flooding and communicable diseases fact sheet*. Access in Apr. the 20th, 2020. n.d. URL: https://www.who.int/hac/techguidance/ems/flood_cds/en/ (cit. on pp. 2, 5, 10, 11).

[WHO n.d.(b)] WHO. *Water sanitation hygiene: Water-related diseases, Dengue and Dengue Haemorrhagic Fever*. Access in Apr. the 16th, 2020. n.d. URL: https://www.who.int/water_sanitation_health/diseases-risks/diseases/dengue/en/ (cit. on pp. 3, 5, 6, 8, 11, 59).

[Wilke *et al.* 2023] ABB Wilke, A Mhlanga, AG Kummer, C Vasquez, and et al. Moreno M. "Diel activity patterns of vector mosquito species in the urban environment: implications for vector control strategies". In: *PLOS Neglected Tropical Diseases* 17.1 (2023). URL: https://doi.org/10.1371/journal.pntd.0011074 (cit. on p. 11).

[Winsor 1932] CP Winsor. "The gompertz curve as a growth curve". In: *Proceedings of the National Academy of Sciences of the United States of America* 18.1 (1932), pp. 1–8. URL: https://doi.org/10.1073/pnas.18.1.1 (cit. on p. 37).

[G. Yang *et al.* 2009] GJ Yang, BW Brook, and CJA Bradshaw. "Predicting the timing and magnitude of tropical mosquito population peaks for maximizing control efficiency". In: *PLOS Neglected Tropical Diseases* 3.2 (2009). e385, pp. 1–9. URL: https://doi.org/10.1371/journal.pntd.0000385 (cit. on pp. 1, 2).

[H. Yang 2014] HM Yang. "Assessing the influence of quiescence eggs on the dynamics of mosquito *Aedes aegypti*". In: *Applied Mathematics* 5.17 (2014), pp. 2696–2711. URL: http://dx.doi.org/10.4236/am.2014.517257 (cit. on pp. 29, 40, 44–46, 63).

[H. Yang *et al.* 2009] HM Yang, ML Macoris, KC Galvani, MTM Andrighetti, and DMV Wanderley. "Assessing the effects of temperature on the population of *Aedes Aegypti*, the vector of dengue". In: *Epidemiol Infect.* 137.8 (2009), pp. 1188–1202. URL: https://doi.org/10.1017/S0950268809002040 (cit. on pp. 1, 28–33, 40, 46, 47, 63, 64).

[Yusoff *et al.* 2012a] N Yusoff, H Budin, and S Ismail. "Simulation of population dynamics of *Aedes aegypti* using climate dependent model". In: (Feb. 2012). URL: https://doi.org/10.5281/zenodo.1058625 (cit. on pp. 1, 28, 30, 41).

[Yusoff *et al.* 2012b] N Yusoff, H Budin, and S Ismail. "Stage-structured population dynamics of *Aedes aegypti*". In: *International Journal of Modern Physics: Conference Series*. International Conference Mathematical and Computational Biology 2011, International Journal of Modern Physics: Conference Series Vol. 9 (2012). World Scientific Publishing Company, 2012, pp. 364–372. URL: https://doi.org/10.1142/S2010194512005430 (cit. on pp. 1, 28–30, 34, 41, 59).